# Electrical energy storage scheduling

## Short-term scheduling for the intraday market using stochastic programming

Andrea Krijgsman


Delft University of Technology

TU Delft

# Electrical energy storage scheduling

## Short-term scheduling for the intraday market using stochastic programming

by

Andrea Krijgsman

to obtain the degree of Master of Science
at the Delft University of Technology,
to be defended publicly on Tuesday November 28, 2023 at 14:30.


| | | |
|---|---|---|
| Student number: | 5424763 | |
| Project Duration: | April, 2023 - November, 2023 | |
| Thesis committee: | Dr. ir. J.T. van Essen | TU Delft, Responsible supervisor |
| | Prof. dr. A. Papapantoleon | TU Delft, Committee member |
| | T. van der Vliet | Northpool B.V., Committee member |




TU Delft

# Abstract

The global push for renewable energy faces challenges due to the unpredictable and inconsistent nature of wind and solar sources. These inherent characteristics of renewable energy sources add volatility to the electricity markets. In response, electrical energy storage (EES) emerges as a solution for maintaining grid flexibility, stability, and reliability. Therefore, it is important to understand the potential interdependence of the wholesale electricity markets and the EESs.

This thesis focuses on short-term EES scheduling, comparing pumped hydropower storage (PHS), compressed air energy storage (CAES), and battery energy storage systems (BESS). This thesis aims to optimize EES scheduling, which includes charging and discharging actions, in the intraday electricity market, considering market price uncertainties. Storage decisions are optimized for one day (24 hours) from the perspective of the storage owner, and its objective is to maximize its profit through market operations. The research introduces a two-stage stochastic programming approach with a rolling horizon method (SORH) to adapt to changing conditions of the intraday market throughout the day.

The results of SORH, its deterministic counterpart (DORH), and simple deterministic optimization (DO) are compared by implementing a case study organized in four typical days based on trading data from the German electricity market. SORH consistently outperforms DORH and DO and is a suitable optimization strategy. SORH reaches on average 72 percentage of the theoretical optimum, where all prices are known in advance. Moreover, SORH offers opportunities for speculative trading using the storage as an option rather than only physically operating the storage. For a practical application of the model, future research could explore methods to match the current day with representative typical days to construct relevant price scenarios.

# Acknowledgements

This thesis was written as the final part in the fulfillment for the degree of Master of Science in Applied Mathematics at the Delft University of Technology. This research was done in the research group Discrete Mathematics and Optimization.

This project could not have been successful if it were not for several people. I would like to express a special thanks.

First of all, I would like to thank my supervisor, Theresia van Essen. You became my supervisor in the middle of the process, and it was inspiring to see how quickly you adapted to the problem without any knowledge of financial products. You always gave me a lot to think about in meetings, which contributed immensely to my progress. The welcoming atmosphere you fostered in your office made every discussion feel like an opportunity for growth. Additionally, I enjoyed our personal discussions in between mathematical topics.

This thesis was performed in cooperation with Northpool B.V. under the supervision of Thomas van der Vliet. I want to thank you for your continuous dedication in guiding me through the complexities of this research. Our countless discussions on modeling the problem gave me a profound sense of support. Therefore, I eagerly anticipate joining your team in March 2024.

I also want to thank all other employees from Northpool who supported me throughout this process. Northpool is a proprietary trading firm active in the energy commodity markets. Founded in 2013 by Roald van Noort, Northpool mainly trades electricity, gas, and carbon contracts. Alongside trading, Northpool also provides ancillary services to the system operators to help balance the electricity grid.

Finally, I want to thank Antonis Papapantoleon for guiding me through the first months of the thesis process and for being part of the thesis committee. Your experienced knowledge of applied probability helped me not take any wrong directions.

In conclusion, I sincerely thank all those mentioned above for their invaluable contributions. Their support has significantly influenced this thesis, and I am thankful for the opportunity to work alongside such dedicated individuals.

***Andrea Krijgsman***
*Delft, November 2023*

# Contents

# Nomenclature

## List of Abbreviations

| Abbreviation | Definition |
|---|---|
| BESS | Battery Energy Storage System |
| CAES | Compressed Air Energy Storage |
| DA | Day-ahead |
| DO | Deterministic Optimization |
| DORH | Deterministic Optimization with Rolling Horizon |
| EES | Electrical Energy Storage |
| ID | Intraday |
| IOHMM | Input/Output Hidden Markov Model |
| MCS | Monte Carlo Simulation |
| MILP | Mixed Integer Linear Programming |
| OTC | Over-the-Counter |
| PHS | Pumped Hydropower Storage |
| RES | Renewable Energy Sources |
| RH | Rolling Horizon |
| SoC | State of Charge |
| SORH | Stochastic Optimization with Rolling Horizon |
| TO | Theoretical Optimization |
| TSO | Transmission System Operator |
| VaR | Value at Risk |
| VPP | Virtual Power Plant |

## List of Sets

| Set | Definition |
|---|---|
| $I$ | Set of solution steps |
| $T$ | Set of time |
| $\Omega$ | Set of scenarios |

## List of Parameters

| Parameter | Definition |
|---|---|
| $C_t^{0,i}$ | Initial charging decision at time $t \in T$ in solution step $i \in I$ |
| $C^{\max}$ | Power limit per time step for charging decisions |
| $D_t^{0,i}$ | Initial discharging decision at time $t \in T$ in solution step $i \in I$ |
| $D^{\max}$ | Power limit per time step for discharging decisions |
| $\eta_c$ | Charging efficiency |
| $\eta_d$ | Discharging efficiency |
| $\eta_s$ | Use-independent loss rate |
| $p_t^{DA}$ | Day-ahead price for time $t \in T$ |
| $p_t^i$ | Intrady price for time $t \in T$ observed in solution step $i \in I$ |
| $p_t^\omega$ | Simulated intraday price for time $t \in T$ for scenario $\omega \in \Omega$ |

| Parameter | Definition |
|---|---|
| $S$ | Cardinality of $\Omega$ |
| $SoC^{0,i}$ | Initial SoC level in solution step $i \in I$ |
| $SoC_{end}$ | Final SoC level |
| $SoC^{\min}$ | Lower bound for the State of Charge |
| $SoC^{\max}$ | Upper bound for the State of Charge |
| $\mathcal{T}$ | Time horizon |
| $\phi^{\omega,i}$ | Probability of scenario $\omega \in \Omega$ in solution step $i \in I$ |

## List of Variables

| Variable | Definition |
|---|---|
| $c_t^{1,i}$ | First-stage charging decision at time $t \in T$ in solution step $i \in I$ |
| $\Delta c_t^{2,\omega,i}$ | Second-stage charging decision at time $t \in T$ for scenario $\omega \in \Omega$ in solution step $i \in I$ |
| $d_t^{1,i}$ | First-stage discharging decision at time $t \in T$ in solution step $i \in I$ |
| $\Delta d_t^{2,\omega,i}$ | Second-stage discharging decision at time $t \in T$ for scenario $\omega \in \Omega$ in solution step $i \in I$ |
| $\mathcal{R}^i$ | Revenue from charging/discharging operations in solution step $i \in I$ |
| $SoC_t^{1,i}$ | First-stage SoC at time $t \in T$ in solution step $i \in I$ |
| $SoC_t^{2,\omega,i}$ | Second-stage SoC at time $t \in T$ for scenario $\omega \in \Omega$ in solution step $i \in I$ |
| $y_t^{1,i}$ | First-stage binary variable which is 1 when charging at time $t \in T$ in solution step $i \in I$ and 0 when discharging |
| $y_t^{2,\omega,i}$ | Second-stage binary variable which is 1 when charging at time $t \in T$ for scenario $\omega \in \Omega$ in solution step $i \in I$ and 0 when discharging |

# List of Figures

# List of Tables

# 1 Introduction

As the global demand for sustainable energy increases, nations worldwide are grappling with the challenges of the energy transition. In this context, the European Green Deal stands out as a prominent initiative aiming to address climate change by striving for no net emissions in greenhouse gases by 2050. One key aspect of this initiative involves a substantial increase in the European Union's share of renewable energy, expected to nearly double from 37 percent in 2021 to 69 percent in 2030, and reaching around 80 percent by 2050 (European Commission, 2023). However, the transition to a greener energy mix, mainly reliant on wind and solar sources, introduces challenges in forecasting due to their dependency on unpredictable weather conditions (Maciejowska, 2020). This shift towards more uncertain and volatile electricity generation necessitates a flexible approach to managing a country's energy system. According to the European Commission (European Commission, 2023), the overall flexibility requirements surge notably as the percentage of renewable energy surpasses the 74 percent mark. In recent years, the energy market has already exhibited a more unbalanced outlook, reflected in the heightened volatility of European electricity prices (Schüle et al., 2023).

## 1.1. Introduction to storage

Energy storage is a potential solution to address the challenges of shifting to renewable energy sources. This solution becomes increasingly important in maintaining flexibility, stability, and reliability within the grid. Excess energy is stored during periods of abundance and can be subsequently drawn from storage during periods of scarce electricity. Notably, the European energy storage capacity is poised for substantial growth, forecast to rise from 60 Gigawatts (GW) in 2022 to 200 GW in 2030 and an impressive 600 GW by 2050 (European Commission, 2023). This surge in energy storage capacity underscores the importance to optimize the utilization of energy storage.

There are several types of energy storage, each designed to address specific needs. This thesis focuses on electrical energy storage (EES), which encompasses various forms. One of the oldest and widely used forms is hydro storage, involving the storage of water and harnessing its energy potential to generate electricity. Hydro storage can be either seasonal or short-term. Seasonal pumped hydropower storage, typically situated in mountainous regions, collects meltwater. Short-term storage systems are defined by a discharging duration of less than 24 hours (Klaas & Beck, 2021). Pumped hydropower storage (PHS), a short-term storage solution, is commonly located alongside large rivers with elevation differences. Notably, Norway stands out in Europe, holding almost half of the continent's reservoir capacity and achieving an outstanding hydropower share of about 95 percent (Quaranta et al., 2022).

Another technique is compressed air energy storage (CAES), which uses electricity to compress and store air underground. The primary concept is to store surplus electricity generated during times of abundance by converting it into compressed air. This compressed air is then stored underground. When renewable energy sources cannot meet demand, the stored air is decompressed, and the released air generates electricity. Like other short-term storage systems, CAES contributes to the stability the power grid. Notably, this process relies on natural underground spaces, such as salt caverns, for storing compressed air.

Battery energy storage systems (BESS) offer an alternative for regions where geological conditions do not favor PHS or CAES. BESS technology utilizes batteries to store electrical energy for later use, contributing to a more robust and flexible energy infrastructure. However, it is worth noting that BESS are not as widely deployed on a utility scale compared to other storage technologies.

These three storage technologies, PHS, CAES, and BESS, are included in this thesis due to their distinct characteristics and potential applications. In addition to them, other options include flywheel energy storage, molten salt storage, hydrogen energy storage, and thermal energy storage. As technology advances, these diverse storage solutions become increasingly important to ensure a stable and reliable electricity supply in the future.

## 1.2. Introduction to electricity markets

We must examine Europe's electricity markets to understand how EESs can solve the increasing renewable energy production. These markets are a dynamic system where electrical power is generated, bought, and sold. Markets ensure we have a safe and reliable electricity supply to meet demand. These markets are designed to be efficient, competitive, and reliable.

On the wholesale electricity markets, both renewable and traditional electricity producers offer their electricity to wholesalers, retailers, and large consumers. Prices fluctuate based on supply and demand. The day-ahead and intraday markets are part of the wholesale markets. On the day-ahead market, participants trade electricity for the following day. They submit bids indicating how much electricity they can supply or require. Clearing prices are set to match supply with expected demand. The intraday market operates closer to real-time. This marketplace allows participants to adjust their positions as the day progresses. It offers flexibility for unforeseen changes in demand or supply.

Closest to the delivery of the electricity, the grid operators manage the balancing market to maintain real-time grid stability. Their only mandate is to procure additional electricity or curtail generation as needed to keep the grid balanced. Therefore, prices can become extreme in this market.

Europe's interconnected grid enables electricity to flow across borders. Surplus energy in one area can be sold to neighboring regions. National governments, regulatory authorities, and the EU regulate and coordinate all markets. They aim to balance economic efficiency and environmental responsibility while delivering dependable electricity to all consumers.

## 1.3. Research questions and outline

Delving into the interaction between EES technologies and electricity markets is essential to devise practical strategies in this field. In this master thesis, we investigate suitable techniques for making optimal storage scheduling decisions on wholesale markets, specifically for the intraday market. Electricity bought from the market will be stored, and discharged electricity will be sold to the market again. This research focuses on short-term storage and follows the perspective of the storage operator. The objective is to maximize their profit through market operations. The research question is formulated as follows:

- How can one optimize EES scheduling on the intraday market, considering the uncertainty in market prices?

The main goal of this thesis is to answer this question. However, the following sub-questions are formulated to support the main question:

- How should the short-term EES be modeled?
- What is the most suitable optimization technique for finding a daily EES schedule?
- How should the intraday price's uncertainty be considered in the model?

To answer all research questions, the outline of this thesis is as follows. First, in Chapter 2, the theoretical background required to understand this thesis is displayed. Three EES systems, the relevant electricity markets and their dynamics, stochastic programming, the rolling horizon approach, and price simulation methods are explained. In Chapter 3, an overview of the literature on this topic is provided. It starts by providing a classification on EES management literature, elaborates on related works, and concludes with literature gaps to be filled. After that, in Chapter 4, the model formulation is explained.

The objective function and constraints of the optimization problem are presented. In Chapter 5, the solution methods and the construction of price scenarios are explained. After that, the case study data for this research is presented in Chapter 6, organized into four groups of typical days. In Chapter 7, the results of the optimization strategies are presented. Finally, Chapter 8 is a conclusion on the findings and provides recommendations for further research.

# 2

# Theoretical Background

In this chapter, we describe the theoretical background necessary to understand this thesis. In Section 2.1, three different energy storage technologies are explained. In Section 2.2, an overview of the European electricity market is provided, explaining its markets and characteristics. In Section 2.3, we explain multi-stage stochastic programming. Next, we introduce the rolling horizon approach in Section 2.4. Finally, Monte Carlo simulation is explained in Section 2.5, which is the price simulation technique.

## 2.1. Energy storage technology

In this section, we describe and compare three distinct electrical energy system (EES) technologies: pymped hydropower storage (PHS), compressed air energy storage (CAES), and battery energy storage system (BESS). These technologies are intriguing to analyze due to their unique advantages and limitations. Understanding their characteristics and applications is crucial for stakeholders in the energy sector. PHS and CAES are mechanical storage systems harnessing energy through kinetic or gravitational forces. On the other hand, BESSs fall under electrochemical storage systems. To provide a comparison, we delve into the principles of each technology, assess their geographic feasibility, and evaluate their efficiency. By focusing on these aspects, we aim to highlight the distinctive features of PHS, CAES, and BESS, aiding stakeholders in making informed decisions.

### 2.1.1. PHS

PHS uses the power of gravity to generate electricity. Water is pumped from a lower reservoir to a higher reservoir when there is excess electricity. When electricity is scarce, the water is released to drive a turbine in the powerhouse to generate electricity. That powerhouse is connected to the grid. In Figure 2.1, one variant of the PHS is shown, the off-river PHS. The second variant is a closed-loop PHS continuously connected to a water source, like a river.

PHS has the world's largest energy storage capacity, accounting for 94 percent of the global capacity, according to the International Hydropower Association (2023). They estimate the total capacity can store up to 9000 gigawatt hours (GWh) of electricity. For comparison, a data center can consume 25 GWh of electricity in one year (CEVA Logistics, 2023). This volume underscores the substantial role PHS plays in meeting global energy demands.

There is still much potential to scale the PHS. However, not all countries have suitable geographical locations. The PHS requires elevation difference between the upper and lower reservoir and significant land use. The efficiency differs between mountainous regions and flat terrains due to variations in elevation. Similarly, the availability of natural water reservoirs significantly affects the feasibility and efficiency of PHS installations. PHS still exhibits relatively high efficiency, typically ranging from 70 to 85 percent (Ma et al., 2014; Blakers et al., 2021).

Another storage parameter to consider is the energy-to-power ratio, calculated by dividing the energy storage capacity (measured in MWh) by the power capacity (measured in MW). Energy storage capacity represents the amount of energy that can be stored, and power capacity indicates the maximum instantaneous electric power that can be generated. This ratio is also known as duration or discharge

time. Real-world and example cases show that the energy-to-power ratio typically ranges between 6 to 10 hours (Ruiz et al., 2022; EnBW, 2023; PORR Group, 2023; Garcia-Gonzalez et al., 2008).

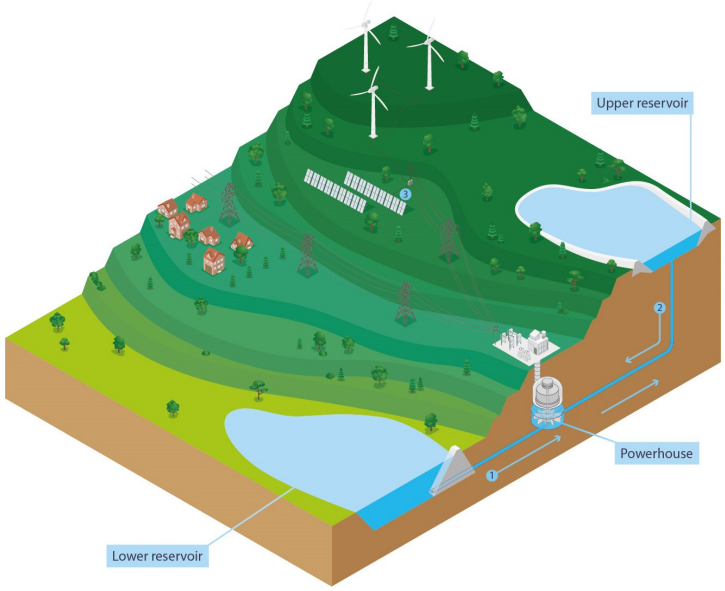


**Figure 2.1:** Schematic explanation off-river pumped hydropower storage (International Hydropower Association, 2023).

### 2.1.2. CAES

CAES uses electricity to compress air and store it underground in a cavern or above ground in a container. During periods of excess electricity generation or low energy demand, surplus electricity is used to operate a compressor (Figure 2.2). The compressor draws in atmospheric air and compresses it to very high pressures. Typically, two main types of underground storage caverns store the air. The first is a salt cavern, artificially created by dissolving underground salt deposits with water, leaving behind large caverns. This type is the preferred choice for CAES since the salt effectively seals the cavern. The second type is porous rock formations, such as depleted natural gas reservoirs or aquifers. Rock formations may require additional measures to prevent air leakage than salt caverns. During periods of scarce electricity or high energy demand, the electricity is recuperated when the compressed air is released from the cavern. The compressed air is sent from the storage tanks to an expander, essentially a large turbine. This generated electricity is then supplied to the grid.

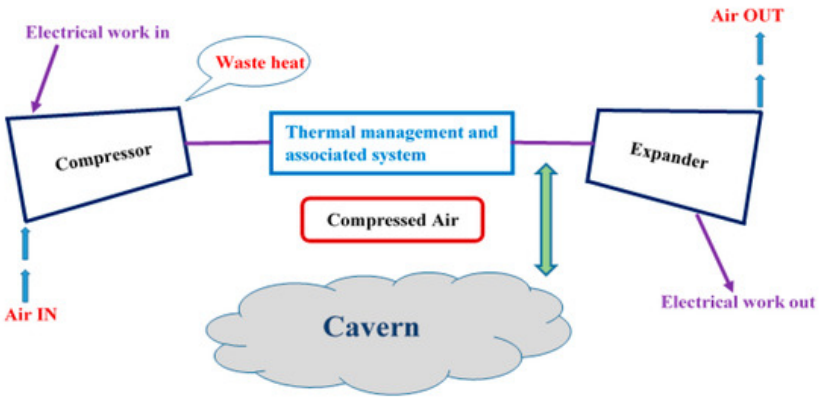


**Figure 2.2:** Schematic explanation compressed air energy storage (Chakraborty et al., 2022).

The main drawback of CAES is the need for a suitable geographical location for the cavern. Another drawback is the low efficiency, around 50 percent for a round trip (Chakraborty et al., 2022). Elmegaard

& Brix (2011) estimate the efficiency slightly lower, around a maximum of 45 percent. However, CAES has the benefit of a large energy storage capacity. In China, the world's largest CAES system can store more than 132 GWh of electricity annually, providing electricity for 40 to 60 thousand households during peak electricity consumption (Bellini, 2022). Another large-scale CAES example is the 290 MW Huntorf plant in Germany (Rabi et al., 2023) with an energy storage capacity of 480 MWh. Therefore, its discharge time is 1.7 hours.

### 2.1.3. BESS

BESS is a system that stores electrical energy in the form of chemical energy in batteries. They can include Lead-Acid batteries, Nickel-Cadmium batteries, Lithium-Ion (Li-Ion) batteries, Sodium-sulfur batteries, Sodium-Nickel-Chloride batteries. The Li-Ion battery is the most important form of storage in portable and mobile applications.

Figure 2.3 shows a schematic explanation of a Li-Ion battery. This electrochemical cell comprises a cathode and an anode, which are the positive and the negative sides of the battery, respectively. Between them lies a thin plastic separator, and the entire structure is filled with an electrolyte liquid containing numerous Li-Ions. Notably, the use of lithium, known for its lightweight properties, enhances the efficiency of the battery.

In the charging process, electrons move from the cathode to the anode. As electrons detach from the cathode, Li-Ions migrate through the electrolyte towards the anode, where they react with both the electrons and the material of the anode, typically graphite. When this cycle is complete, the battery is fully charged. During discharge, the reverse reaction occurs. Electrons come off the anode and move to the cathode, while Li-Ions move through the electrolyte to the cathode, reacting with the electrons and the material on the cathode. The movement of electrons and Li-Ions in these cycles powers the functioning of the battery.

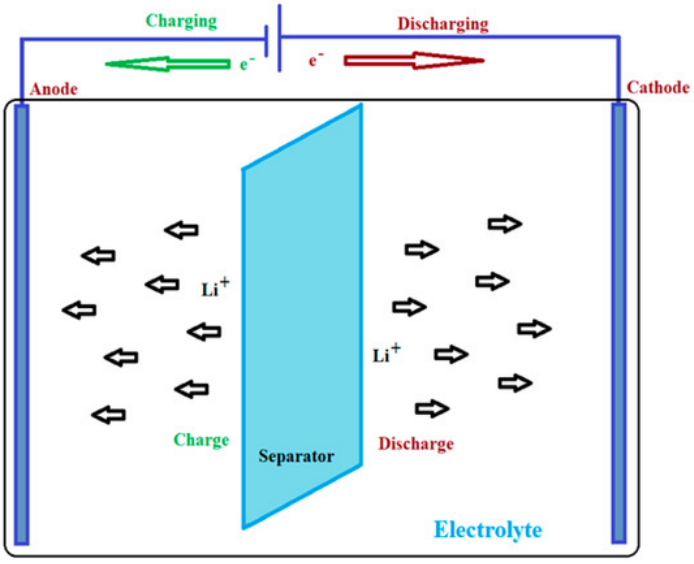


**Figure 2.3:** Schematic explanation Lithium-Ion battery (Chakraborty et al., 2022).

BESS consists of packs of multiple battery cells set up at the same voltage. Batteries are the most efficient forms of storage. For example, Li-Ion batteries' charging and discharging efficiencies are around 95 percent (E. Oh & Wang, 2020). These efficiencies combined result in a round-trip efficiency of approximately 90 percent. Another advantage of BESS is its high charging and discharging power capacities. The German energy firm RWE recently confirmed its utility-scale battery storage project in the Netherlands with a 35 MW power capacity and a discharge time of 1.2 hours (ETN News, 2023). A recently installed Californian project has 30 MW power capacity and a discharge time of 0.7 hours (Power Engineers, 2023).

However, BESS technology also has its limitations. BESS systems have limited energy storage capacity compared to other forms of EES, such as PHS and CAES (Chakraborty et al., 2022), which

may restrict their ability to supply electricity for extended periods. The world's first big Li-Ion BESS is installed in 2017 in Australia. They installed only 129 MWh of energy storage capacity. Moreover, S. Oh et al. (2023) and E. Oh & Wang (2020) restrict the maximum energy storage capacity at 90 percent of the total capacity, resulting in a lower storage flexibility. Moreover, batteries degrade over time, leading to an even more reduced capacity and lifespan.

## 2.2. Electricity markets

Since the deregulation and introduction of competitive markets in the 1990s and 2000s, electricity has been considered a commodity and traded on different competitive markets (Mayer & Trück, 2018). All electricity contracts have a specific delivery time and location. In financial terminology, this is referred to as a forward or futures contract. A forward contract is a legal agreement in which two parties commit to purchasing or selling a specific commodity, asset, or security at a predetermined price on a specified future date. The buyer of a forward contract commits to acquire and take possession of the underlying asset when the contract is delivered. Conversely, the seller commits to supply and deliver the underlying asset on the agreed-upon delivery date. Futures are standardized forward contracts designed to be uniform in quality and quantity to streamline trading on futures exchanges. The largest electricity spot exchanges in Europe are EPEX Spot and Nord Pool. Forwards are traded bilaterally or over-the-counter (OTC). In that case, trading partners directly contact each other.

In Figure 2.4, it is shown that the markets are organized depending on the delivery time of their contracts. On the forward market, electricity is traded between five years and one month before delivery. After that, participants can sell and buy electricity for the next day in hourly blocks on the day-ahead market. The intraday market starts after the day-ahead market is cleared, and buyers and sellers can adjust their volumes when more information comes in. Both day-ahead and intraday markets are called spot markets. Finally, the balancing market manages the real-time imbalances between electricity supply and demand. The following sections explain each of them in more detail.

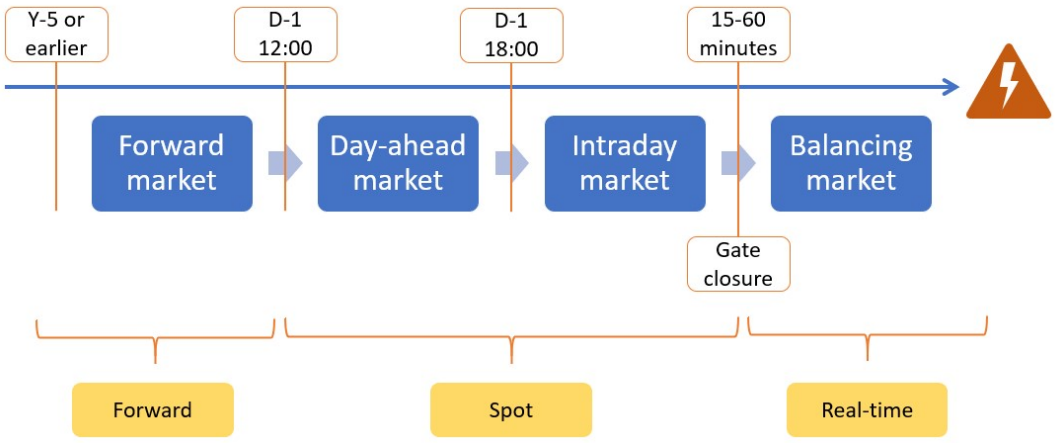


**Figure 2.4:** Time outline of the electricity markets (KYOS, 2023).

Compared to other commodities, the behavior of electricity prices differs significantly due to several distinctive characteristics. Most importantly, electricity must be consumed at the same time as it is created to keep the grid in balance. This requirement dictates that the supply of electricity must always match the demand from consumers. Consequently, this real-time synchronization can lead to extreme price changes within small periods. In Section 2.2.5, the leading pricing principles of electricity are explained.

### 2.2.1. Forward market

The forward market is a financial marketplace where participants can buy and sell contracts for the future delivery of electricity. Contracts can have various durations, ranging from days to years, allowing participants to manage their electricity needs for different time horizons. Participants, such as electricity producers, distributors, and large consumers, hedge against price volatility using the forward market.

By entering into forward contracts, they can lock in prices, reducing their exposure to unpredictable fluctuations in electricity prices.

### 2.2.2. Day-ahead market

The day-ahead market operates as an auction where suppliers and consumers submit bids for the next day's 24-hour period. The auction is held at 12.00. There is a separate futures contract for each hour of the day, 00.00-01.00, 01.00-02.00, etc. The market operator employs a clearing algorithm to determine which bids will be accepted and which will be rejected. The intersection of aggregated supply and demand curves in the auction results in day-ahead spot prices for each hour. These spot prices best reflect the expected value of electricity for the corresponding hours. The prices are determined per bidding zone, which corresponds mainly to the borders of Europe.

### 2.2.3. Intraday market

The intraday market operates closer to the delivery time and opens after the day-ahead market has been cleared. In the intraday market, trading occurs at hourly and quarter-hourly intervals, offering participants the flexibility to adjust their positions and respond to changing demands as the delivery time approaches. Trades can be executed up to a few minutes before the actual delivery of electricity. In the intraday market, trades are concluded using the pay-as-bid principle. This principle implies that buy and sell bids are matched based on their respective prices, and the trades are concluded at the specified prices in the bids.

As the delivery time approaches, the accuracy of demand estimates improves due to the incorporation of real-time data, such as weather updates and information on events that may influence demand patterns or the latest data on power plant outages. However, the intraday market can still be more volatile than the day-ahead market. This increased volatility can be attributed to sudden shifts in consumer behavior or unexpected changes in energy supply. Additionally, the tighter time frame for decision-making in the intraday market amplifies the impact of even minor fluctuations, leading to increased price volatility compared to the day-ahead market, where transactions are planned the day before delivery.

So far, volumes traded on the day-ahead market are significantly higher than on the intraday market (EPEX SPOT, 2023). However, the volumes on the intraday market are expected to rise with the growing share of renewable energy sources (RES) in the market. The inherent uncertainty in RES supply underscores the necessity for adjustments closer to delivery, where the intraday market can play a crucial role.

### 2.2.4. Balancing market

The balancing market operates in real-time to address imbalances between scheduled electricity generation and actual consumption, ensuring a stable and reliable power system. The transmission system operator (TSO) is responsible for maintaining this equilibrium on the grid. Entities participating in the balancing market, such as generators and demand response providers, submit bids indicating the quantity of electricity they can provide or consume. The TSO evaluates these bids in real-time and dispatches the most cost-effective offers to balance the grid. These imbalances can arise due to unforeseen changes in electricity demand, unexpected generator outages, or other factors affecting supply-demand equilibrium.

### 2.2.5. Pricing

In a competitive electricity market, pricing is determined by two key principles: marginal pricing and merit order. Marginal pricing sets electricity prices based on the variable cost of the most expensive plant required to meet demand. The most expensive plant is referred to as the marginal plant. The merit order ranks generators by operating costs, with cheaper plants dispatched first and more expensive ones dispatched last, setting the electricity price at the level of the last generator dispatched, which is the marginal plant. The price bid by the marginal plant becomes the clearing price. This means that all generators receive the same price per unit of electricity they produce, equal to the price set by the marginal plant. The merit order effect is displayed in Figure 2.5. RES power plants tend to have the lowest operating cost, followed by nuclear plants, coal plants, and natural gas-fired plants. This dispatch process ensures that electricity is produced most cost-effectively, with the cheapest sources

being used before more expensive ones.

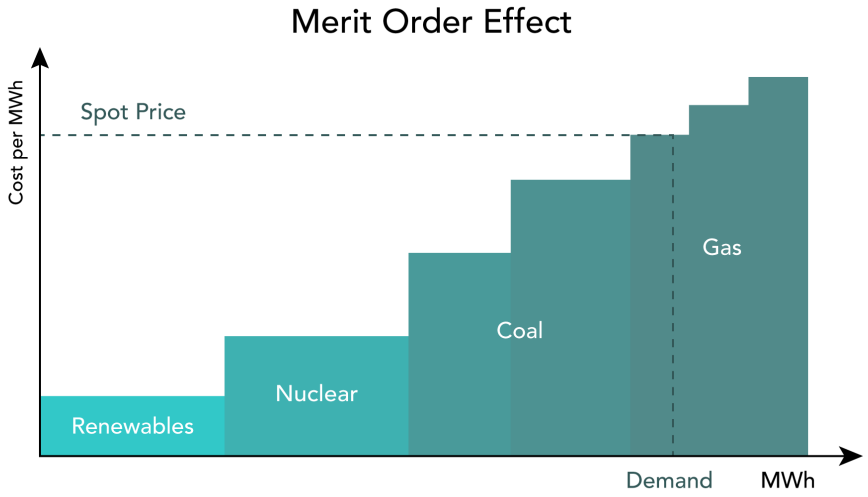


**Figure 2.5:** Visual representation merit order effect of electricity markets (Bowden, 2023).

## 2.3. Optimization under uncertainty

Optimization is a process that aims to maximize or minimize an objective function by evaluating potential values across a set of decision variables. It plays a crucial role in various fields, from mathematics and engineering to economics and data science, enabling the discovery of optimal solutions that enhance efficiency, performance, and decision-making processes. A simple optimization problem is generally written in the following form:

$$\min_{x \in X} f(x) \tag{2.1}$$

In this notation, $X$ is the feasible region, the vector $x$ defines the decision variables, and $f$ is the objective function. The standard form is to minimize the objective function but this can easily be transformed into a maximization problem.

In real-world scenarios, many situations occur where the parameters of the objective function are not known before the optimization is performed. We introduce a stochastic programming approach to account for this uncertainty in parameter values. This approach incorporates randomness into specific parameters, allowing for optimization under variable or unpredictable conditions. The two-stage paradigm divides the decision variables into two subsets (Sahinidis, 2004). The first-stage decision variables $x$ have to be decided before the realization of the uncertain parameters. They are often referred to as the *here-and-now* decisions. After the occurrence of random events, the variables $\boldsymbol{y}$ of the second-stage, or *recourse*, are determined to optimize the objective. The *recourse* variables can be interpreted as adjustments or corrections to the first-stage solution. In stochastic programming, it is assumed that the probability distribution of the random parameters is known (Birge & Louveaux, 2011). We define the random parameters as the random vector $\boldsymbol{\xi}$. We use boldface to indicate the vector is a random variable. $\Omega$ represents the set of random events. Given a random event $\omega \in \Omega$, we define $\xi(\omega)$ as a realization of the random vector $\boldsymbol{\xi}$. The sequence of events is best described below:

$$x \rightarrow \xi\left(\omega\right) \rightarrow y\left(\omega, x\right) \tag{2.2}$$

Sequence (2.2) indicates that first, the first-stage decisions are made, afterwards, the realizations of the random vector $\xi(\omega)$ become known, and finally, the second-stage decisions are made based on the decisions of the first-stage and the random realizations. A standard formulation of the two-stage linear program is

$$\min_{x \in X} \left(f(x) + E_{\boldsymbol{\xi}}\left(Q\left(x, \boldsymbol{\xi}\right)\right)\right), \tag{2.3}$$

where $E_{\boldsymbol{\xi}}(\cdot)$ denotes the common notation of the mathematical expectation with respect to the random vector $\boldsymbol{\xi}$. $Q(x, \boldsymbol{\xi})$ is the optimal value of the second-stage problem and is defined as

$$Q(x, \boldsymbol{\xi}) = \min_{y \in Y} g(\boldsymbol{y}, x, \boldsymbol{\xi}). \tag{2.4}$$

In this approach, $Y = Y(x, \xi)$ is the feasible region for the second-stage decisions. We write $Y$ as a function of $x$ and $\xi$ to indicate that the feasibility is dependent on the first-stage decisions and the realization $\xi$. $g(\boldsymbol{y}, x, \boldsymbol{\xi})$ is the objective function of the second-stage, given the first stage solution $x$ and a realization of $\boldsymbol{\xi}$ of the random data. It is also minimized in this standard formulation.

In a lot of research, it is assumed that the random vector $\boldsymbol{\xi}$ follows a discrete distribution (Birge & Louveaux, 2011). Therefore, the random vector $\boldsymbol{\xi}$ has finite possible realizations or scenarios. If we assume $K$ possible scenarios, $\xi_1, ..., \xi_K$, and corresponding probabilities $p_1, ..., p_K$, then the optimization problem can be written as

$$\min_{x \in X} \left( f(x) + \sum_{k=1}^{K} p_k \left( Q\left(x, \xi_k\right) \right) \right). \tag{2.5}$$

## 2.4. Rolling horizon approach

The rolling horizon approach is a dynamic solution approach to solve problems that evolve over time. The term rolling horizon is used to indicate that a time-dependent model is solved repeatedly and that the planning interval is moved forward in time during each solution step. In this method, the optimization problem is divided into a series of shorter planning periods, typically referred to as horizons. For each horizon, only a portion of the problem is solved, considering current information and constraints, while the future portions remain uncertain or unmodeled. As time progresses, the optimization horizon rolls forward, allowing for periodic updates and revisions to the plan based on new data or changing circumstances. This iterative process enables decision-makers to make more informed and adaptable choices while efficiently managing computational complexity. The rolling horizon approach finds applications in various fields, where real-time adjustments and flexibility are crucial for making decisions in uncertain environments. Figure 2.6 shows an example of the rolling horizon approach for a planning problem. The planning horizon is separated into a fixed and changeable planning period and is rolled forward in time. The changeable part allows for revisions compared to the initial planning.

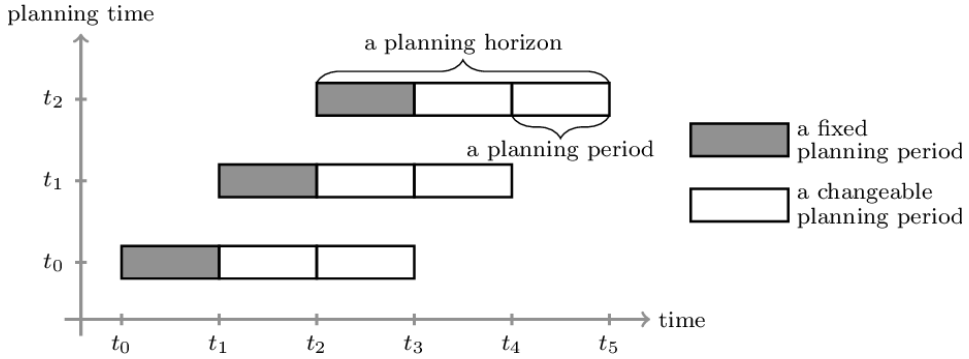


**Figure 2.6:** Example rolling horizon approach for a planning problem (Wang & Kopfer, 2015).

## 2.5. Monte Carlo simulation

Monte Carlo simulation (MCS) is a computational technique that relies on random sampling. It involves running simulations of a system or process multiple times, each time using different random inputs based on known probability distributions. By repeatedly sampling from these distributions, the technique generates a diverse set of scenarios, allowing to observe the behavior of the system. The randomness introduced through sampling is a key aspect of the method, enabling it to explore complex systems and handle situations with high uncertainty. MCS is widely used in various fields for both estimating outcomes and pure simulation purposes.

Multivariate MCS extends the basic approach to handle scenarios with multiple input variables. In many real-world scenarios, the behavior of a system depends not only on a single input but on multiple interrelated inputs. Multivariate MCS allows us to capture these dependencies and model the system more accurately.

The Cholesky decomposition is a technique used in multivariate MCS for efficiently generating correlated random samples. It is applied to the correlation matrix $R$ of the input variables, decomposing it in a lower triangular matrix $L$ and its transpose $L^T$, such that $R = LL^T$. The uncorrelated samples for each input variable are then generated from a known distribution, typically the multivariate standard normal distribution. Afterwards, the uncorrelated random samples are transformed by $L$ to obtain correlated random samples. The simulation model is run with the correlated samples following the required correlation structure. This method stands out for its computational efficiency and simple integration of the correlation structure into the simulated samples.

# 3

# Literature Review

In this chapter, the existing literature on electrical energy storage (EES) management is reviewed. A classification framework from previous literature is introduced in Section 3.1. After that, relevant papers are explained and discussed in Section 3.2. Finally, the literature gaps are identified, and the expected contributions of this thesis are stated in Section 3.3.

## 3.1. Classifying literature on EES management

Research on the management of EES systems has received more and more attention and covers many different directions. We start with explaining the framework presented in Weitzel & Glock (2018). They classify the literature on managing EES systems using a conceptual framework of three pillars: contextual characteristics, mathematical formulation, and optimization (Figure 3.1).

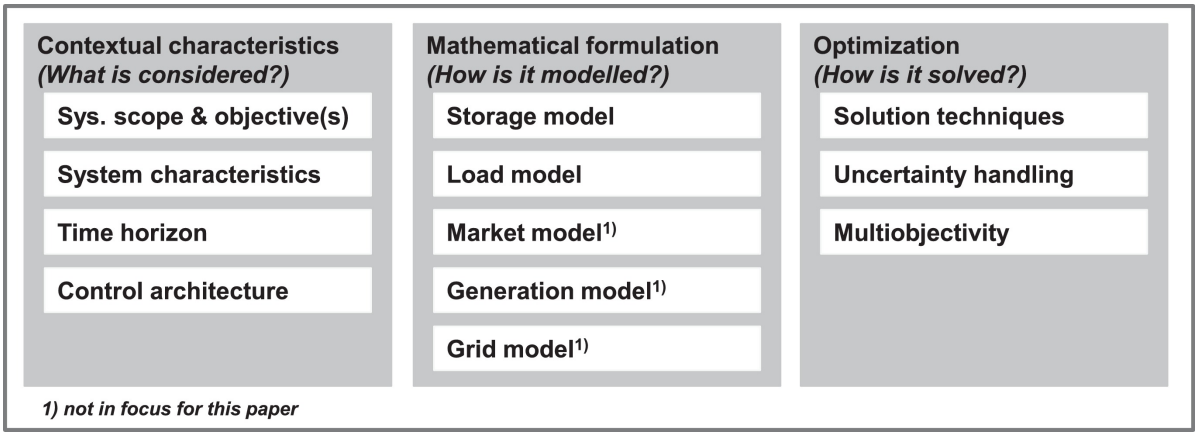


**Figure 3.1:** Conceptual framework of Weitzel & Glock (2018) to classify literature on managing EES systems.

**Contextual characteristics** This pillar answers the question *"What is considered?"*. The system scope defines the type of participants and their relations. This scope can be storage-only, including consumers and producers, or even a full microgrid. The objective is closely related to the system scope and can be economical, technical, environmental, consumption strategy, or a combination. Next, the type of storage system should be defined. Examples are pumped hydropower storage (PHS) and compressed air energy storage (CAES). The time horizon is another aspect of defining contextual characteristics. Storage management for a few hours or several days can be very different. The time horizon is mainly defined by including different electricity markets or their combination. Finally, the control architecture defines how different storage elements communicate. This architecture is relevant for a storage system with multiple participants.

**Mathematical formulation** This pillar answers the question *"How is it modeled?"*. The problem formulation can take different forms. The most basic form is a deterministic multi-period decision problem. This can be expanded by adding stochastic variables, or the linear formulation can become quadratic. Another form of problem formulation is a Markov decision process. It is an alternative sequential decision process formulation including uncertainty. Weitzel & Glock (2018) argue that most optimization problems mentioned, considered in their paper, are modeled as a mixed integer linear program (MILP). MILP is a way to model problems where some decision variables are required to take integer values while the objective function and constraints are linear. Moreover, all discussed papers include a model that represents storage capabilities. Depending on the contextual characteristics, load, market, generation, and grid models are added.

**Optimization** This pillar answers the question *"How is it solved?"*. The solution techniques discussed in Weitzel & Glock (2018) range from exact solution approaches to heuristics. They are mainly coupled to the mathematical formulations. For example, all MILP problem formulations considered in Weitzel & Glock (2018) are solved by a MILP solver, like CPLEX and Gurobi. The next component of this pillar is the handling of uncertainty. The main distinction is made between deterministic and stochastic modeling. Under stochastic modeling, many options are available. A final option to include in research is multi-objectivity, where the system follows multiple objectives at the same time. This component defines how it deals with multiple objectives.

## 3.2. Related works

In this section, an overview of related works is provided. Only papers with a stochastic programming formulation are discussed since other mathematical formulations are too different from this thesis' model formulation, discussed in Chapter 4.

Garcia-Gonzalez et al. (2008) investigate the combined optimization of a wind farm and a pumped-storage facility from the point of view of a generation company. It is modeled as a two-stage stochastic programming problem. The optimal bids for the day-ahead spot market are the *here-and-now* decisions and are not scenario-dependent. They form the first-stage decisions. The optimal operation of the facilities are the *recourse* variables and follow different scenarios. They are the second-stage decisions. The input/output hidden Markov model (IOHMM) approach generates hourly electricity price scenarios for the day-ahead market. A joint configuration is modeled and compared with an uncoordinated operation. They conclude that stochastic programming is an effective method to model decision-making and that a joint operation increases profit.

Kim et al. (2021) also propose a two-stage stochastic model for optimizing the operation of energy storage. The two model stages correspond to scheduling day-ahead and real-time charging and discharging. The energy storage operator is assumed to be a price-maker, and the prices are assumed to have a linear relation to the energy storage operations. The transactions scheduled in the day-ahead market are the *here-and-now* decisions. The transactions scheduled in the real-time markets are optimized for different scenarios of the real-time price and are, therefore, the *recourse* decisions. They conclude that in cases where market prices do not react to charging and discharging decisions and when energy storage can fully adjust its real-time operations relative to the day-ahead schedule, a stochastic modeling framework does not provide any added value.

Löhndorf et al. (2013) integrate a more complex model in which short-term intrastage decisions are integrated with long-term interstage decisions to optimize operations of a PHS system with multiple connected reservoirs. The operators participate in the wholesale electricity markets. The intrastage problem is formulated as a two-stage stochastic mixed-integer quadratic program. The first stage consists of fixing price-dependent bidding curves for the day-ahead market. The day-ahead prices are represented by 48 linear models, with regressors comprising gas price, temperature, wind power production, water inflow, and daily electricity demand. Realizations of the price process create a finite set of scenarios. Since the bidding curves should be set before the realizations of the market prices, the price points are fixed in advance. The second stage closes all positions using storage capacities from all the reservoirs and the intraday market. The intraday market prices are assumed to have a linear relation to the amount of electricity sold or purchased at the intraday market itself. They demonstrate the efficiency of the solution approach using a case study of an existing hydro storage system.

Qi et al. (2023) propose a two-stage stochastic optimization model to optimize a virtual power plant (VPP) portfolio, including generic energy storage. A virtual power plant is a system that aggregates distributed energy resources to optimize power generation, consumption, and grid stability. The VPP is assumed to be a price-taker and participates in the day-ahead and real-time balancing market. The day-ahead market price scenarios are generated from Nord Pool price data and clustered in representative scenarios using K-means. The first-stage decisions are the day-ahead offering strategies and the value at risk (VaR), independent of the scenarios. VaR is a measure to estimate the potential loss of an investment, including making more risk-averse decisions. The second stage decisions are varied with scenarios and are the balancing market decisions. For convenience, the balancing market prices are set relative to the day-ahead market prices.

Nease & Adams II (2014) implement a rolling horizon optimization strategy for an integrated solid-oxide fuel cell and a CAES plant. They divide the optimization process into intervals and formulate a mixed integer non-linear program for each interval. The objective function aims to achieve a trade-off between maximizing total revenue and improving overall load-following capabilities. Load-following capabilities allow a power plant to increase or decrease its output in real-time or near-real-time to match the changing electricity demand. The optimization process relies on forecasts for the electricity spot prices (no market is specified) and demand for each time interval over the optimization horizon. Only the uncertainty in the demand forecast is considered by adding measurement noise and generating scenarios using Monte Carlo simulation (MCS). Adding a rolling horizon to the optimization significantly reduces the sum-of-squared errors between the demand and supply profiles.

Another paper that applied the rolling horizon approach is from Klaas & Beck (2021). They implemented a MILP for revenue maximization of a CAES plant. The plant operators participate in the day-ahead market and the minute-reserve market, which is part of the balancing markets. The day-ahead price forecasts are captured in a simple model that simulates the uncertainty closely related to the actual day-ahead prices. They intentionally did not include a very advanced simulation method since it was not the objective of the research. The results of their analysis indicate that the operation of the storage plant, when approached economically, offers the potential for generating substantial revenues.

From the literature, it becomes clear that many different techniques are used to handle uncertainty in market prices. The discussed methods are the IOHMM, a linear relation to the energy storage operations, separate regression models for each hour, clustering methods to generate representative scenarios, point forecasts, or simple simulation models. Few papers employ a rolling horizon approach, which is valuable for adapting to incremental information in an uncertain environment. Moreover, we see that a combination of two markets is used in many studies. The day-ahead market is often used to plan the first-stage decisions, and the intraday or real-time market is used to adjust that planning in the second stage.

## 3.3. Literature gaps

To the best of our knowledge, the following gaps in the literature have been identified.

- The intraday market is not often used as a primary market to participate in storage decisions.
- The uncertainty in the intraday market price is not modeled to a large extent.
- Papers mainly focus on one storage technology instead of comparing multiple technologies.
- No study considers a case study of typical days. Either the information is incorporated in the regressors, or the type of day is left out of the research.

We aim to address all these literature gaps in our research. The storage operator only participates in the intraday market. Trades occur continuously on the intraday until the contract goes into delivery. Therefore, there is more flexibility in the scheduling problem. During the day, charging and discharging decisions can be adjusted, given fluctuations in the price. Historical correlation is incorporated into the sampling models to handle the uncertainty from the intraday market prices. The literature shows that multiple storage technologies are integrated, e.g., in a microgrid or a VPP. However, in this thesis, different individual EES systems are compared. Therefore, it is possible to conclude which storage technologies are suitable for operating using the intraday market. Finally, a case study is introduced to compare typical days.

# 4

# Model Formulation

The aim of this thesis is to develop a model that optimizes the profit for a storage operator participating in the intraday market. In this chapter, the model necessary to answer the research questions is formulated. First, the objective function of this problem is presented in Section 4.1. After that, the corresponding constraints of the storage technology are explained in Section 4.2. We refer to this as the storage model.

## 4.1. Objective function

To create a profit maximization model for a storage operator, it is essential to have a mathematical representation of the intraday market. While we introduced this market in Section 2.2.3, we now formalize it mathematically. For this thesis, we consider hourly trading intervals exclusively, which means we have a price for all 24 hours of the day. Given the continuous nature of the intraday market, the market establishes prices based on supply and demand for all hourly intervals. We assume the storage operator is a price taker in the intraday market, and therefore, participation in the market has no effect on the market prices. The storage operator's objective is to maximize its revenue over the time horizon $\mathcal{T} = 24$. Therefore, the time set $T = \{1, ..., \mathcal{T}\}$ represents the next day and the time step $\Delta t$ is one hour.

We represent the prices of all contracts in the vector $P = (p_1, p_2, ..., p_{\mathcal{T}})$. For each price $p_t$ in $P$, we associate it with a specific time $i$ at which the price $p_t$ is observed. To simplify our model, we consider that $i$ belongs to the set $I = T$, which represents hourly intervals. We call $i$ the solution step of the problem. Consequently, $p_t^i$ denotes the price observed at time $i$ for the intraday market at time $t$. It is important to note that there is no price $p_t^i$ for $t < i$, as the market does not provide prices for past hours. When all $p_t^i$ values are known in advance, making optimal charging and discharging decisions becomes straightforward. For each solution step $i$, a decision must be made for all $t \in \{i, ..., \mathcal{T}\}$ regarding whether to charge or discharge based on the current intraday price $p_t^i$.

We define the revenue, denoted as $\mathcal{R}$, generated from operating the storage on the intraday market for one day. We compute a double summation to calculate this revenue, considering all solution steps $i \in T$ and remaining times $t \in \{i, ..., \mathcal{T}\}$. Specifically, it is defined as the product of the intraday market price $p_t^i$ at time $i$ for time $t$, and the difference between the scheduled discharging amount $d_t^i$ for solution step $i$ at time $t$, and the scheduled charging amount $c_t^i$ for solution step $i$ at time $t$. Coherently to the intraday market price $p_t^i$, the charging amount $c_t^i$ and discharging amount $d_t^i$ are defined for each solution step $i$ and all $t \in \{i, ..., \mathcal{T}\}$. The objective function (4.1) is now defined as follows:

$$\max \mathcal{R} := \sum_{i=1}^{\mathcal{T}} \sum_{t=i}^{\mathcal{T}} p_t^i (d_t^i - c_t^i). \tag{4.1}$$

In the next section, we introduce the constraints that define the storage model that restricts the charging and discharging decisions based on the limitations imposed by the storage technology.

## 4.2. Constraints

The storage model should represent the electrical energy storage (EES) capabilities. Sioshansi et al. (2021) define the minimum that should be included in EES modeling. Their definition is centered around the State of Charge (SoC) of storage, which indicates the energy level stored in the system at a given time. We have extended the model by adding the time $i$ at which the SoC is observed. It is defined for all $i \in T$ and all $t \in \{i, ..., \mathcal{T}\}$. Therefore, the $SoC_t^i$ is the amount of electrical energy held in the storage at time $t$ based on the cumulative charging and discharging decisions up to time $i$. It is defined by adding the charging amounts of all solution steps up to the current step $i$, $\sum_{j=1}^{i} c_t^j$, to the SoC at time $t-1$ based on the charging and discharging decisions up to time $i$, and subtracting the discharging amounts of all solution steps up to time $i$, $\sum_{j=1}^{i} d_t^j$. We set the initial SoC at a given level, i.e., $SoC_0^0$. This is an input parameter to the problem.

Three efficiencies are taken into account: the use-independent loss rate $\eta_s \in [0, 1)$, the charging efficiency $\eta_c \in (0, 1]$, and the discharging efficiency $\eta_d \in (0, 1]$. The first indicates the rate at which stored electrical energy is lost over time, without considering the system's charge and discharge cycles. The second represents the percentage of the energy effectively stored in a storage system during the charging process. It should be multiplied by the charging amount $c_t^i$ to account for the fact that not all the energy you put into the system during charging gets stored. For discharging, it is the percentage of energy obtained from the system when it is discharged. The scheduled discharging amount $d_t^i$ should be divided by $\eta_d$ to take into account that not all the stored energy is retrievable. This ensures that the discharging amount accurately reflects the usable energy. Equations (4.2) and (4.3) define the SoC at time $t$ based on the decisions up to time $i$.

$$SoC_{i-1}^i = SoC_{i-1}^{i-1}, \qquad \forall i \in T \tag{4.2}$$

$$SoC_t^i = (1-\eta_s) SoC_{t-1}^i + \eta_c \sum_{j=1}^{i} c_t^j - \frac{\sum_{j=1}^{i} d_t^j}{\eta_d}, \quad \forall i \in T,\ \forall t \in \{i, ..., \mathcal{T}\} \tag{4.3}$$

$$SoC^{min} \leq SoC_t^i \leq SoC^{max}, \qquad \forall i \in T,\ \forall t \in \{i, ..., \mathcal{T}\} \tag{4.4}$$

$$0 \leq \sum_{j=1}^{i} c_t^j \leq C^{max} y_t^i, \qquad \forall i \in T,\ \forall t \in \{i, ..., \mathcal{T}\} \tag{4.5}$$

$$0 \leq \sum_{j=1}^{i} d_t^j \leq D^{max}(1 - y_t^i), \qquad \forall i \in T,\ \forall t \in \{i, ..., \mathcal{T}\} \tag{4.6}$$

$$SoC_{\mathcal{T}}^i = SoC_{end} \qquad \forall i \in T \tag{4.7}$$

$$y_t^i \in \{0, 1\}, \qquad \forall i \in T,\ \forall t \in \{i, ..., \mathcal{T}\} \tag{4.8}$$

Constraints (4.4)–(4.8) define the energy storage capacity limits of the SoC and the charging and discharging power limits per time step. $SoC^{min}$ and $SoC^{max}$ represent the lower and upper bounds of the storage capacity. $C^{max}$ and $D^{max}$ indicate the charging and discharging power limits per time step, respectively. The sums $\sum_{j=1}^{i} c_t^j$ and $\sum_{j=1}^{i} d_t^j$ aggregate over all solution steps up to step $i$, ensuring that cumulative power constraints are satisfied as we progress through each solution step. While these sums must adhere to nonnegativity constraints, the hourly decisions, represented by $c_t^j$ and $d_t^j$, may have negative values, allowing for reversing a positive decision made in a previous step.

This flexibility implies the potential to undo previously made charging and discharging decisions in future steps. In such cases, even though trading on storage is feasible, it does not have to result in using stored electricity. The actual electricity utilization from the storage may not occur, and the effective SoC might remain the same. However, profits can be generated without necessarily affecting the effective SoC. These profits are achieved through the strategic scheduling of charging and discharging decisions and the ability to make adjustments before the final delivery of electricity.

Moreover, the SoC at the final time step $\mathcal{T}$ is fixed at $SoC_{end}$ in Constraint (4.7) to mitigate the end-value problem, which typically involves an empty SoC at the final time step. For each $i \in T$ and $t \geq i$, a binary variable, $y_t^i$, is added to Constraints (4.5) and (4.6) to ensure that charging and discharging do not occur simultaneously. When $y_t^i = 1$, the system is charging at time $t$ based on decisions up to solution step $i$; for $y_t^i = 0$, the system discharges at time $t$ based on decisions up to solution step $i$.

In this thesis, it is chosen to express these storage-defining parameters and the SoC in percentages of the total capacities. For example, $SoC_5^i = 0.7$ indicates a SoC of 70 percent at the end of time period 5 for solution step $i$. Moreover, a charging power limit of $C^{max} = 0.25$ implies that in one time step $\Delta t$ the storage can be charged with 25 percent of the full capacity, and it takes 4 time steps to completely charge the storage (without taking the efficiency losses into account). The power limit is the inverse of the energy-to-power ratio, explained in Chapter 2.

# 5

# Solution Methods

In this chapter, the solution methods for the problem formalized in Chapter 4 are provided. Since prices are not available ahead of time, we have to find a suitable approach. We combine two-stage stochastic programming with a rolling horizon approach. The objective function and constraints of each solution step are presented in Section 5.1. Afterwards, the rolling horizon approach is explained in Section 5.2. Finally, in Section 5.3, the handling of the uncertainty of the intraday market prices is explained, and the applied simulation method is provided.

## 5.1. Two-stage stochastic programming

Since the prices $p_t^i$ are not known in advance, we cannot solve the problem formulated in Chapter 4 at once. Instead, we adapt to the situation where the prices $p_t^i$ for each solution step $i$ become available during the day at their respective observed times $i$. Therefore, we treat the market prices as uncertain variables, considering all 24 contracts' prices as random variables. To address this uncertainty, we implement a two-stage stochastic programming model along with a rolling horizon solution method. In this section, we define the objective function and constraints for each solution step within the rolling horizon approach.

For every solution step, a separate optimization problem is formulated as a two-stage stochastic program. In the first stage, we make deterministic hourly charging and discharging decisions based on the current intraday market price. These decisions are established without prior knowledge of future price scenarios and are referred to as *here-and-now* decisions. The second-stage decision variables adjust the charging and discharging quantities of the first stage in reaction to possible price fluctuations. These price fluctuations are presented in the price scenarios. An adjusted charging or discharging decision is associated with each price scenario. We call them the *recourse* decisions.

**Objective function** Each solution step in the rolling horizon approach optimizes over a new objective function. This objective function is the revenue from solution step $i$, $\mathcal{R}^i$, and is maximized so that the storage operator is profit-driven. It is the sum of the profit from the first-stage decisions and the expected profit of the second-stage decisions. We define for each time $i$, $c_t^{1,i}$ as the amount of electricity bought in the market scheduled to be charged at time $t$, and $d_t^{1,i}$ as the amount sold to the market scheduled to be discharged at time $t$. These variables represent the first-stage decision variables of the stochastic optimization problem and are executed against the current intraday market price $p_t^i$.

Moreover, we have a set of random events $\Omega$, which we call the scenarios. Each scenario, $\omega$, represents another price path for the intraday market at time $t$, $p_t^\omega$. We assume a finite cardinality $|\Omega| = S$. Each scenario $\omega \in \Omega$ occurs with a probability $\phi^{\omega,i}$, where the probability depends on the solution step $i$. We require $\sum_{\omega\in\Omega} \phi^{\omega,i} = 1$ for each time $i$. We need to maximize the expected value over all scenarios. $\Delta c_t^{2,\omega,i}$ and $\Delta d_t^{2,\omega,i}$ are the adjustment amounts charged and discharged in solution step $i$ when using the intraday market in scenario $\omega$ and for time $t$. These decision variables are scenario dependent and represent the second-stage decision variables. The objective function for solution step $i$ is provided below.

$$\max \mathcal{R}^i \tag{5.1}$$

$$\mathcal{R}^i := \sum_{t=i}^{\mathcal{T}} p_t^i (d_t^{1,i} - c_t^{1,i}) + \sum_{\omega \in \Omega} \sum_{t=i+1}^{\mathcal{T}} \phi^{\omega,i} \left[ p_t^{\omega} (\Delta d_t^{2,\omega,i} - \Delta c_t^{2,\omega,i}) \right] \tag{5.2}$$

The second stage starts at $t = i + 1$, as the first-stage decisions have already been executed in the market before the realization of $p_t^{\omega}$. By this point, the contract of time $t = i$ has transitioned to the delivery phase, and no further adjustments for that time are possible. As a result, planning for the second stage to start at $t = i$ would be unnecessary, as the second-stage decisions cannot be implemented anymore.

**Constraints** Constraints (5.3)–(5.16) are an extension of the storage model of Section 4.2 to include the two-stage paradigm and the rolling horizon approach and still comply with the physical limits of the storage. Now, the charging and discharging decisions have initial levels for each time $t \in \{i, ..., \mathcal{T}\}$, $C_t^{0,i}$ and $D_t^{0,i}$. They refer to amounts that already have been scheduled to be charged and discharged from the storage from previous solution steps. They are both nonnegative for all $t \in T$. Constraints (5.3)–(5.9) impose the charging limits of the SoC and the power limits for charging and discharging decisions for the first stage. In Constraint (5.4), $SoC_t^{1,i}$ represents the first-stage SoC for solution step $i$ at time $t$. We set the initial level $SoC_{i-1}^{1,i}$ at a fixed level $SoC^{0,i}$ in Constraint (5.3). For $i = 1$, this is an input parameter to the system. For $i > 1$, it is explained in Section 5.2 how each $SoC^{0,i}$ is defined.

It is important to note that each charging decision $c_t^{1,i}$ may have a negative value. However, the only requirement, set in Constraint (5.6), is that the sum of $C_t^{0,i}$ and $c_t^{1,i}$ must be greater than or equal to zero. This sum represents the cumulative charging decisions up to solution step $i$. This implies that, over the rolling horizon, charging decisions made at certain times can be reversed by negative charging decisions in subsequent solution steps. The same principle, stated in Constraint (5.7), applies to discharging decisions $d_t^{1,i}$ which can also take on negative values, but the cumulative discharging for each time $t$ must remain nonnegative. To maintain operational feasibility, we introduce first-stage binary variables $y_t^{1,i}$, defined in Constraint (5.9), to prevent simultaneous charging and discharging. Specifically, for each solution step $i$, $y_t^{1,i} = 1$ indicates charging at time $t$, while $y_t^{1,i} = 0$ indicates discharging at time $t$. This, in conjunction with the flexibility to reverse charging and discharging actions in subsequent solution steps, allows for a transition from charging to discharging and vice versa from one solution step to the next. Moreover, as explained in Section 4.2, the SoC at the final time step $\mathcal{T}$ is fixed at $SoC_{end}$ in Constraint (5.8).

Next, we define in Constraints (5.10)–(5.16) the charging and discharging limits for the intraday adjustment decisions. In Constraint (5.11), $SoC_t^{2,\omega,i}$ indicates the SoC at time $t$, for scenario $\omega$, and in solution step $i$. Note that the constraints for the second stage start at $t = i + 1$ for similar reasons as explained for the objective function. In Constraint (5.10), the initial level $SoC_i^{2,\omega,i}$ is set at $SoC_i^1$ since there are no second-stage decisions for $t = i$. That means we start to calculate $SoC_t^{2,\omega,i}$ at the first-stage decisions of $t = i$.

As for the first-stage constraints, the second-stage decisions $\Delta c_t^{2,\omega,i}$ and $\Delta d_t^{2,\omega,i}$ can have negative values, but the sum of all charging and discharging decisions for each time $t$ should be nonnegative, as enforced by Constraints (5.13) and (5.14). Again, binary variables $y_t^{2,\omega,i}$, defined in Constraint (5.16), are added to prevent the storage from charging and discharging simultaneously. When $y_t^{2,\omega,i} = 1$, it indicates the storage is charging at time $t$ and for scenario $\omega$, whereas $y_t^{2,\omega,i} = 0$ indicates the storage is discharging at time $t$ and for scenario $\omega$. Using the same rationale as mentioned earlier, this allows for the possibility of flipping a charging decision for a given time $t$ into a discharging decision for that same time in the subsequent solution step. This flexibility enables dynamic adjustments in the charging and discharging strategies over the course of the optimization process. Finally, the SoC at the final time step $\mathcal{T}$ is fixed at $SoC_{end}$ for all $\omega \in \Omega$ in Constraint (5.15). For this thesis, $\eta_s$ is omitted since this loss is negligible on an hourly time interval (Fajinmi et al., 2023).

$$SoC_{i-1}^{1,i} = SoC^{0,i} \tag{5.3}$$

$$SoC_t^{1,i} = SoC_{t-1}^{1,i} + \eta_c(C_t^{0,i} + c_t^{1,i}) - \frac{(D_t^{0,i} + d_t^{1,i})}{\eta_d}, \ \forall t \in \{i, ..., \mathcal{T}\} \tag{5.4}$$

$$SoC^{\min} \leq SoC_t^{1,i} \leq SoC^{max}, \qquad \forall t \in \{i, ..., \mathcal{T}\} \tag{5.5}$$

$$0 \leq C_t^{0,i} + c_t^{1,i} \leq C^{max} y_t^{1,i}, \qquad \forall t \in \{i, ..., \mathcal{T}\} \tag{5.6}$$

$$0 \leq D_t^{0,i} + d_t^{1,i} \leq D^{max}(1 - y_t^{1,i}), \qquad \forall t \in \{i, ..., \mathcal{T}\} \tag{5.7}$$

$$SoC_{\mathcal{T}}^{1,i} = SoC_{end} \tag{5.8}$$

$$y_t^{1,i} \in \{0, 1\}, \qquad \forall t \in \{i, ..., \mathcal{T}\} \tag{5.9}$$

$$SoC_i^{2,\omega,i} = SoC_i^{1,i} \qquad \forall \omega \in \Omega \tag{5.10}$$

$$SoC_t^{2,\omega,i} = SoC_{t-1}^{2,\omega,i} + \eta_c(C_t^{0,i} + c_t^{1,i} + \Delta c_t^{2,\omega,i}) - \frac{(D_t^{0,i} + d_t^{1,i} + \Delta d_t^{2,\omega,i})}{\eta_d}, \ \forall t \in \{i+1, ..., \mathcal{T}\}, \ \forall \omega \in \Omega \tag{5.11}$$

$$SoC^{min} \leq SoC_t^{2,\omega,i} \leq SoC^{max}, \qquad \forall t \in \{i+1, ..., \mathcal{T}\}, \ \forall \omega \in \Omega \tag{5.12}$$

$$0 \leq C_t^{0,i} + c_t^{1,i} + \Delta c_t^{2,\omega,i} \leq C^{max} y_t^{2,\omega,i}, \qquad \forall t \in \{i+1, ..., \mathcal{T}\}, \ \forall \omega \in \Omega \tag{5.13}$$

$$0 \leq D_t^{0,i} + d_t^{1,i} + \Delta d_t^{2,\omega,i} \leq D^{max}(1 - y_t^{2,\omega,i}), \qquad \forall t \in \{i+1, ..., \mathcal{T}\}, \ \forall \omega \in \Omega \tag{5.14}$$

$$SoC_{\mathcal{T}}^{2,\omega,i} = SoC_{end}, \qquad \forall \omega \in \Omega \tag{5.15}$$

$$y_t^{2,\omega,i} \in \{0, 1\}, \qquad \forall t \in \{i+1, ..., \mathcal{T}\}, \ \forall \omega \in \Omega \tag{5.16}$$

## 5.2. Rolling horizon

A rolling horizon approach is introduced to iteratively solve the optimization problem, wherein the planning interval is incrementally moved forward in time for each solution step. This approach is added since we do not know each price $p_t^i$ in advance, but only when we move forward in time. The times when the prices $p_t^i$ are observed align with the solution steps and are indexed as $i \in I$, where $I = T$. This chosen solution approach allows us to adjust our planning throughout the day dynamically. For the first solution step, we execute the first-stage charging and discharging plan for all 24 hours of the next day. That means we buy and sell the scheduled amounts in the intraday market. The decisions for the first planning hour are final when the first hour has passed. No further adjustments are possible after it has gone into the delivery phase. However, altering the remaining hours' decisions is possible until they go into delivery. Therefore, only the decisions for time $t = i$ are final in each solution step $i$.

After each solution step, the constraints are updated, taking into account the executed decisions from the previous solution step. These executed decisions affect the flexibility of the current stage decisions. The previous solution sets the $SoC^{0,i}$, where $i$ indicates the solution step it is entering. For solution step $i$, it is updated as follows:

$$SoC^{0,i} := SoC_{i-1}^{1,i-1}, \ \ \forall i > 1 \tag{5.17}$$

Moreover, the $C_t^{0,i}$ and $D_t^{0,i}$ should be updated for the next solution step. It is the sum of the previous initial charging and discharging decisions and the previously executed market decisions from the first-stage decisions. For the first solution step $i = 1$, we set $C_t^{0,1}$ and $D_t^{0,1}$ at a fixed level, which describe the planning before the day has started. Find below the formulas for solution steps $i > 1$.

$$C_t^{0,i} := C_t^{0,i-1} + c_t^{1,i-1}, \ \ \forall t \in \{i, ..., \mathcal{T}\} \tag{5.18}$$

$$D_t^{0,i} := D_t^{0,i-1} + d_t^{1,i-1}, \ \ \forall t \in \{i, ..., \mathcal{T}\} \tag{5.19}$$

## 5.3. Construction intraday price scenarios

We use Monte Carlo simulation (MCS) to generate the price scenarios for the intraday market. We have 24 different contracts on the intraday, each price being set by the market's current supply and

demand behavior. We represent the prices of all contracts in the multivariate random variable $P = (p_1, p_2, ..., p_{24})$. For each $p_t$ in $P$, we define its deviation from the day-ahead (DA) spot price $p_t^{DA}$, i.e.

$$\Delta p_t = p_t - p_t^{DA}, \tag{5.20}$$

where the mean $\mu_t$ of $\Delta p_t$ becomes

$$\mu_t = \mathbb{E}[\Delta p_t] = \mathbb{E}[p_t - p_t^{\mathrm{DA}}], \tag{5.21}$$

and standard deviation $\sigma_t$ of $\Delta p_t$

$$\sigma_t = \sqrt{\mathbb{E}[(\Delta p_t - \mu_t)^2]}. \tag{5.22}$$

Since the prices in $P$ are correlated, we need to define the correlation matrix $R$ where

$$R_{s,t} = \frac{\mathbb{E}\big[(\Delta p_s - \mu_s)(\Delta p_t - \mu_t)\big]}{\sigma_s \sigma_t}, \quad \forall s, t \in T. \tag{5.23}$$

For each hourly contract $p_t$, $S$ random values are required to simulate $S$ price scenarios. These random draws from the normal distribution are denoted as $Z_t^\omega$ for $t \in T$ and $\omega \in \Omega$. We have $Z_t^\omega \sim N(\mu_t, \sigma_t)$ for all $t \in T$. Taking the DA price $p_t^{\mathrm{DA}}$ as a starting point, we create through basic MCS the following price scenarios:

$$p_t^\omega = p_t^{DA} + Z_t^\omega. \tag{5.24}$$

To incorporate the correlation among different hours, we adopt the Cholesky decomposition method. This technique involves decomposing the correlation matrix $R$ into the product of a lower triangular matrix $L$ and its transpose $L^T$, denoted as $R = LL^T$. By applying the transformation using matrix $L$ to the uncorrelated variables $Z$, we create correlated variables $Y$. The revised formulation for the Monte Carlo simulation is as follows:

$$p_t^\omega = p_t^{DA} + Y_t^\omega. \tag{5.25}$$

Here, $Y_t^\omega = \sum_{j=1}^{T} L_{t,j} Z_j^\omega$ for $t \in T$.

The price scenarios represent the second-stage intraday prices. They are independent of solution step $i$. The first-stage price is determined by randomly selecting a scenario from the set of price scenarios and adding a random term to account for the inherent uncertainty in predicting future prices. This first-stage price, denoted as $p_t^i$, reflects the current intraday market price. As we progress through each solution step, a new price is selected randomly from the available price scenarios. This dynamic process represents how the market's prices change over time and can be formally defined as:

$$p_t^i = p_t^\omega + \lambda \epsilon_t, \quad \forall t \in \{i, ..., \mathcal{T}\}. \tag{5.26}$$

In Equation (5.26), $p_t^i$ represents the intraday price at solution step $i$ for time $t$, $p_t^\omega$ represents the price based on a randomly chosen scenario, $\lambda$ is a scaling factor, and $\epsilon_t$ is a random value drawn from a standard normal distribution. Introducing the scaling factor $\lambda$ is to incorporate noise that reflects prediction errors. This factor ensures that the introduced noise does not deviate significantly from the magnitude of the randomly chosen price scenario, thereby minimizing the risk of $p_t^i$ resembling another price scenario. We define $\lambda$ as

$$\lambda = \frac{\max_{t,\omega}(p_t^\omega) - \min_{t,\omega}(p_t^\omega)}{S}. \tag{5.27}$$

In Equation (5.27), $\max_{t,\omega}(p_t^\omega)$ and $\min_{t,\omega}(p_t^\omega)$ represent the maximum and minimum price across all available scenarios and all times, and $S$ is the number of scenarios.

To enhance the stochastic optimization, we calculate probabilities using quadratic distances, denoted as $d^{\omega,i}$, between the first-stage price and the scenario prices. These probabilities are recalculated at each solution step to accommodate the evolving first-stage price. The objective is to assign greater

probability to scenarios closely aligning with the current first-stage price, amplified by the choice of squared distances. The calculation of these probabilities is as follows:

$$\phi^{\omega,i} = \frac{1/d^{\omega,i}}{\sum_{\omega\in\Omega}(1/d^{\omega,i})}, \quad \forall i \in T,\ \forall \omega \in \Omega, \tag{5.28}$$

where

$$d^{\omega,i} = \sum_{t=i}^{\mathcal{T}} \left(p_t^{\omega} - p_t^{i}\right)^2, \quad \forall i \in T,\ \forall \omega \in \Omega. \tag{5.29}$$

In Equation (5.28), the probabilities are normalized so that they sum up to one.

# 6 Data

In this chapter, the data that form the foundation of our case study is presented. We start in Section 6.1 by providing an overview of the case study and explain how it is divided into four cases that represent typical days. In Section 6.2, we match the typical days with the available day-ahead (DA) and intraday (ID) trading data to retrieve historical price information. Furthermore, we conduct a descriptive analysis for both DA and ID price distributions, providing valuable insights into the data. Finally, we discuss the input parameters crucial to our optimization problem in Section 6.3.

## 6.1. Selection typical days

In this section, we explain the selection process of the typical days that share comparable characteristics. Given the substantial influence of demand, weather conditions, and neighboring countries' transmission on the DA and ID market price behavior, we refer to these features as the fundamentals. For our case study, we have collected fundamental data from Germany and other European countries, covering the period from June 29, 2019 to August 7, 2023, resulting in 1501 days. All weather-related data are converted into power metrics, expressed in megawatts (MW), to ensure consistency in our analysis. These metrics represent the amount of power generated by weather-dependent sources. They reflect the influence of weather on energy dynamics. This data is provided by Northpool.

Firstly, we partition all data into four sets, each corresponding to a season and distinguishing between weekends and weekdays. These sets consist of the following: spring weekend data, summer weekday data, autumn weekday data, and winter weekday data. From each set, a group of typical days is selected using K-means clustering. We use the elbow method to determine the optimal number of clusters (K) for this process. The elbow method calculates the within-cluster sum of square (WCSS), which measures the sum of squared distances between data points within a cluster and their respective cluster center. By analyzing the WCSS graph, we identify the best K value for K-means clustering. This clustering aims to capture specific characteristics from the fundamentals for each set. The clustering relies on the following ten fundamentals present in our data set. They play a crucial role in understanding the interplay between electricity demand, weather conditions, and the dynamics of electricity prices.

1. German electricity demand
2. German hydroelectric generation (run of river)
3. German solar photovoltaic generation
4. German offshore wind generation
5. German onshore wind generation,
6. German total renewable generation
7. German residual load
8. Central Western Europe (CWE) residual load (including Germany, France, Belgium, and the Netherlands)
9. Scandinavian residual load (including Denmark, Norway, and Sweden)

10. European residual load (adding Austria, Switzerland, UK, Spain, Portugal, and Italy)

The first fundamental is the daily German electricity demand. The second fundamental refers to the electricity generated by hydroelectric power plants in Germany that are primarily driven by the natural flow of rivers. The third fundamental is the total German solar photovoltaic generation, i.e., generation from solar panels. Fundamentals 4 and 5 refer to wind power generation, offshore and onshore, respectively. In 2022, wind energy remained the leading contributor to German electricity production, exceeding brown coal and other energy sources (Bundesverband WindEnergie, 2022). The sixth fundamental is the total renewable generation for Germany, adding biomass. The term residual load refers to the difference between electricity demand and the available generation from renewable energy sources. In other words, it is the amount of electricity needed by conventional power sources (such as fossil fuels or nuclear) to meet the remaining demand after accounting for the contribution from renewables like wind, solar, and hydropower. Fundamentals 7 to 10 represent the total residual loads per indicated area.

The chosen clusters and their corresponding cluster centers can be found in Table 6.1. We have identified four clusters. The clusters contain 59 days for Spring Weekend, 133 days for Stormy Summer, 123 days for Cloudy Autumn, and 126 days for Windy Winter.

**Table 6.1:** Cluster centers of chosen clusters representing Spring Weekend, Stormy Summer, Cloudy Autumn, and Windy Winter.

| Fundamentals | Spring Weekend | Stormy Summer | Cloudy Autumn | Windy Winter |
|---|---|---|---|---|
| German demand | 46020MW | 56938MW | 64026MW | 63323MW |
| German hydro | 1603MW | 1705MW | 1219MW | 1304MW |
| German solar pv | 9603MW | 8232MW | 1774MW | 3420MW |
| German offshore wind | 2598MW | 3033MW | 2760MW | 4511MW |
| German onshore wind | 10995MW | 11505MW | 8182MW | 23301MW |
| German total renewable | 24800MW | 24467MW | 13937MW | 32539MW |
| German residual load | 21220MW | 32470MW | 50089MW | 30783MW |
| CWE residual load | 58285MW | 76839MW | 120747MW | 90159MW |
| Scandinavian residual load | 12090MW | 11103MW | 20039MW | 17496MW |
| European residual load | 70653MW | 90412MW | 145496MW | 111861MW |

After filtering for spring weekend days, the K-means algorithm was applied for several values of K to select the optimal K value. For that optimal K, the K-means clustering was performed based on the fundamentals. The cluster with the highest renewable generation was chosen as the group of typical days for Spring Weekend. The cluster center indicates low demand due to the weekend and low residual load due to high renewable energy generation. This results in an expectation of market prices dropping below zero during the day.

Next, we focused on summer weekdays. After applying K-means clustering to this subset of the data using the optimal K value, we identified a cluster characterized by high wind energy generation along with significant solar photovoltaic generation. The days of this cluster were selected to represent our Stormy Summer case. These Stormy Summer days typically exhibit medium-to-high electricity demand, as indicated in Table 6.1. This can be explained by the cooling systems in buildings required for hot summer days. This choice of typical days allows us to research price patterns with strong wind and solar energy generation during the summer months.

The third case is based on autumn weekday data. The clustering method displayed one cluster with a low solar photovoltaic production. The corresponding days were chosen as our Cloudy Autumn case. Moreover, it can be seen in Table 6.1 that the cluster center has the lowest total renewable generation, resulting in a high residual load. Therefore, prices are expected to be higher for the trading data of these typical days.

The fourth and final data subset comprises winter weekdays. The K-means clustering identified a cluster characterized by high wind energy generation in this data set. This cluster exhibits the highest total renewable generation center, despite having the second-lowest solar photovoltaic generation. The cluster center for German electricity demand is also high, likely due to cold weather conditions during the winter months. This clustering resulted in a cluster representing the Windy Winter typical days.

## 6.2. DA and ID price data

In this section, we match the DA and ID price data with the corresponding typical days. To manage data volume, we focus exclusively on the price data from the year 2021. This year is chosen since, in 2019, the data only begins in June, and 2023 is still ongoing. This led us to consider 2020, 2021, and 2022 as the options for our analysis. We settled on 2021 due to its relative stability, making it the least impacted by external factors like the COVID-19 pandemic or the Russian invasion of Ukraine. The resulting lockdowns of the COVID-19 pandemic mainly caused the electricity demand to decrease. In 2021, although it still experienced COVID-19 lockdowns, the influence was less severe than in 2020. On the contrary, the Russian-Ukrainian war resulted in high gas prices, consequently driving up the overall market prices of electricity. Therefore, 2021 provides the most recent and relevant data for our case study. The DA data includes all auction results for the typical days for the German price area. This resulted in 8 trading days for Spring Weekend, 13 for Stormy Summer, 44 for Cloudy Autumn, and 21 for Windy Winter. Figure 6.1 shows the distribution of the DA price data. We observe distinct shapes and distributions throughout the day, highlighting the variability in market dynamics for each case.

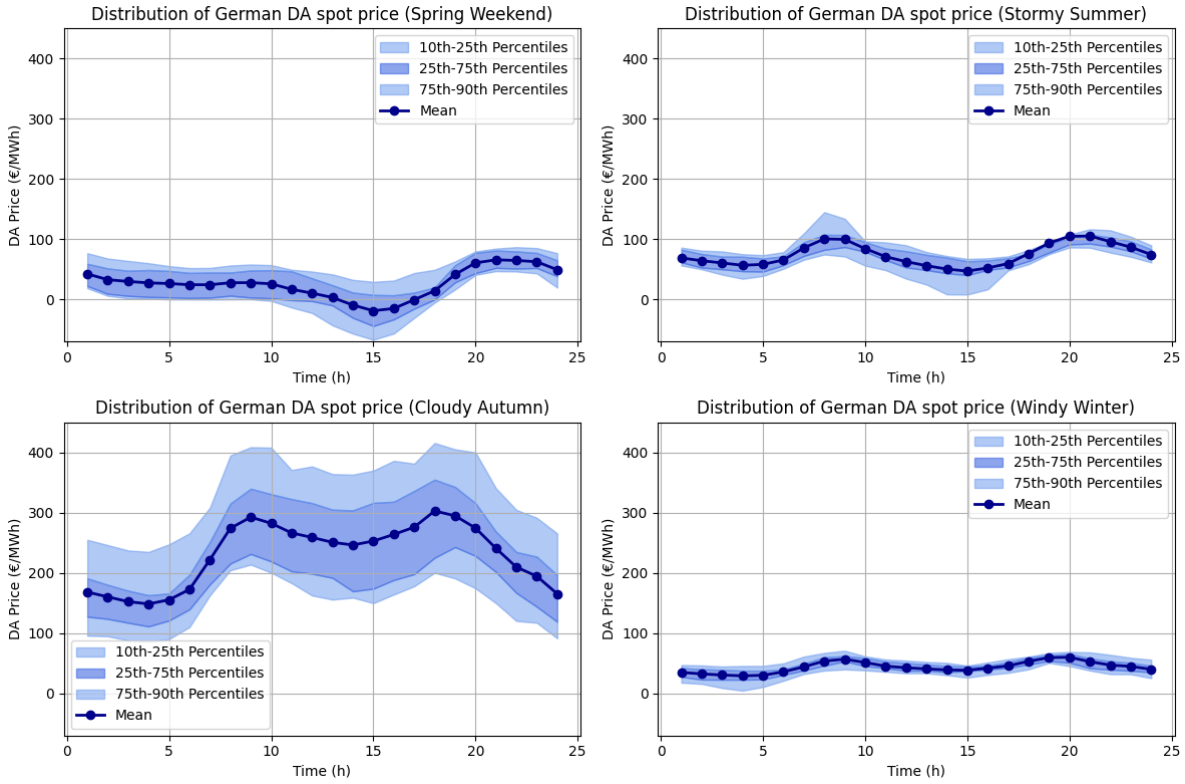


**Figure 6.1:** Distributions German DA spot price based on price data from 2021.

Firstly, the mean DA price in Spring Weekend drops below zero in the afternoon due to low demand and high renewable production (Table 6.1). This indicates that buyers in the market are essentially paid to consume electricity. In these hours, the spread between the maximum and minimum DA prices is more pronounced, indicating higher market uncertainty. Towards the end of the day, the spread gradually narrows, implying a more predictable pattern in DA prices. However, it is worth noting that the mean DA price increases towards €65/MWh in the evening. This upward trend is mainly attributed to decreased solar photovoltaic generation during the evening hours.

For the second, third, and fourth cases, we see a clear pattern with two peaks, which are often referred to as the shoulders. In electricity markets, the shoulders represent the two periods of the day with the highest electricity prices, typically occurring during the morning and evening when demand is relatively high but not at its peak. Moreover, renewable production is typically at a low level. These periods often have elevated prices due to increased residual load, and they are referred to as shoulders because they appear as peaks on a daily price curve. Moreover, the prices of Stormy Summer are

generally higher than in Spring Weekend due to a higher residual load.

An obvious observation from the DA price distribution of Cloudy Autumn is that the mean price is nearly three times as high as compared to the first two cases. During the peak hours, the mean price is around €300/MWh. This surge in prices can be attributed to the high residual load. As temperatures drop during autumn, there is typically an increase in electricity demand. However, due to the lack of sunlight and wind, the limited renewable energy production for this case fails to meet the heightened demand, resulting in a price hike.

Windy Winter has the most concentrated distribution compared to the other cases. It has a comparable demand (Table 6.1) as Cloudy Autumn, again caused by cold temperatures. However, offshore and onshore wind power generation are very high, leading to a lower residual load. Therefore, prices do not pass €100/MWh. In conclusion, these four cases underline the importance of considering all relevant factors together to comprehend the specific behaviors of electricity prices.

Next, we consider the ID price data. Since the ID market is continuous, all trades from the German ID market in 2021 are selected. This resulted in 664309 trades for Spring Weekend, 956915 trades for Stormy Summer, 3587884 trades for Cloudy Autumn, and 2100933 trades for Windy Winter. The variation in the number of trades is attributed to Spring Weekend having fewer trading days and Cloudy Autumn having the most. To analyze the deviation of the trades from the DA price, we subtracted all DA prices from the corresponding ID prices for the same delivery hour. Figure 6.2 provides an overview of the price differences through boxplots for each case.

It should be noted that the price deviation data in the boxplots aggregate values across all 24 hours of the day. On average, the price deviations of the ID trades are highest for Cloudy Autumn, with an average difference of approximately €4/MWh lower than the DA price across all 24 hours of the day. It shows the most significant spread, possibly due to the larger number of trades in its data set and a more extensive spread in the DA data. The large spread in DA indicates a broad range of price behavior, also affecting the ID market. This connection highlights how the diversity of prices in the DA market can propagate and influence the ID market. Conversely, Windy Winter displays the smallest spread, corresponding to the concentrated distribution of the DA price shown in Figure 6.1.

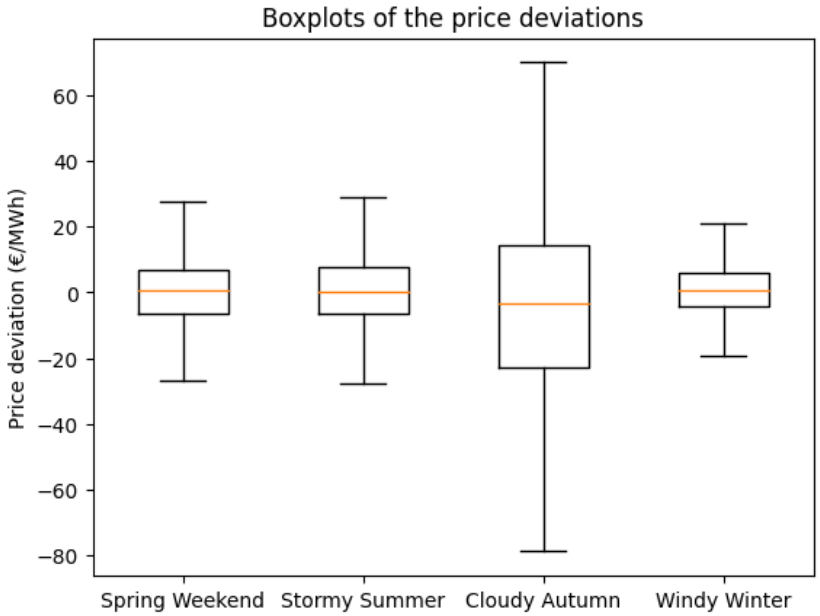


**Figure 6.2:** Boxplots of ID market trades subtracted by DA price based on price data from 2021.

We calculate the hourly means, standard deviations, and correlations from these price deviations. The values for all four cases are presented in Appendix A.1. These metrics provide more understanding of the price evolution during the day than the aggregated descriptive analysis. Following Equation (5.25), we generate price scenarios for all four cases. These scenarios are based on a single DA price as the starting point. In the next chapter, these scenarios serve as input for stochastic optimization and represent the ID price paths.

## 6.3. Input parameters

Table 6.2 presents the key parameters implemented in this thesis for three different energy storage technologies: PHS, CAES, and BESS. These parameters serve as inputs for modeling and analyzing the performance of these storage systems and are based on the examples of Section 2.1.

**Table 6.2:** Defining parameters for three storage technologies, PHS, CAES, and BESS.

| Storage technology | $\eta_c$ | $\eta_d$ | $SoC^{min}$ | $SoC^{max}$ | $C^{max}$ | $D^{max}$ |
|---|---|---|---|---|---|---|
| PHS | 0.85 | 0.85 | 0 | 1 | 0.125 | 0.125 |
| CAES | 0.60 | 0.80 | 0 | 1 | 0.60 | 0.60 |
| BESS | 0.95 | 0.95 | 0 | 0.9 | 1 | 1 |

It is important to note that the choices of these parameters represent averages and generalizations for each technology. In reality, the performance characteristics of energy storage systems can vary significantly based on various factors, including geographical location, system design, operational conditions, and technological advancements. For example, the efficiency of a PHS system may differ between mountainous regions and flat terrains due to variations in elevation and water availability. As for the capacities, storage capacity degradation over time can be influenced by factors like battery aging in BESS or sediment buildup in PHS.

Input parameters that are not related to any specific storage technology are explained next. We set the initial SoC level at 0.5. The final SoC level is also 0.5 for all $i$. This is chosen to prevent the system from being empty at the end of the day. All the initial levels of charging and discharging are set to 0 since no planning decisions have been made before our planning starts. Therefore, we have for $i = 1$:

$$SoC^{0,1} = 0.5 \tag{6.1}$$

$$SoC_{end} = 0.5 \tag{6.2}$$

$$C_t^{0,1} = 0, \quad \forall t \in T \tag{6.3}$$

$$D_t^{0,1} = 0, \quad \forall t \in T. \tag{6.4}$$

# 7

# Results

In this chapter, we present the results when using various optimization techniques. In Section 7.1, we determine the solution when using the DA prices to give the reader some insight into the problem and solutions. Secondly, in Section 7.2, the effect of the increase in the number of price scenarios is examined. Finally, in Section 7.3, we investigate the effects of incorporating rolling horizon and price uncertainty on the optimization results.

The optimization process is implemented in Python, utilizing the Jupyter Notebook interface, and solved using the commercial Gurobi MILP-solver. The computing environment is equipped with an Intel Core i7-1185G7 CPU running at 3.00GHz and 16 GB of RAM.

## 7.1. Deterministic solutions for DA prices

We begin our analysis by presenting deterministic optimization (DO) solutions. Compared to the stochastic optimization with a rolling horizon, explained in Chapter 5, the DO model formulation exclusively involves first-stage decision variables and is solved only for the first solution step, i.e., $i = 1$. Consequently, it incorporates only a single price input. For this section, the first-stage decisions are based on the DA price, and the resulting profits offer insights into the intrinsic value of storage for each case. Figure 7.1 shows the specific DA prices used to calculate these DO solutions.

In the Cloudy Autumn case, the highest DA prices are observed, and its price curve during the day is the most extreme. Consequently, we expect high profits for this case. While Stormy Summer and Windy Winter share a similar price trend, Stormy Summer prices are more elevated. In the Spring Weekend case, the price profile is interesting as prices drop below zero in the afternoon hours and rise afterwards to the highest price level of the day.

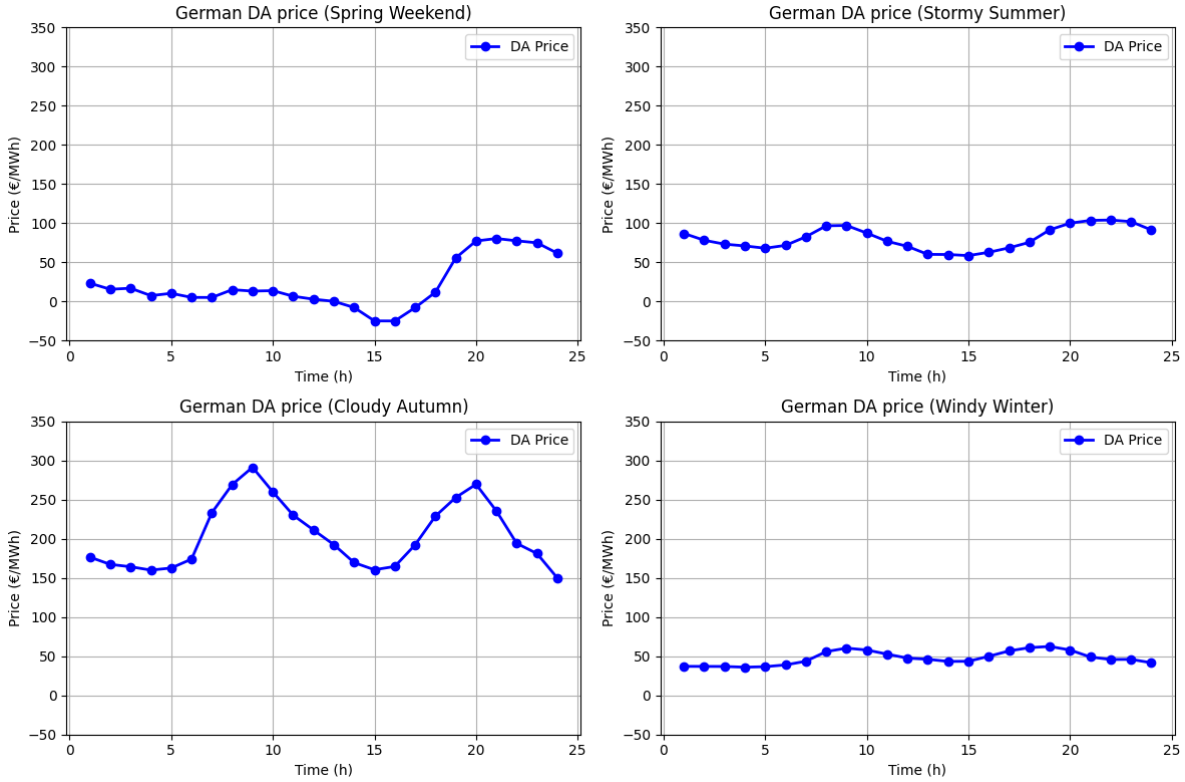


**Figure 7.1:** Hourly DA prices for DO. The exact dates are May 23, July 6, October 8, and February 19, 2021.

In Table 7.1, we present the profits obtained from selling and buying against the DA price for each storage technology and case. Notably, these profits are calculated per unit of storage capacity since we have defined the charging and discharging decisions as percentages of the total capacities. Therefore, we express the profit without a unit. Compressed air energy storage (CAES) proves to be the least profitable storage technology under these DA prices. It generates a profit only on the Spring Weekend day, which can be attributed to relatively low charging and discharging efficiencies. However, the profit of 77.68 for CAES on the Spring Weekend day exceeds the profit of 46.47 for pumped hydropower storage (PHS). This could be linked to PHS's low power limit per hour of 12.5 percent. In contrast, the highest profit of 181.36 is achieved using a battery energy storage system (BESS) on the Cloudy Autumn day. This outcome aligns with our expectations for two reasons. Firstly, BESS offers the most flexibility in charging and discharging, with minimal efficiency losses. Secondly, Cloudy Autumn has the most significant price differences, benefiting high profits.

**Table 7.1:** Profits of DO on DA market across all storage technologies and typical days.

| Storage technology | Spring Weekend | Stormy Summer | Cloudy Autumn | Windy Winter |
|---|---|---|---|---|
| PHS | 46.47 | 7.81 | 28.48 | 4.31 |
| CAES | 77.68 | 0 | 0 | 0 |
| BESS | 80.88 | 45.27 | 181.36 | 26.87 |

Figure 7.2 provides a detailed view of the DO solution for a BESS on a Cloudy Autumn day. The first plot out of four shows the BESS' charging decisions over time. The second plot displays the BESS' discharging decisions over the time. The third plot illustrates the corresponding profits and losses generated by the BESS based on its charging and discharging actions. Finally, the fourth plot presents the prices against which the charging and discharging decisions are executed, which coincides with Figure 7.1. We observe a clear pattern of charging at the lowest price levels and discharging at the price peaks.

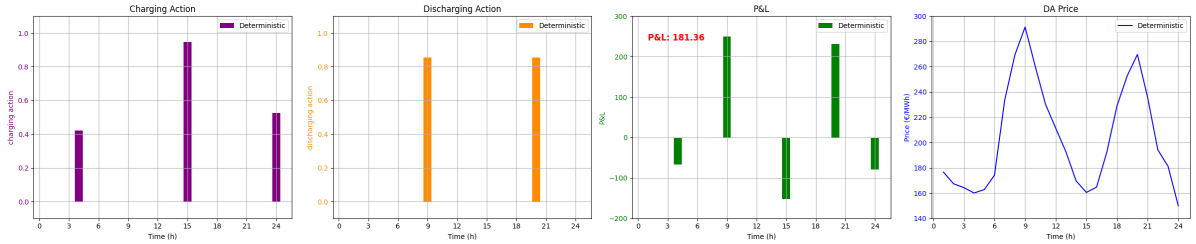


**Figure 7.2:** Optimal charging and discharging decisions, profits and losses, and DA price for DO for a BESS on October 8, 2021.

From Table 7.1, we make another observation: the Spring Weekend day yields the highest profits for PHS and CAES. This can be explained by the significant price fluctuations in the Spring Weekend price profile, which transitions from approximately €-20/MWh in the afternoon to around €80/MWh in the evening. Consequently, profits can be generated in both periods by charging at a negative price and discharging at a high positive price. An overview of how charging and discharging decisions are made throughout the day and the corresponding profits and losses resulting from these actions can be found in Figure 7.3 for PHS and Figure 7.4 for CAES. It becomes clear that the solution for CAES makes less charging and discharging actions due to higher charging and discharging power capacities.

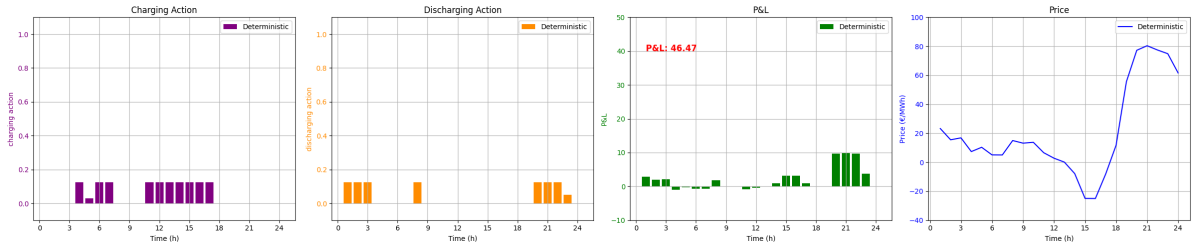


**Figure 7.3:** Optimal charging and discharging decisions, profits and losses, and DA price for DO for a PHS on May 23, 2021.

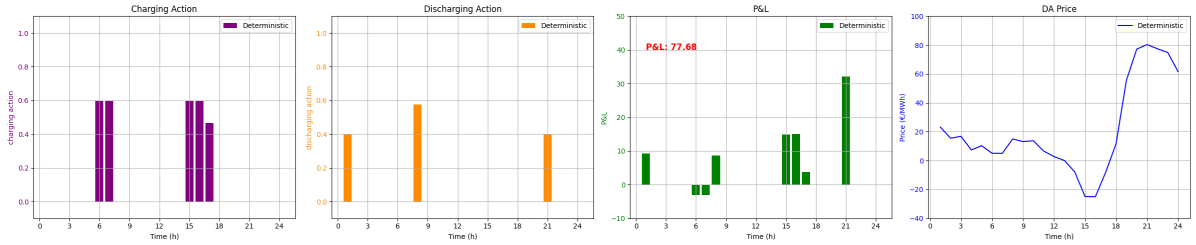


**Figure 7.4:** Optimal charging and discharging decisions, profits and losses, and DA price for DO for a CAES on May 23, 2021.

## 7.2. Varying the number of scenarios

In this section, we determine the number of scenarios we need for the second stage. We want to balance between ensuring an adequate number of price scenarios to provide valuable information to the model and maintaining a reasonable runtime for the calculations. We start with 50 price scenarios to ensure a quick runtime. However, this approach only partially captures the complexity of real-world conditions, where numerous price scenarios can unfold over a 24-hour day. To better align with reality, the number of scenarios is increased in this section.

Our analysis takes into account the maximum runtime for a single solution step. It is crucial to note that the first-stage decisions rely on the current market price, and if the computation time for a solution step is too long, the market prices can change significantly when our model completes its calculations.

In this discussion, we explore scenario quantity by comparing two approaches: deterministic optimization with a rolling horizon approach (DORH) and stochastic optimization with a rolling horizon

approach (SORH). The DORH approach is similar to the SORH approach, however, the model formulation does not include the second part of the objective function and the constraints related to the second-stage decision variables. Therefore, our focus centers on understanding the value added by the SORH and the impact of increasing the number of price scenarios. The profits of DORH and SORH are computed similarly based on the first-stage decisions. These profits encompass the cumulative profits and losses acquired from the first-stage decisions over all solution steps. Since the first-stage prices are the same for both approaches, the disparities in profit can be attributed to the divergent charging and discharging decisions made in the two approaches.

The first-stage prices are selected from a comprehensive scenario set, which encompasses a total of 5000 scenarios. This selection process follows the methodology outlined in Equation (5.26). It is worth noting that as the number of scenarios increases, the likelihood of the first-stage price closely aligning with one of the price scenarios also increases. Consequently, the expanding scenario set contributes to a more accurate representation of potential market price behaviors.

The hypothesis revolves around how the number of scenarios affects SORH profit. On the one hand, using a higher number of scenarios might result in a reduction in SORH profit because it represents a more risk-averse approach, considering a broader spectrum of potential scenarios. Conversely, we anticipate a point at which profit stabilizes beyond a certain number of scenarios, since the first-stage prices are all represented in the scenarios.

We start by comparing the most extreme cases, Cloudy Autumn and Windy Winter. Cloudy Autumn shows the highest prices and the most apparent shape of the four cases. Windy Winter has relatively low prices and much less shape during the day. Figure 7.5 shows 50 price scenarios generated for Cloudy Autumn, and Figure 7.6 shows 50 price scenarios generated for Windy Winter. The different scaling of the axes in these figures is intentional. It helps highlight the disparities in price behavior between the two cases, making them more visually distinguishable.

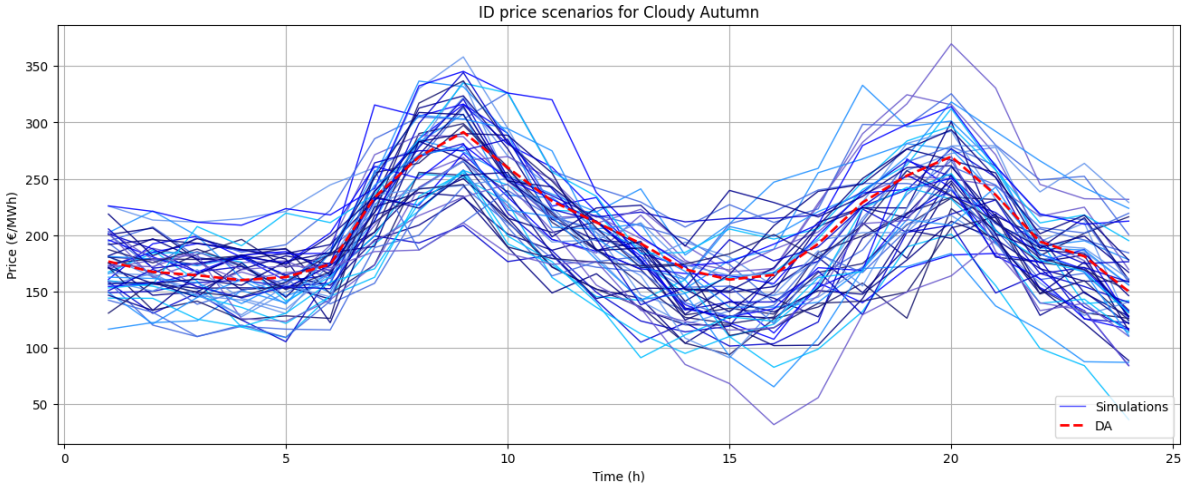


**Figure 7.5:** 50 simulations ID price based on DA price and hourly mean, standard deviation, and correlation for Cloudy Autumn.

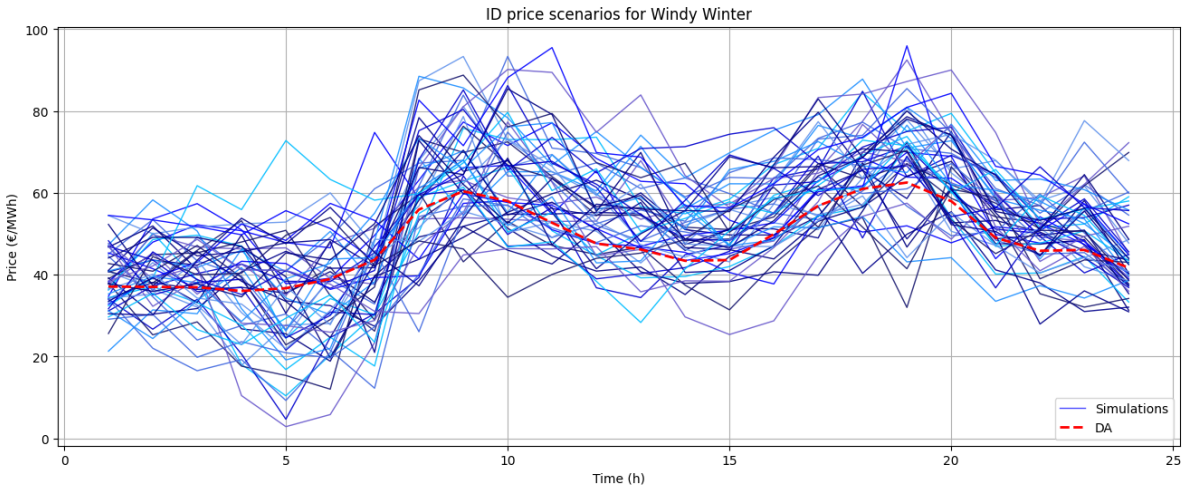


**Figure 7.6:** 50 simulations ID price based on DA price and hourly mean, standard deviation, and correlation for Windy Winter.

First, our investigation focuses solely on PHS. Table 7.2 presents the results for the Cloudy Autumn case when using PHS and including different numbers of scenarios. We have structured our analysis to include progressively larger sets of scenarios, ensuring that each set encompasses the smaller ones. This approach allows us to evaluate how increasing the number of scenarios not only impacts runtime but also how the SORH solution stabilizes as scenario numbers increase. We have also included the profit of the DORH solution, which remains constant across all scenario counts due to the use of the same first-stage prices. To assess the added value of the SORH model, the stochastic value column indicates the percentage increase relative to the DORH results. The last column provides the maximum runtime for a single solution step in the SORH.

We observe a DORH profit of 322.37 with a total runtime of 7 seconds. The SORH profit fluctuates from 609.55 up to 625.68. The stochastic value is on average 92 percent which indicates that the profit nearly doubles when adding a second-stage with price scenarios. We observe that the SORH profit does not clearly stabilize over a certain number of scenarios. However, for 250 scenarios, we have a maximum runtime of the solution step of almost one minute, which is the reasonable upper limit from a trading perspective. We aim for at least 80 percent of the solutions steps taking less than 60 seconds. Therefore, these results indicate that selecting 250 scenarios balances representing market variability and maintaining a reasonable runtime. It exhibits a percentage increase of 91.6 percent compared to the DORH profit and a reasonable maximum runtime of 58 seconds.

**Table 7.2:** Results of DORH and SORH for a PHS for Cloudy Autumn.

| Number of scenarios | DORH profit | SORH profit | Stochastic value | Maximum runtime |
|---|---|---|---|---|
| 50 | 322.37 | 618.25 | 91.8% | 8s |
| 100 | 322.37 | 620.34 | 92.4% | 16s |
| 250 | 322.37 | 617.68 | 91.6% | 58s |
| 500 | 322.37 | 619.61 | 92.2% | 162s |
| 750 | 322.37 | 625.68 | 94.1% | 327s |
| 1000 | 322.37 | 609.66 | 89.1% | 416s |

To be sure that 250 is the highest number of scenarios that can be included, meeting our intended goal of 80 percent of the solution steps below 60 seconds, we look at Figure 7.7. This figure illustrates the SORH's runtime per solution step, including 500 scenarios. The maximum runtime is 162 seconds. While an occasional runtime peak exists in the first solution steps, the runtime steadily decreases for the subsequent steps. This reduction can be attributed to the decreasing number of decision variables considered for each solution step, as we only optimize for the remaining periods. However, we observe that it does not meet our goal to have 80 percent of the solution steps below 60 seconds of runtime.

This analysis encourages us to select 250 scenarios. We conduct a similar analysis for the Windy Winter case to strengthen this consideration.

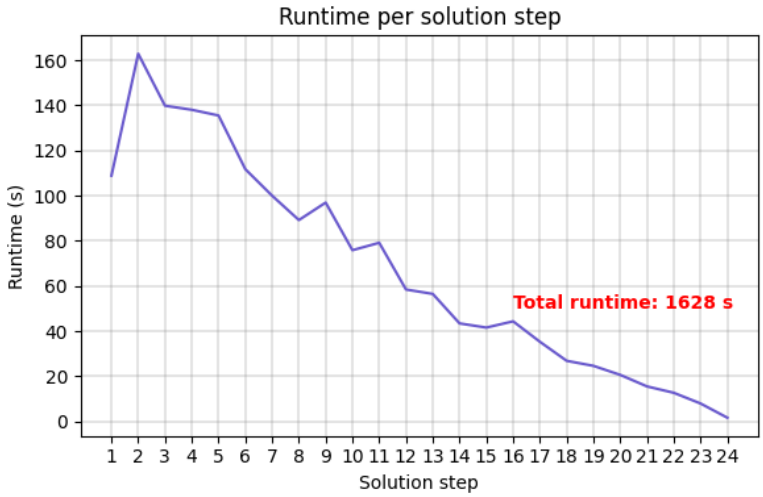


**Figure 7.7:** Runtime decay per solution step of SORH including 500 scenarios, solved for a PHS for Cloudy Autumn.

Table 7.3 shows the same analysis as the previous but for Windy Winter. Firstly, we observe lower profits due to the lower prices in Windy Winter. Moreover, we observe a lower stochastic value, around 63 percent. That implies that the effect of including the second stage is more significant for Cloudy Autumn than for Windy Winter. The higher variability in the Cloudy Autumn prices explains this. Anticipating more extreme cases can have a positive effect on the total profit.

The SORH profit shows a more stable pattern across the increasing number of scenarios. For 500 and 1000 scenarios, a clear drop to 193 is observed. For the other numbers, the stochastic value is approximately 64. This can be attributed to less variability in the price scenarios of Windy Winter. In terms of computational performance, when comparing the maximum runtimes, we see that the order of size remains the same for each increase in the number of scenarios. For 250 scenarios, the maximum runtime remains below 60 seconds. This leaves us to examine the runtime decay for 500 scenarios.

**Table 7.3:** Results of DORH and SORH for a PHS for Windy Winter.

| Number of scenarios | DORH profit | SORH profit | Stochastic value | Maximum runtime |
|---|---|---|---|---|
| 50 | 121.15 | 198.67 | 64.0% | 8s |
| 100 | 121.15 | 198.69 | 64.0% | 17s |
| 250 | 121.15 | 201.11 | 66.0% | 54s |
| 500 | 121.15 | 192.88 | 59.2% | 207s |
| 750 | 121.15 | 198.55 | 63.9% | 362s |
| 1000 | 121.15 | 192.77 | 59.1% | 612s |

Figure 7.8 shows the decay in the runtime per solution step for 500 scenarios for Windy Winter. This plot exhibits a slightly higher total runtime of 1773 seconds compared to the Cloudy Autumn case. Again, after jumpy solution steps, the runtime decays. The goal of 80 percent of the runtime below 60 seconds is not met again. Therefore, this analysis reaffirms our choice of using 250 scenarios to continue this research. This number balances between accuracy and computational feasibility. In Appendix A.2, we display four more tables, similar to Table 7.3 but solved for other storage technologies and typical days, that back this choice.

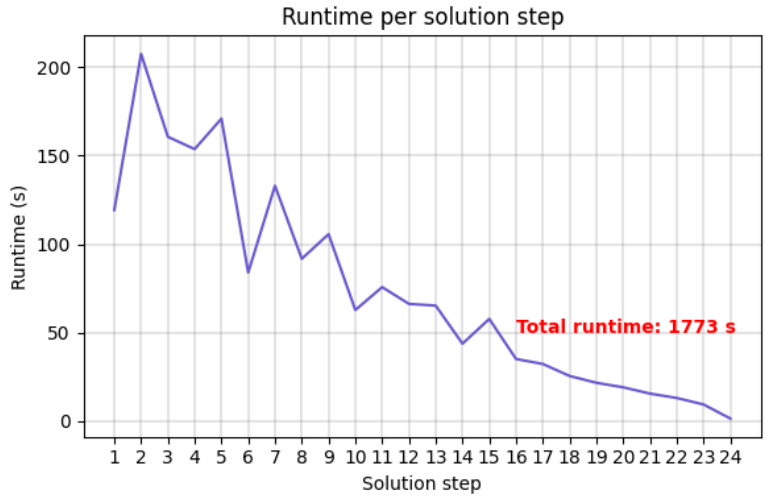


**Figure 7.8:** Runtime decay per solution step of SORH including 500 scenarios, solved for PHS for Windy Winter.

## 7.3. Comparing stochastic to deterministic approaches

In this section, we compare the SORH results with the two deterministic optimization (DO and DORH) results. DO involves straightforward decision-making as in Section 7.1. Charging and discharging decisions are based on the first-stage price of the first solution step. Note that this price differs from the DA prices of Section 7.1. Compared to DO, DORH incorporates a rolling horizon. While decisions can be adjusted against the new first-stage prices of each solution step, it is essential to note that no second-stage decisions are considered in this approach. Consequently, this approach does not consider future price scenarios during decision-making. Based on the analysis in Section 7.2, 250 scenarios are used for all SORH results.

### 7.3.1. Spring Weekend

Figure 7.9 presents the price scenarios employed in the SORH for Spring Weekend. The red dashed line represents the initial DA price used as the starting point of the simulations. This figure presents 250 simulations as chosen as the number of scenarios used to generate all SORH results.

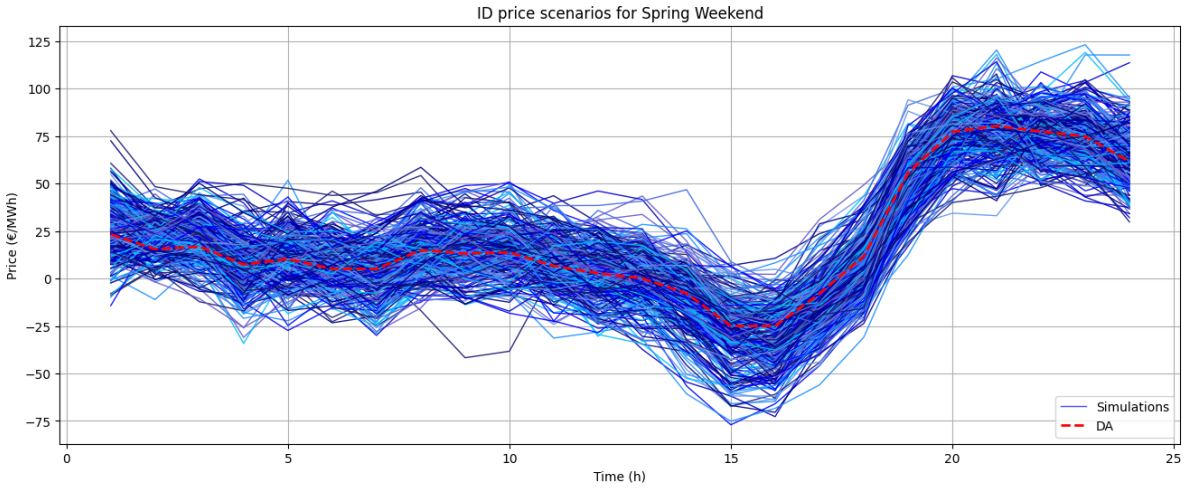


**Figure 7.9:** 250 simulations ID price based on DA price and hourly mean, standard deviation, and correlation for Spring Weekend.

The results of Spring Weekend and for all storage technologies are provided in Table 7.4. The profits of DO, DORH, and SORH are all stated. The RH value indicates the percentage increase from the DO

profit to the DORH profit, providing insight into the added value of the rolling horizon approach. Similar to Tables 7.2 and 7.3, columns for stochastic value and maximum runtime are included. Additionally, the performance column is added to assess the performance of SORH compared to the theoretical optimization (TO). TO represents the theoretical optimum in the ideal setting discussed in Chapter 4. The performance metric reflects the percentage of the theoretical optimum reached by SORH, providing a measure of its effectiveness in approaching the theoretical result.

A first observation that aligns with our expectations is that, across all storage technologies, employing DORH leads to greater profits than employing DO. Furthermore, it becomes clear that employing SORH results in higher profits than DORH. This shows the additional value brought by the rolling horizon approach and two-stage stochastic programming. The performance indicates SORH reaches on average 73 percent of the TO profit.

Secondly, across all optimization strategies, it is evident that BESS outperforms CAES, which itself outperforms PHS. This difference in performance can be linked to the varying flexibility of each storage technology. PHS has the lowest power limit per hour for charging and discharging, while BESS has the highest. However, this observation might not hold for all typical days, as the results from DO in Section 7.1 show that CAES resulted in zero profits for all typical days except for Spring Weekend. In the following sections, this hypothesis is further explored.

Thirdly, it is notable that the RH value increases from PHS to BESS, while the stochastic value decreases. This can also be linked to the differing flexibility of each storage technology. When incorporating the rolling horizon into the DO approach, storage with high charging and discharging power benefits significantly from iterative problem solving. However, when introducing the second stage with information about future price scenarios, it becomes more advantageous for PHS storage with lower power limits, indicating reduced flexibility. Again, we are interested in examining how these dynamics play out in other cases.

Finally, we observe an unexpectedly high maximum runtime of 360 seconds for CAES. We consider this an outlier and do not adjust our strategy of including 250 scenarios in the stochastic solution.

**Table 7.4:** Results of DO, DORH, and SORH for Spring Weekend.

| Storage | DO | DORH | RH value | SORH | Stochastic value | Performance | Max runtime |
|---|---|---|---|---|---|---|---|
| PHS | 43.41 | 124.95 | 188% | 335.17 | 168% | 76% | 62s |
| CAES | 80.62 | 433.92 | 438% | 1001.91 | 131% | 72% | 360s |
| BESS | 112.75 | 768.36 | 581% | 1137.93 | 48% | 70% | 75s |

To analyze the SoC behavior in both DORH and SORH solutions, we depict the SoC actions for the first solution step for a CAES in Figure 7.10 for DORH and in Figure 7.11 for SORH. The results of the first solution step of SORH involve more frequent charging and discharging actions than for DORH. However, despite these more frequent actions, the system tends to make more minor adjustments, resulting in the storage capacity being maintained at intermediate levels rather than consistently near empty or full. This cautious approach may originate from the system's anticipation of extreme price scenarios in the second stage. By doing so, it ensures that the storage remains flexible, ready to take potentially profitable opportunities in future solution steps.

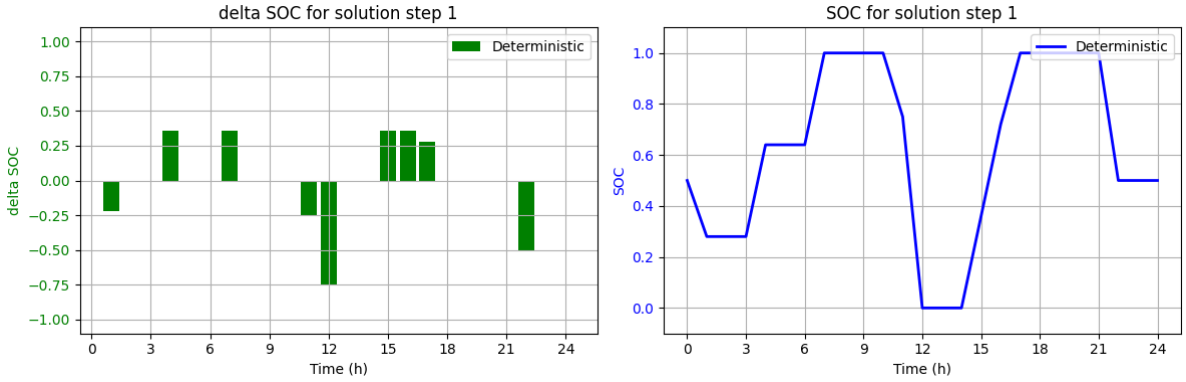


**Figure 7.10:** Storage planning first solution step DORH for a CAES for Spring Weekend.

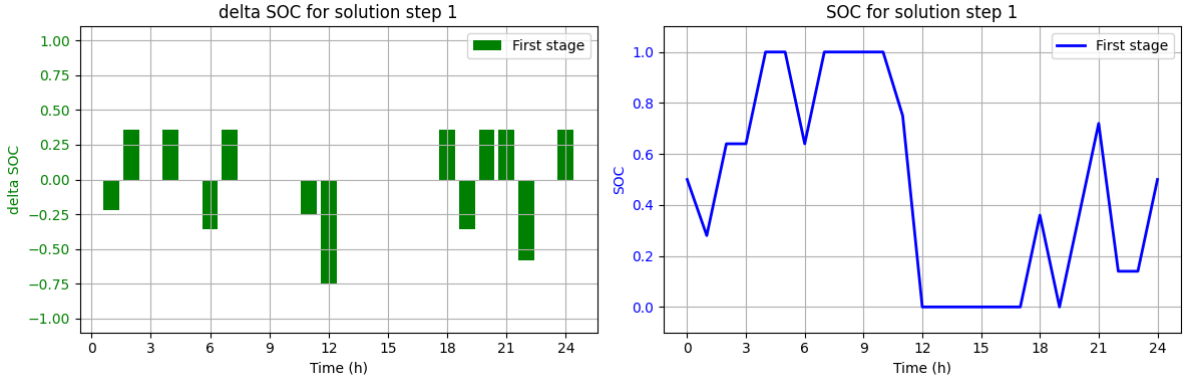


**Figure 7.11:** Storage planning first solution step SORH for a CAES for Spring Weekend.

Moving on to the second solution step for both approaches, we examine their optimal charging and discharging actions displayed in Figures 7.12 and 7.13. Notably, the results of the second solution step for SORH exhibit a significantly higher frequency of charging and discharging actions than for DORH. This approach results in a higher profit of 175.47, whereas the DORH profit is 48.20. From these observations, it becomes evident that SORH strategically makes more frequent but restrained choices in one solution step, possibly intending to generate a higher profit in subsequent steps. This approach allows it to maintain a degree of flexibility for future decision-making. In the following section, we further explore this concept by implementing the Stormy Summer case, aiming to confirm this pattern through additional examples.

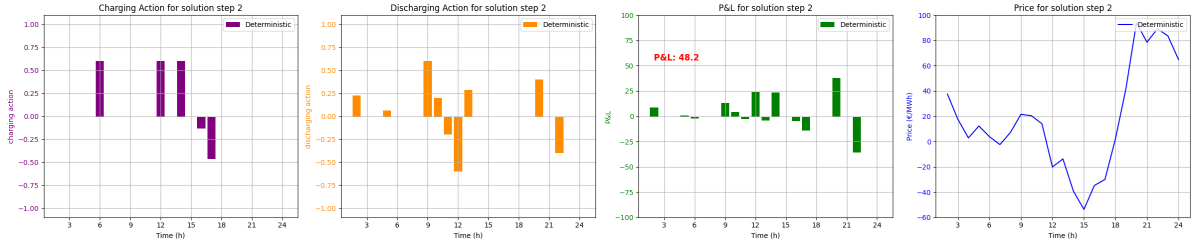


**Figure 7.12:** Optimal charging and discharging decisions, profits and losses, and ID price for the second solution step of DORH for a CAES for Spring Weekend.

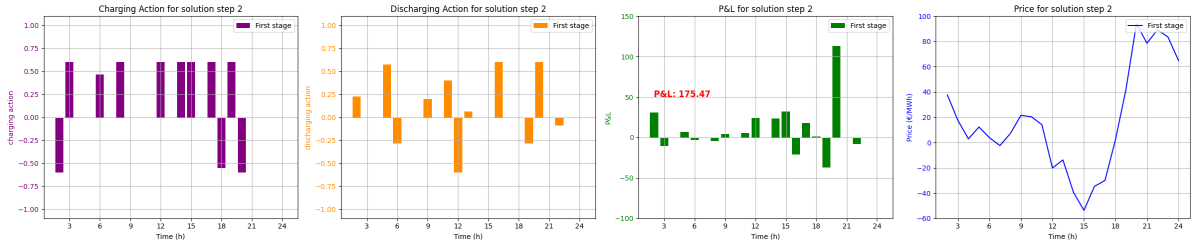


**Figure 7.13:** Optimal charging and discharging decisions, profits and losses, and ID price for the second solution step of SORH for a CAES for Spring Weekend.

### 7.3.2. Stormy Summer

Price scenarios for Stormy Summer are illustrated in Figure 7.14. These scenarios display a different pattern compared to the Spring Weekend, with higher variability, especially during the evening hours.

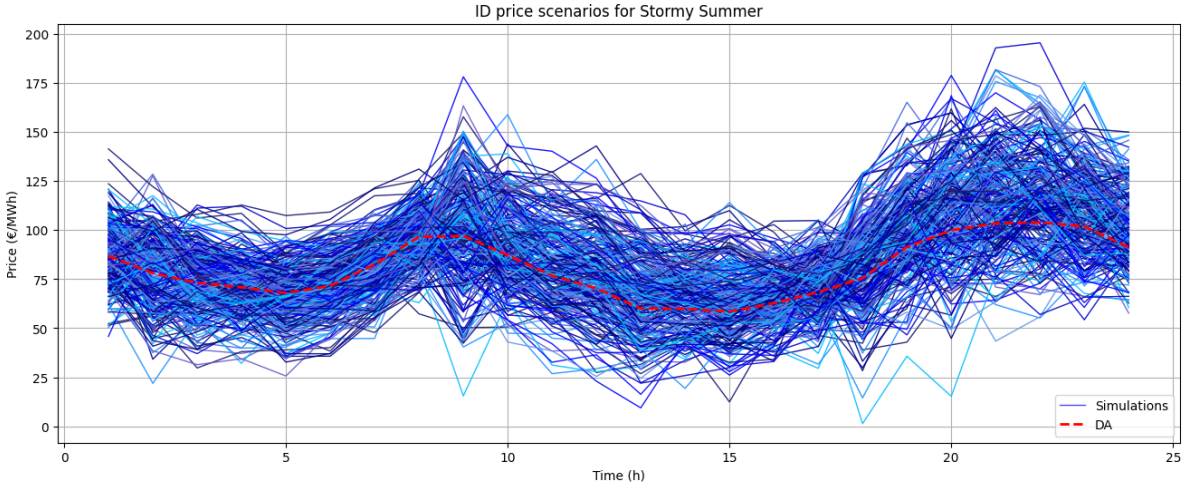


**Figure 7.14:** 250 simulations ID price based on DA price and hourly mean, standard deviation, and correlation for Stormy Summer.

The results for Stormy Summer, across all storage technologies, can be found in Table 7.5. For a CAES, DO still yields a profit of zero. Apart from that zero profit, we observe consistent outcomes as in the Spring Weekend case. Across all storage technologies, the results show that the highest profit is achieved with SORH, followed by DORH, and the lowest with DO. This scheme remains consistent for all storage technologies. The performance for Stormy Summer lies higher than for Spring Weekend, around 76 percent.

Additionally, the profitability for both rolling horizon approaches ranks similarly considering the storage technologies separately. BESS generates the highest profits, followed by CAES and PHS, yielding the lowest profits across all optimization approaches. These results confirm the hypothesis introduced in the previous section. For BESS, we observe the highest RH value but the lowest stochastic value. We delve deeper into the details of the BESS solution.

**Table 7.5:** Results of DO, DORH, and SORH for Stormy Summer.

| Storage | DO | DORH | RH value | SORH | Stochastic value | Performance | Max runtime |
|---|---|---|---|---|---|---|---|
| PHS | 18.30 | 212.80 | 1063% | 449.74 | 111% | 80% | 50s |
| CAES | 0 | 310.21 | - | 1472.48 | 375% | 76% | 60s |
| BESS | 80.72 | 1464.31 | 1714% | 1825.33 | 25% | 72% | 50s |

We depict the SoC actions for the first solution step of a BESS in Figure 7.15 for DORH and in Figure 7.16 for SORH. Similar to Spring Weekend, the results of the first solution step for SORH

involve more frequent charging and discharging actions than for DORH. However, SORH yields a profit of 62.26 for the first solution step, compared to 80.72 for DORH. We expect that the model intends this to anticipate on major price fluctuations in the next solutions steps.

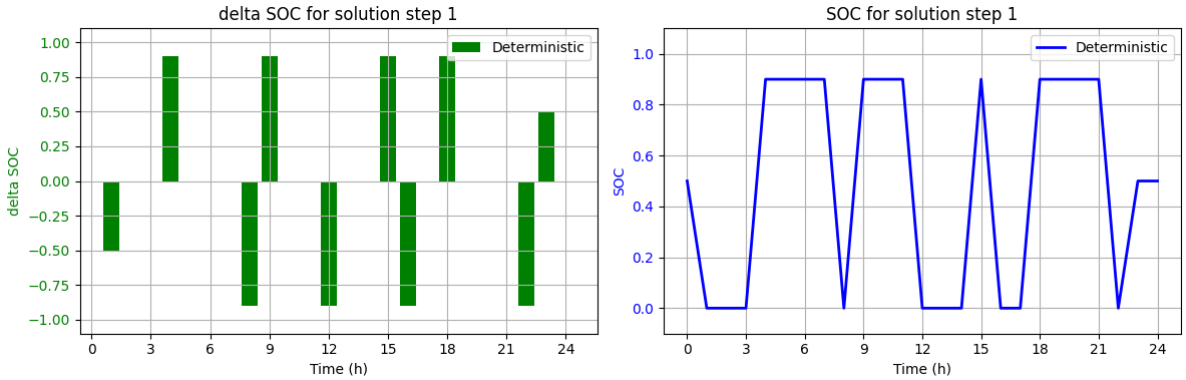


**Figure 7.15:** Storage planning for the first solution step of DORH for a BESS for Stormy Summer.

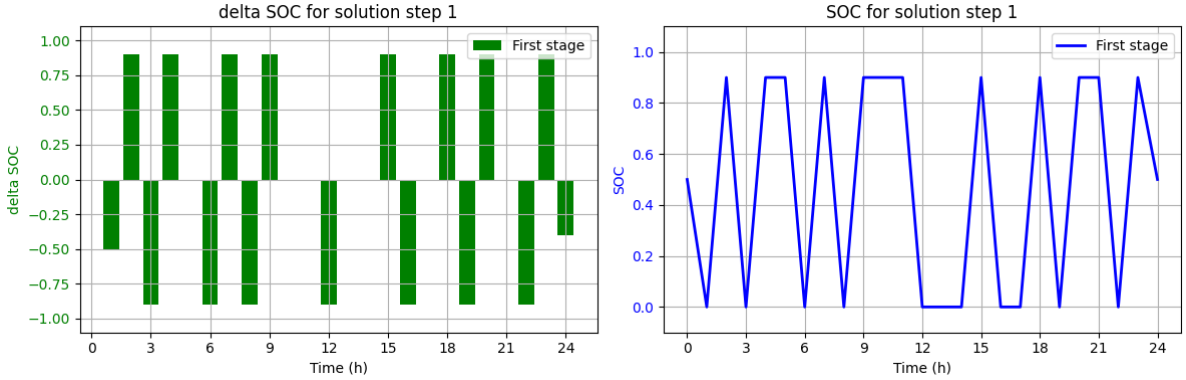


**Figure 7.16:** Storage planning for the first solution step of SORH for a BESS for Stormy Summer.

Now, we again examine the optimal charging and discharging actions of the results for the second solution step of DORH and SORH, displayed in Figures 7.17 and 7.18. The results for SORH exhibit a significantly higher frequency of charging and discharging actions than for DORH. This approach results in a higher profit of 344.62, whereas the DORH profit is 237.21. These observations again confirm the hypothesis that SORH strategically makes charging and discharging decisions in one solution step, intending to generate a higher profit in subsequent steps.

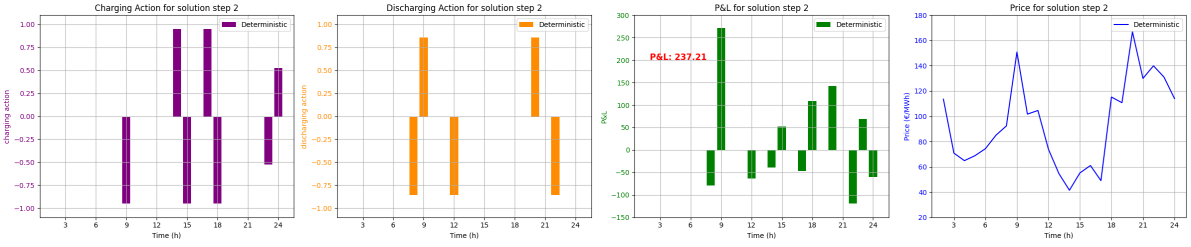


**Figure 7.17:** Optimal charging and discharging decisions, profits and losses, and ID price for the second solution step of DORH for a BESS for Stormy Summer.

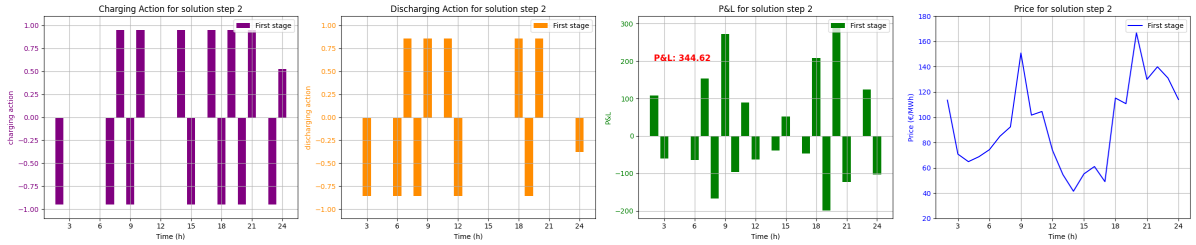


**Figure 7.18:** Optimal charging and discharging decisions, profits and losses, and ID price for the second solution step of SORH for a BESS for Stormy Summer.

### 7.3.3. Cloudy Autumn

In Figure 7.19, we observe the price scenarios for Cloudy Autumn, where prices fluctuate between €100/MWh and €400/MWh. This price range is higher than in previous cases and shows increased volatility. We expect that these price dynamics improve our profits.

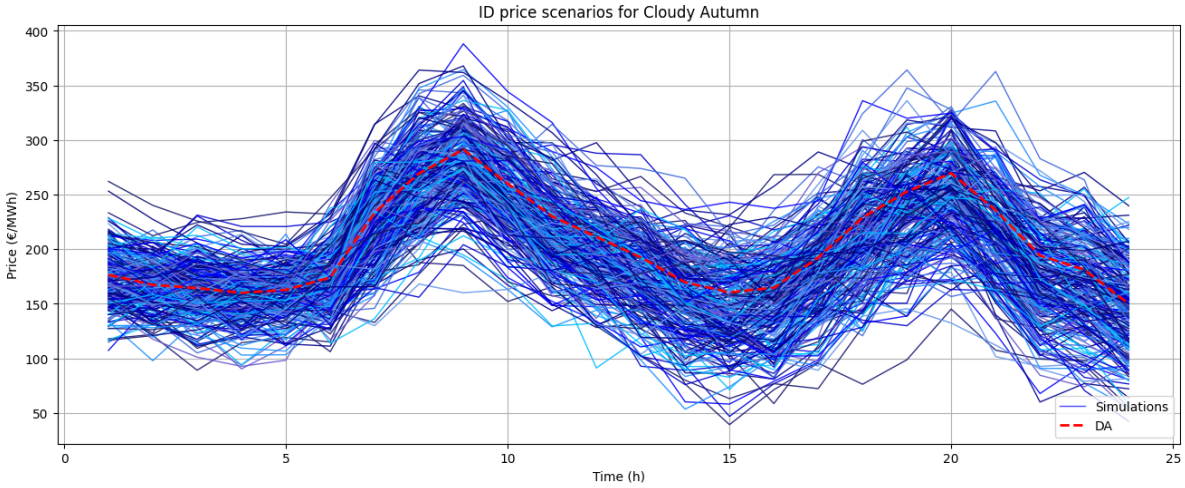


**Figure 7.19:** 250 simulations ID price based on DA price and hourly mean, standard deviation, and correlation for Cloudy Autumn.

The results for Cloudy Autumn, for all storage technologies, are presented in Table 7.6. Notably, we observe the highest profits achieved by SORH compared to all other typical days, which can be attributed to high price levels and significant volatility of Cloudy Autumn. The performance of SORH is stable around 71 percent. Deviating from our earlier findings, PHS exhibits a high RH value and the lowest stochastic value. This prompts a closer examination of the results.

**Table 7.6:** Results of DO, DORH, and SORH for Cloudy Autumn.

| Storage | DO | DORH | RH value | SORH | Stochastic value | Performance | Max runtime |
|---|---|---|---|---|---|---|---|
| PHS | 47.87 | 322.37 | 573% | 617.68 | 92% | 72% | 58s |
| CAES | 0.01 | 515.28 | - | 1932.09 | 275% | 72% | 63s |
| BESS | 200.48 | 1004.55 | 401% | 2379.05 | 137% | 69% | 59s |

Figure 7.20 offers an overview of the charging and discharging decisions made during the first solution step of SORH, including the resulting profits and losses and the first-stage ID price. Notably, we observe frequent charging and discharging actions, which result in a loss of 21.11. In contrast, the first solution step of the DORH yields a profit of 47.87, as indicated in Table 7.6.

We notice that the results for SORH demonstrate more frequent charging and discharging actions in subsequent solution steps when compared to DORH. While DORH yields a substantial increase in profits compared to DO, SORH seizes more advantages during each solution step. For a more detailed

examination of storage management during the fourth solution step, refer to Figure 7.21, illustrating the resulting changes in SoC and SoC planning for DORH. In contrast, Figure 7.22 portrays the storage planning for SORH. These figures reveal that decisions for SORH consistently capitalize on anticipated flexibility, leaving no idle hours.

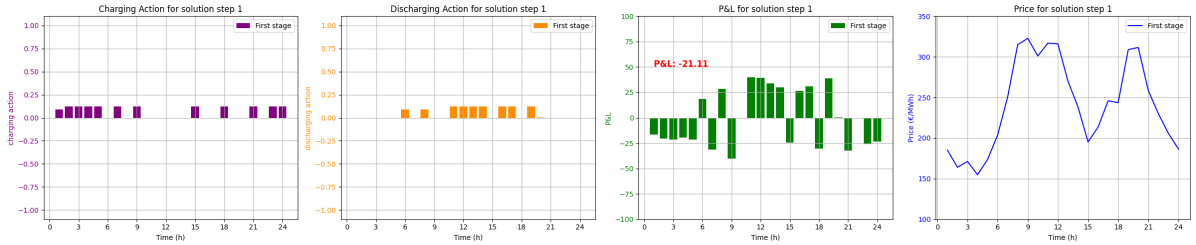


**Figure 7.20:** Optimal charging and discharging decisions, profits and losses, and ID price of the first solution step of SORH for a PHS for Cloudy Autumn.

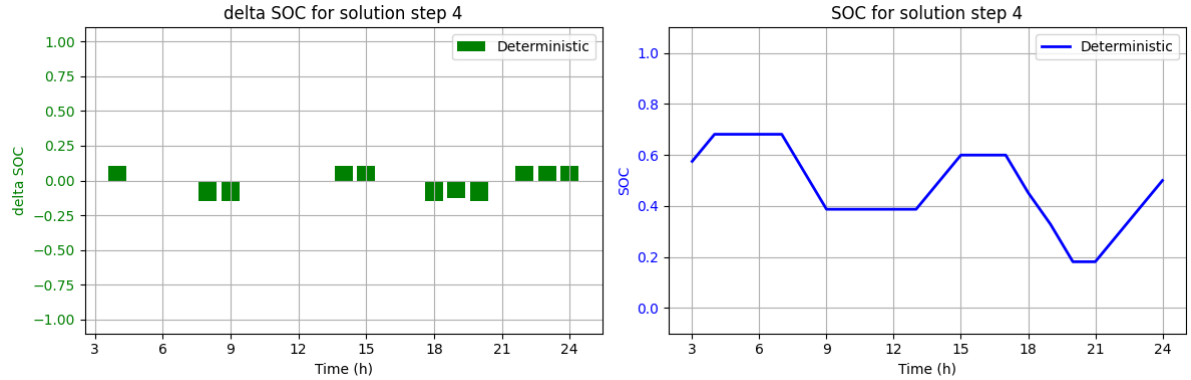


**Figure 7.21:** Storage planning for the fourth solution step of DORH for a PHS for Cloudy Autumn.

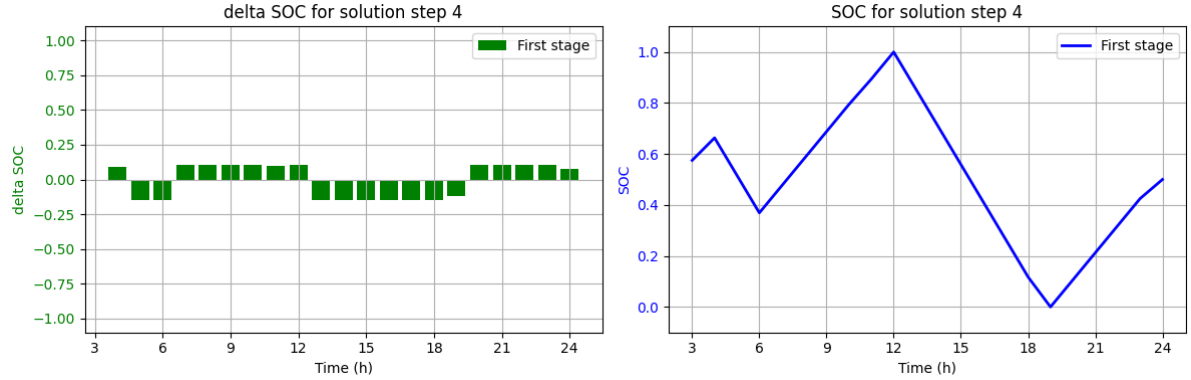


**Figure 7.22:** Storage planning for the fourth solution step of SORH for a PHS for Cloudy Autumn.

In Figure 7.23, we display the effective charging and discharging actions achieved through the SORH after 24 solution steps. The effective outcomes represent the decisions made regarding the charging and discharging operations within the storage system. At each solution step $i$, only the planning for the first feasible hour ($t = i$) is considered final and effectively changes the level of the SoC. This result differs from the planned charging and discharging decisions for all remaining hours ($t > i$), which can still be adjusted if more rolling horizon steps remain. It becomes clear that the effective planning does not have charging and discharging activities for every hour. Seemingly, this is not optimal in this case, but was optimal in intermediate storage plannings.

When compared to the effective charging and discharging actions of a BESS, as shown in Figure 7.24, a distinct pattern emerges. Both systems involve charging and discharging operations at similar intervals, but the key difference lies in the reduced duration of these actions for BESS due to its higher power limits.

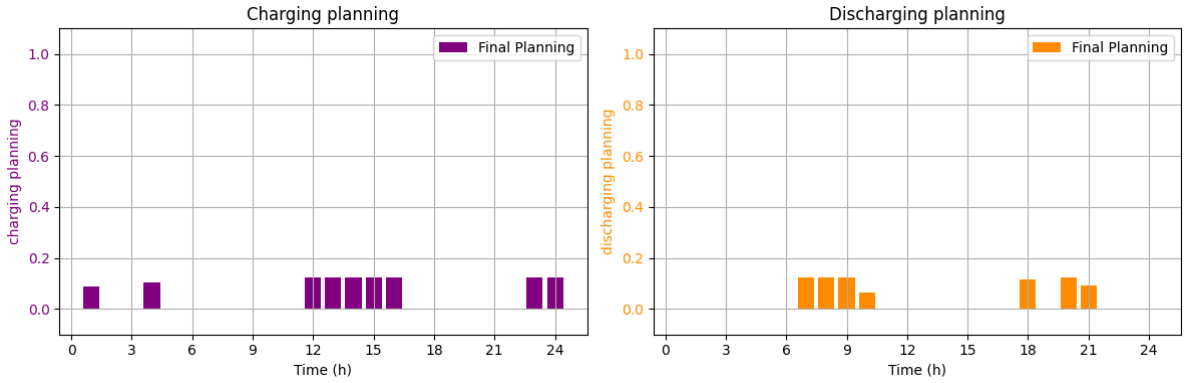


**Figure 7.23:** Effective charging and discharging actions for SORH for a PHS for Cloudy Autumn.

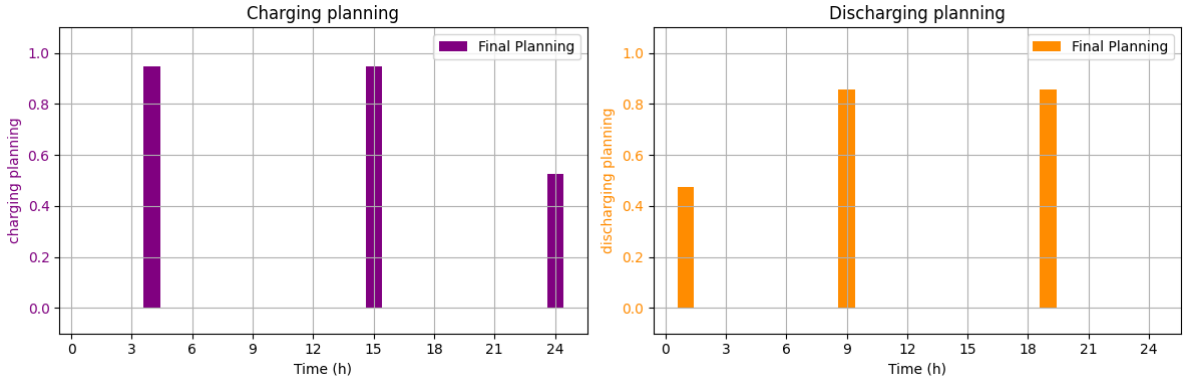


**Figure 7.24:** Effective charging and discharging actions for SORH for a BESS for Cloudy Autumn.

### 7.3.4. Windy Winter

For Windy Winter, price scenarios can be observed in Figure 7.25. It is worth noting that these prices are significantly lower than Cloudy Autumn's prices. Furthermore, the price range demonstrates less variability, which we expect to translate into a reduced profit for the system.

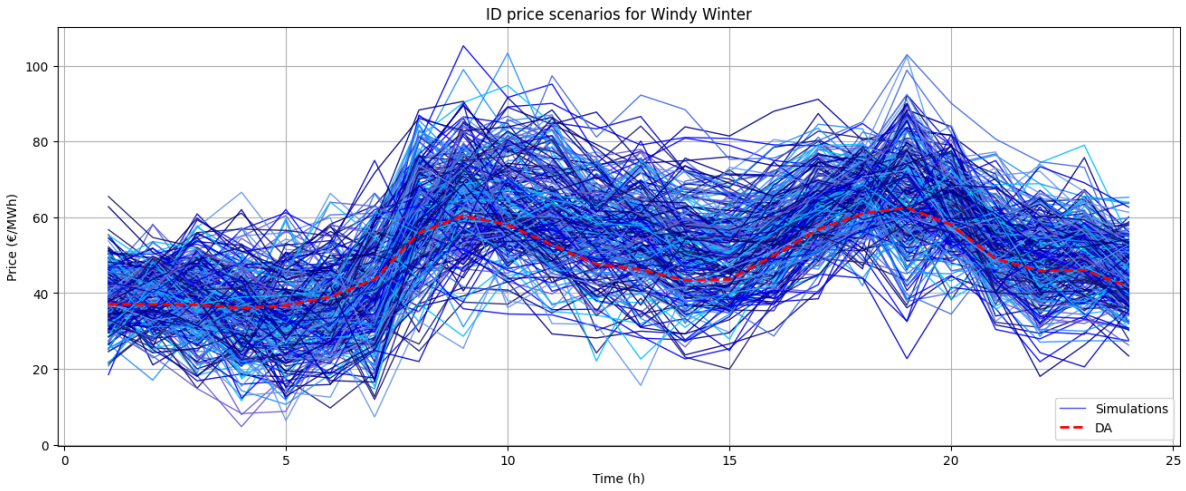


**Figure 7.25:** 250 simulations ID price based on DA price and hourly mean, standard deviation, and correlation for Windy Winter.

Indeed, the profits for Windy Winter, as shown in Table 7.7, are lower than those for Cloudy Autumn. Nevertheless, no extreme or unexpected outcomes are observed. Cloudy Autumn shows the lowest performance of SORH of 70 percent on average. We delve deeper into the results for a CAES in both rolling horizon approaches since they exhibit a high RH value and stochastic value.

**Table 7.7:** Results of DO, DORH, and SORH for Windy Winter.

| Storage | DO | DORH | RH value | SORH | Stochastic value | Performance | Max runtime |
|---|---|---|---|---|---|---|---|
| PHS | 17.94 | 121.15 | 575% | 201.11 | 66% | 69% | 55s |
| CAES | 10.53 | 176.28 | 1574% | 722.21 | 310% | 71% | 61s |
| BESS | 54.65 | 653.30 | 1095% | 918.66 | 41% | 70% | 50s |

Figures 7.26 and 7.27 represent the aggregated profits and losses for each solution step. Each aggregated profit or loss is the result from executing the first-stage charging and discharging decisions of the remaining hours in the intraday market. In DORH, no losses are incurred, as the system operates without knowledge of future price scenarios. Therefore, it will never decide to take a loss and instead not charge or discharge anything. However, after reaching its peak at solution step 4, the DORH profits show only modest gains.

Conversely, in SORH, a deliberate strategy is employed. An initial loss of 55.32 is accepted in the first step, and the system breaks even in the second solution step. This approach is designed to maximize profits in subsequent solution steps. The outcome is a remarkable quadrupling of the total expected profit.

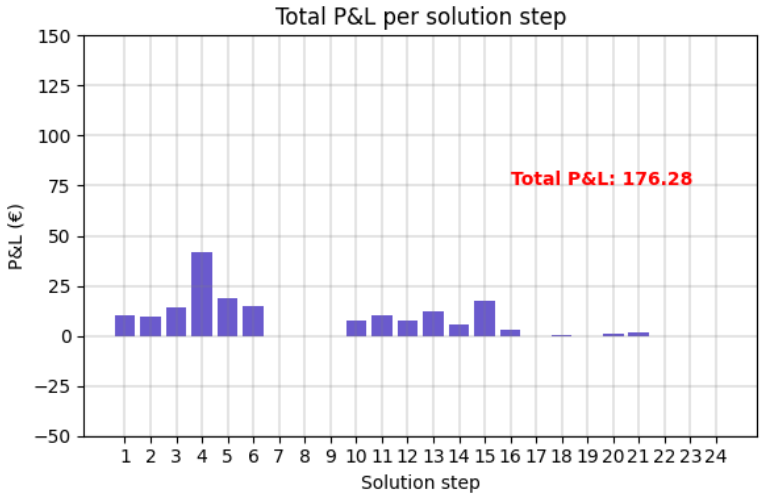


**Figure 7.26:** Total profits per solution step for DORH for a CAES for Windy Winter.

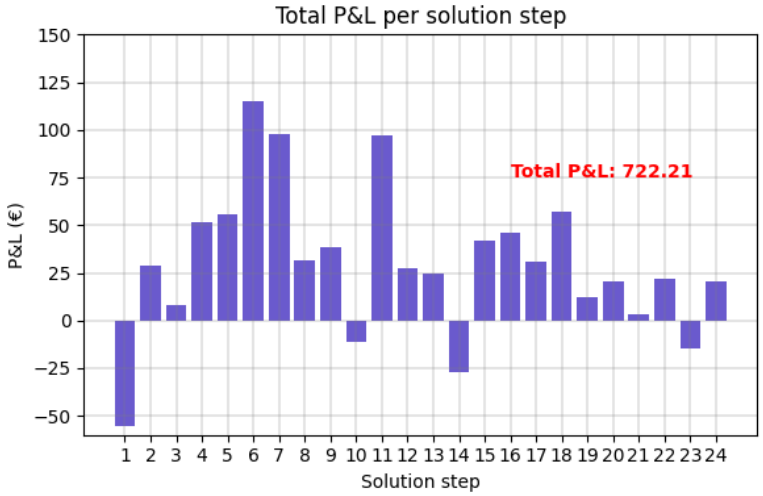


**Figure 7.27:** Total profits per solution step for SORH for a CAES for Windy Winter.

Figure 7.28 and Figure 7.29 illustrate the effective storage planning after completing all solution steps for both DORH and SORH for CAES. It is the result of what effectively is stored at each time, in contrasts to the storage planning of each solution step. For each solution step $i$, the planning for hour $t = i$ becomes definitive as it proceeds to delivery and is executed within the storage system.

It is remarkable that the effective storage planning for DORH appears almost non-existent, and there is a complete absence of change in the SoC for SORH. This observation is particularly intriguing given the substantial profit increase of 299 percent for SORH compared to DORH. Since both approaches result in high profits, it suggests that the system performs many actions that are canceled out in later solution steps, effectively not engaging in significant charging and discharging in the effective storage planning.

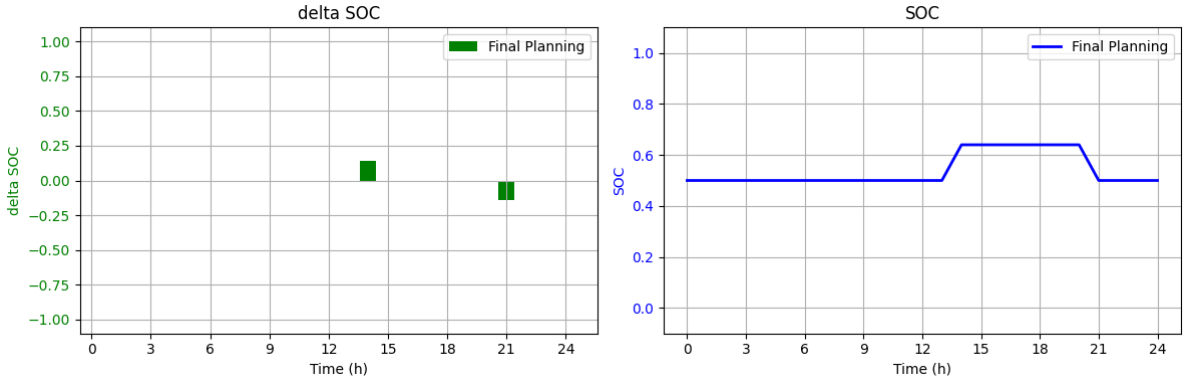


**Figure 7.28:** Effective storage planning after 24 solution steps for DORH for a CAES for Windy Winter.

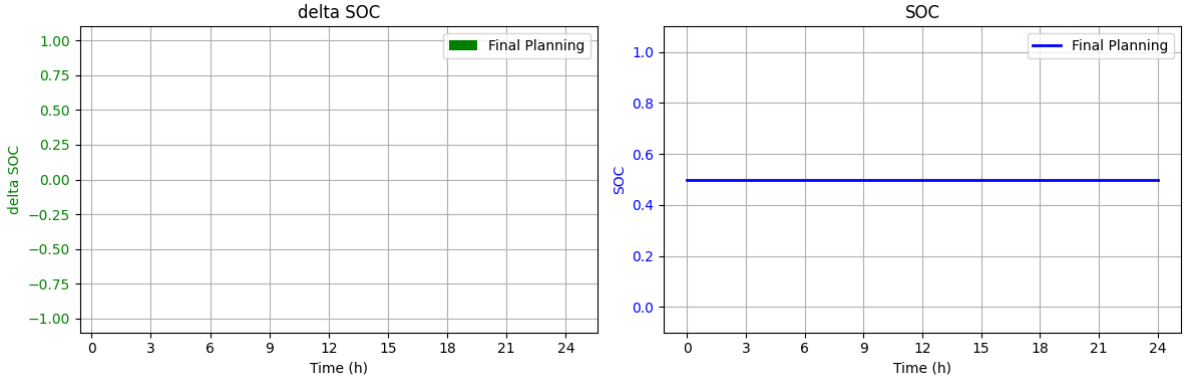


**Figure 7.29:** Effective storage planning after 24 solution steps for SORH for a CAES for Windy Winter.

A thorough investigation of all solution steps is conducted to gain a deeper understanding of this phenomenon. It appears that, for each planning already established for a specific time $t$ in preceding solution steps, the intended action is effectively canceled out during solution step $i = t$ when that particular hour transitions into the delivery phase. To illustrate this, we consider solution steps 4 and 5.

Looking at Figure 7.30, which presents the storage planning for the fourth solution step, we can see that there is no storage planning for hour 4, i.e., $t = i$. However, a discharge is planned for hour 5. Now, in the second plot of Figure 7.31, we observe that this previously planned discharging activity is effectively canceled by a negative discharging action. Consequently, when hour 5 enters the delivery phase, nothing is effectively stored.

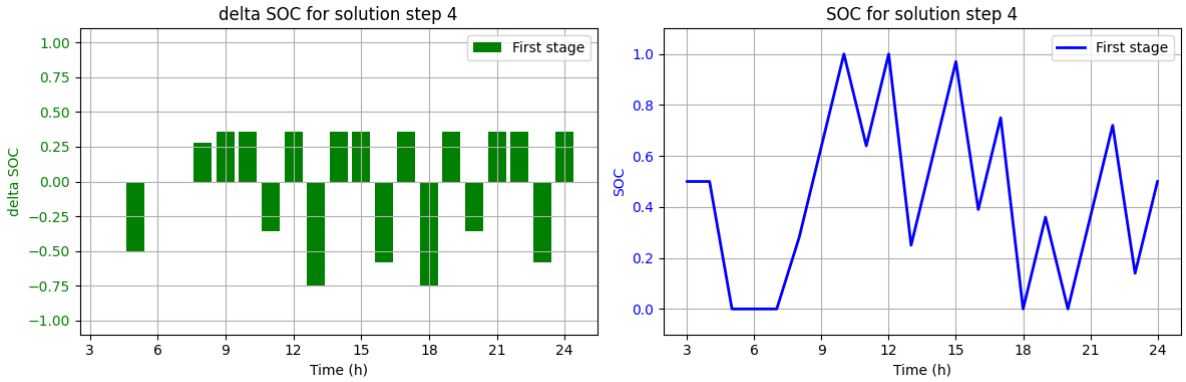


**Figure 7.30:** Storage planning for the fourth solution step of SORH for a CAES for Windy Winter.

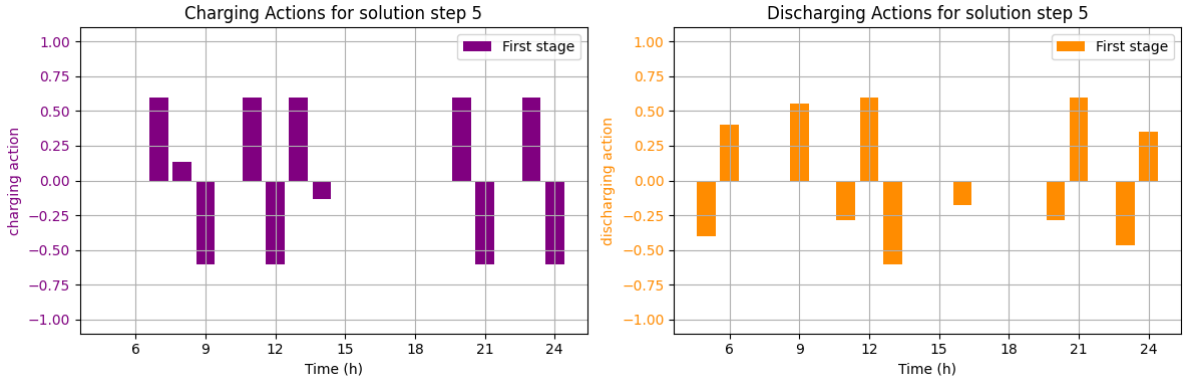


**Figure 7.31:** Optimal charging and discharging decisions for the fifth solution step of SORH for a CAES for Windy Winter.

# 8

# Conclusions and Recommendations

In this chapter, the conclusions and recommendations for this thesis are presented. In Section 8.1, the conclusions of the research carried out during this thesis are presented. After that, the directions for further research are proposed, and recommendations are made in Section 8.2.

## 8.1. Conclusions

For this master thesis, the research question was: How can one optimize electrical energy storage (EES) scheduling on the intraday market, considering the uncertainty in market prices?

This research demonstrates that a two-stage stochastic program including a rolling horizon approach (SOHR) is an effective way to optimize EES scheduling on the intraday market. The model includes the uncertainty in the market prices through price scenarios in the second stage of the stochastic program. By executing the first-stage charging and discharging decisions for each solution step in the market, the SORH always reaches a higher profit concerning the deterministic approaches.

The achieved computation time for each solution step is reasonable for trading purposes. We aimed for 80 percent of the solution steps to be completed within 60 seconds, and this target was achieved by incorporating 250 scenarios in the second stage. This goal is crucial because prolonged calculation times can lead to significant changes in market prices. Using 250 scenarios, we balance obtaining valuable information about potential future price fluctuations and ensuring a timely solution.

The performance of SORH concerning theoretical optimization (TO) results in an average of 72 percent across all cases. This result implies that the SORH profit reaches 72 percent of the theoretical optimum, in which all prices are known in advance. However, the performance of SORH depends on the quality of price scenarios and is expected to drop if price scenarios do not correctly represent future prices.

There were three sub-questions to support the main question. They are all answered below.

**How should the short-term EES be modeled?** We have adopted a model that can accommodate various storage technologies by adjusting the relevant storage parameters. This approach was chosen deliberately, as the literature needs more extensive comparisons between different storage technologies. As of now, many papers predominantly focus on a single storage technology. The comparison of pumped hydropower storage (PHS), compressed air energy storage (CAES), and battery energy storage systems (BESS) could be made using our storage model.

Our model is built around the State of Charge (SoC), which is the central variable in the model. It describes the energy level stored within the system at any given moment. We incorporate the charging and discharging costs in our model by accounting for the efficiency losses incurred during the charging and discharging processes. While our model simplifies the representation of real-world complexities, it effectively captures each storage technology's principal advantages and disadvantages.

**What is the most suitable optimization technique for finding a daily EES schedule?** A careful review of the existing literature influenced our choice of optimization technique. This review identified specific gaps in the literature among the already extensive research on short-term storage scheduling.

One notable gap was the limited use of the intraday market in many research papers. We recognized the inherent advantages of the intraday market for short-term storage. This market enables close-to-delivery adjustments to capitalize on price fluctuations and accommodate fast charging and discharging. We designed a model that addresses this research gap. Our model adopts an iterative approach to solve the optimization problem, resulting in a deterministic optimization problem repeatedly solved using the rolling horizon method (DORH). This approach aligns with our goal to utilize the intraday market for short-term storage effectively.

From Chapter 7, we observe that the DORH approach consistently outperforms the deterministic optimization (DO) approach. Therefore, including a rolling horizon is a suitable optimization technique for short-term storage.

**How should the intraday price's uncertainty be considered in the model?** Our model employs a two-stage stochastic programming approach to account for the uncertainty in intraday market prices. In the first stage, deterministic decisions are made based on the current intraday market price. We also incorporate future price scenarios to anticipate potential price fluctuations. The second-stage decisions are adjustments to the deterministic decisions following these price scenarios. This stochastic approach is combined with the rolling horizon approach and enables our solution to adapt to the price scenarios in subsequent solution steps.

The results presented in Chapter 7 demonstrate the advantages of incorporating a stochastic paradigm. The stochastic value is a metric for measuring improved profit from SORH to DORH. Our findings indicate that the stochastic value is positive for all storage technologies. Notably, it offers the most significant benefits for storage technologies with lower flexibility, such as PHS, where the model's ability to anticipate future price fluctuations is particularly advantageous. Storage technologies with higher flexibility, such as BESS, can rapidly adjust their charging and discharging plans. As a result, they are less susceptible to the impact of price fluctuations, making them less reliant on the quality of the price scenario simulations.

The intraday price scenarios are generated using a Monte Carlo simulation (MCS), incorporating historical price data from the German electricity market from 2021. These scenarios are categorized into four cases, each representing a typical day. They entail Spring Weekend, Stormy Summer, Cloudy Autumn, and Windy Winter. This categorization aims to offer a diverse range of inputs, enabling us to observe how the model performs under various conditions. Intriguingly, these cases yield different results, providing valuable insights into the most opportune days for short-term storage operations and the optimal strategies to apply.

## 8.2. Recommendations for future research

In this section, we identify interesting directions for future research and make recommendations. They are categorized into five key areas: computational, storage modeling, optimization model, price input, and practical application.

**Computational** The robustness of our study could be enhanced by comparing different sets of first-stage prices rather than relying on a single set for each case. The current approach introduces a significant random element into the analysis since first-stage prices are randomly selected from price scenarios. A more robust methodology would entail analyzing multiple sets of first-stage prices and presenting the distribution of the outcomes. This approach could provide insight into the variability of different first-stage price selections.

**Storage modeling** It should be acknowledged that this research employs a simplified representation of electrical energy storage. There are several opportunities for enhancing the complexity of the model, bringing it closer to real-world scenarios. In the existing model, storage parameters are expressed as a percentage of total capacity. The model could incorporate specific real-world storage examples to refine precision and enable more accurate estimations of expected profits and charging and discharging decisions. This enhancement facilitates a more nuanced comparison among storage technologies, considering their substantial differences in size.

Furthermore, additional characteristics could be introduced, such as the degradation of batteries over time or investments costs. This inclusion would offer a more comprehensive view of the long-term

performance and sustainability of energy storage systems. It could improve the model's practical applicability, providing insights into EES scheduling in real-world settings.

**Optimization model** We employed a single method to determine probabilities within the stochastic programming framework. However, it is worth exploring different probability assignment methods. These different methods can assign probabilities to the price scenarios with varying degrees of risk tolerance, ranging from risk-averse to risk-seeking. In this way, we could better understand how risk different profiles impact decisions and overall profitability. Expanding the research in this direction will enrich the findings and provide a more comprehensive understanding on decision-making under uncertainty in short-term EES scheduling.

**Price input** There are several possibilities to create a more realistic price input. Firstly, the distribution choice in the MCS for generating price scenarios can be refined. It is recommended to assess whether intraday market prices follow a normal distribution. This step was not included in the research. For example, Wozabal & Rameseder (2020) investigate the family of normal inverse Gaussian distributions to model electricity prices. These distributions allow for heavy tails and asymmetries, usually present during peak hours.

We suspect the next two price input factors contributing to optimistic profit outcomes. In the current methodology, the first-stage prices are randomly selected from the price scenarios with the addition of a noise term. This method allows prices to jump between scenarios, with the potential of artificially boosting profit outcomes. Future research could incorporate correlation between successive first-stage prices, providing a more realistic representation of evolving intraday prices. This modification would better capture that first-stage prices are not expected to transition abruptly from one scenario to the next within a single solution step.

Secondly, the volatility incorporated in the simulation is derived from trading data of all hours. However, when a trade is made within one hour of delivery, the volatility tends to be much higher compared to earlier hours. Therefore, there is a possibility that the overall volatility has been overestimated, resulting in more profitable price scenarios.

Finally, the research could be improved by introducing quarter-hourly trading intervals. This adjustment would be particularly relevant for flexible storage technologies, such as BESS, as it could leverage the opportunities presented by quarter-hourly price fluctuations. However, it is important to consider that this modification may increase the maximum runtime per solution step. This potential drawback should be weighed against the benefits, especially considering the smaller decision windows in quarter-hourly trading intervals.

**Practical application** This research offers a practical application for storage operators actively participating in the intraday market. The proposed model is designed for successive implementation of the SORH approach and provides significant added value compared to the straightforward DO approach.

In practice, the price scenarios used in the SORH approach should be simulated based on the day-ahead price, which is already available when the intraday market opens. The first-stage price aligns with the current intraday price and is observable from the market. This price should not be chosen from the constructed price scenarios as in our case study. In each solution step, SORH calculates first-stage charging and discharging decisions, which are then executed in the intraday market. After updating the storage planning based on these decisions, the next first-stage price is observed from the market, and the process repeats.

However, the hourly means, standard deviations, and correlations derived from the case study may not directly apply, as they are based on only four typical days. When optimizing EES for a specific day in practice, the methodology must be extended to encompass a broader range of typical days and establish connections with historical trading data. Future research could explore methods to match the current day with a representative typical day to retrieve the historical means, standard deviations, and correlations for constructing price scenarios.

# References


Bellini, E. (2022). *World's largest compressed air energy storage project goes online in china.* Retrieved September 19, 2023, from https://www.pv-magazine.com/2022/10/06/worlds-largest-compressed-air-energy-storage-project-goes-online-in-china

Birge, J. R., & Louveaux, F. (2011). *Introduction to stochastic programming.* Springer Science & Business Media.

Blakers, A., Stocks, M., Lu, B., & Cheng, C. (2021). A review of pumped hydro energy storage. *Progress in Energy*, *3*(2), 022003.

Bowden, C. (2023). *Understanding power markets: Merit order and marginal pricing.* Retrieved August 6, 2023, from https://www.squeaky.energy/blog/understanding-power-markets-merit-order-and-marginal-pricing

Bundesverband WindEnergie. (2022). *German wind energy in numbers.* Retrieved October 9, 2023, from https://www.wind-energie.de/english/statistics/statistics-germany

CEVA Logistics. (2023). *Gigawatt hour.* Retrieved September 19, 2023, from https://www.cevalogistics.com/en/glossary/gigawatt-hour

Chakraborty, M. R., Dawn, S., Saha, P. K., Basu, J. B., & Ustun, T. S. (2022). A comparative review on energy storage systems and their application in deregulated systems. *Batteries*, *8*(9), 124.

Elmegaard, B., & Brix, W. (2011). Efficiency of compressed air energy storage. In *24th international conference on efficiency, cost, optimization, simulation and environmental impact of energy systems.*

EnBW. (2023). *Enbw to invest in hydropower and pumped storage in forbach.* Retrieved September 11, 2023, from https://www.enbw.com/company/investors/news-and-publications/enbw-to-invest-in-hydropower-and-pumped-storage-in-forbach.html

EPEX SPOT. (2023). *Trading products.* Retrieved July 24, 2023, from https://www.epexspot.com/en/tradingproducts

ETN News. (2023). *Rwe confirms 35 mw/ 41 mwh bess at its biomass plant in netherlands.* Retrieved September 11, 2023, from https://etn.news/buzz/rwe-utility-scale-battery-storage-eemshaven-netherlands

European Commission. (2023). *Recommendations on energy storage.* Retrieved July 28, 2023, from https://energy.ec.europa.eu/topics/research-and-technology/energy-storage/recommendations-energy-storage_en

Fajinmi, O., Munda, J. L., Hamam, Y., & Popoola, O. (2023). Compressed air energy storage as a battery energy storage system for various application domains: A review. *Energies*, *16*(18), 6653.

Garcia-Gonzalez, J., de la Muela, R. M. R., Santos, L. M., & Gonzalez, A. M. (2008). Stochastic joint optimization of wind generation and pumped-storage units in an electricity market. *IEEE Transactions on Power Systems*, *23*(2), 460–468.

International Hydropower Association. (2023). *Pumped storage hydropower.* Retrieved July 27, 2023, from https://www.hydropower.org/factsheets/pumped-storage

Kim, H. J., Sioshansi, R., & Conejo, A. J. (2021). Benefits of stochastic optimization for scheduling energy storage in wholesale electricity markets. *Journal of Modern Power Systems and Clean Energy*, *9*(1), 181–189.

Klaas, A.-K., & Beck, H.-P. (2021). A milp model for revenue optimization of a compressed air energy storage plant with electrolysis. *Energies*, *14*(20), 6803.

KYOS. (2023). *What is spot power trading?* Retrieved July 31, 2023, from `https://www.kyos.com/faq/what-is-spot-power-trading/`

Löhndorf, N., Wozabal, D., & Minner, S. (2013). Optimizing trading decisions for hydro storage systems using approximate dual dynamic programming. *Operations Research*, *61*(4), 810–823.

Ma, T., Yang, H., & Lu, L. (2014). Feasibility study and economic analysis of pumped hydro storage and battery storage for a renewable energy powered island. *Energy Conversion and Management*, *79*, 387-397. Retrieved from `https://www.sciencedirect.com/science/article/pii/S0196890413008236` doi: https://doi.org/10.1016/j.enconman.2013.12.047

Maciejowska, K. (2020). Assessing the impact of renewable energy sources on the electricity price level and variability–a quantile regression approach. *Energy Economics*, *85*, 104532.

Mayer, K., & Trück, S. (2018). Electricity markets around the world. *Journal of Commodity Markets*, *9*, 77–100.

Nease, J., & Adams II, T. A. (2014). Application of rolling horizon optimization to an integrated solid-oxide fuel cell and compressed air energy storage plant for zero-emissions peaking power under uncertainty. *Computers & chemical engineering*, *68*, 203–219.

Oh, E., & Wang, H. (2020). Reinforcement-learning-based energy storage system operation strategies to manage wind power forecast uncertainty. *IEEE Access*, *8*, 20965–20976.

Oh, S., Kong, J., Yang, Y., Jung, J., & Lee, C.-H. (2023). A multi-use framework of energy storage systems using reinforcement learning for both price-based and incentive-based demand response programs. *International Journal of Electrical Power & Energy Systems*, *144*, 108519.

PORR Group. (2023). *Porr to build caverns and tunnel system for forbach pumped storage power plant.* Retrieved September 11, 2023, from `https://porr-group.com/en/press/press-release/news/porr-to-build-caverns-and-tunnel-system-for-forbach-pumped-storage-power-plant/`

Power Engineers. (2023). *30 mw/20 mwh battery energy storage system (bess).* Retrieved September 11, 2023, from `https://www.powereng.com/library/30-mw--20-mwh-battery-energy-storage-system-bess`

Qi, N., Cheng, L., Li, H., Zhao, Y., & Tian, H. (2023). Portfolio optimization of generic energy storage-based virtual power plant under decision-dependent uncertainties. *Journal of Energy Storage*, *63*, 107000.

Quaranta, E., Georgakaki, A., Letout, S., Kuokkanen, A., Mountraki, A., Ince, E., … others (2022). Clean energy technology observatory: Hydropower and pumped hydropower storage in the european union–2022 status report on technology development, trends, value chains and markets.

Rabi, A. M., Radulovic, J., & Buick, J. M. (2023). Comprehensive review of compressed air energy storage (caes) technologies. *Thermo*, *3*(1), 104–126.

Ruiz, R. A., De Vilder, L., Prasasti, E., Aouad, M., De Luca, A., Geisseler, B., … others (2022). Low-head pumped hydro storage: A review on civil structure designs, legal and environmental aspects to make its realization feasible in seawater. *Renewable and Sustainable Energy Reviews*, *160*, 112281.

Sahinidis, N. V. (2004). Optimization under uncertainty: state-of-the-art and opportunities. *Computers & chemical engineering*, *28*(6-7), 971–983.

Schüle, M., Veillard, X., & Weiss, A. (2023). *Four themes shaping the future of the stormy european power market.* Retrieved September 19, 2023, from `https://www.mckinsey.com/industries/electric-power-and-natural-gas/our-insights/four-themes-shaping-the-future-of-the-stormy-european-power-market`

Sioshansi, R., Denholm, P., Arteaga, J., Awara, S., Bhattacharjee, S., Botterud, A., … others (2021). Energy-storage modeling: State-of-the-art and future research directions. *IEEE Transactions on Power Systems*, *37*(2), 860–875.

Wang, X., & Kopfer, H. (2015). Rolling horizon planning for a dynamic collaborative routing problem with full-truckload pickup and delivery requests. *Flexible Services and Manufacturing Journal*, *27*, 509–533.

Weitzel, T., & Glock, C. H. (2018). Energy management for stationary electric energy storage systems: A systematic literature review. *European Journal of Operational Research*, *264*(2), 582–606.

Wozabal, D., & Rameseder, G. (2020). Optimal bidding of a virtual power plant on the spanish day-ahead and intraday market for electricity. *European Journal of Operational Research*, *280*(2), 639–655.

# A

# Appendix

## A.1. Intraday historical price data

This section presents the hourly mean, standard deviation, and correlations for all four cases, which are utilized in constructing the intraday price scenarios.

**Table A.1:** Hourly mean and standard deviation for Spring Weekend.

| Time | Mean | Standard deviation |
|---|---|---|
| 1 | 2.94 | 15.20 |
| 2 | 4.78 | 10.33 |
| 3 | 1.29 | 11.91 |
| 4 | -0.97 | 15.28 |
| 5 | -0.59 | 15.24 |
| 6 | -0.16 | 12.44 |
| 7 | -2.39 | 16.59 |
| 8 | -2.03 | 16.17 |
| 9 | 0.55 | 14.17 |
| 10 | 2.74 | 13.01 |
| 11 | 4.14 | 11.87 |
| 12 | 0.79 | 14.84 |
| 13 | -1.15 | 15.18 |
| 14 | -3.89 | 17.24 |
| 15 | -1.29 | 16.24 |
| 16 | -2.14 | 16.00 |
| 17 | -3.00 | 15.63 |
| 18 | 0.78 | 15.52 |
| 19 | 0.02 | 13.30 |
| 20 | 0.16 | 14.75 |
| 21 | -3.01 | 16.99 |
| 22 | -1.38 | 10.18 |
| 23 | 0.40 | 14.79 |
| 24 | 4.02 | 18.67 |

**Table A.2:** Correlation matrix for Spring Weekend.

| | 1 | 2 | 3 | 4 | 5 | 6 | 7 | 8 | 9 | 10 | 11 | 12 | 13 | 14 | 15 | 16 | 17 | 18 | 19 | 20 | 21 | 22 | 23 | 24 |
|---|---|---|---|---|---|---|---|---|---|---|---|---|---|---|---|---|---|---|---|---|---|---|---|---|
| 1 | 1.00 | 0.38 | 0.36 | 0.64 | 0.53 | 0.53 | 0.41 | 0.36 | 0.03 | 0.16 | 0.22 | 0.25 | 0.06 | 0.13 | 0.19 | -0.02 | 0.20 | 0.17 | -0.30 | -0.37 | -0.34 | -0.12 | -0.02 | -0.18 |
| 2 | 0.38 | 1.00 | 0.59 | 0.34 | 0.31 | 0.40 | 0.25 | 0.26 | 0.31 | -0.02 | -0.14 | -0.03 | 0.00 | -0.16 | -0.03 | -0.18 | -0.32 | -0.23 | -0.32 | -0.35 | -0.45 | -0.24 | -0.25 | -0.33 |
| 3 | 0.36 | 0.59 | 1.00 | 0.65 | 0.21 | 0.54 | 0.59 | 0.61 | 0.39 | 0.11 | -0.19 | -0.23 | -0.24 | -0.15 | 0.03 | -0.17 | -0.20 | -0.17 | -0.25 | -0.42 | -0.45 | -0.14 | -0.21 | -0.27 |
| 4 | 0.64 | 0.34 | 0.65 | 1.00 | 0.48 | 0.61 | 0.77 | 0.71 | 0.28 | 0.23 | 0.12 | -0.03 | -0.21 | 0.00 | 0.19 | -0.05 | -0.01 | 0.06 | -0.27 | -0.51 | -0.45 | -0.08 | -0.05 | -0.14 |
| 5 | 0.53 | 0.31 | 0.21 | 0.48 | 1.00 | 0.56 | 0.40 | 0.40 | 0.30 | 0.28 | 0.24 | 0.19 | 0.07 | -0.05 | 0.10 | 0.08 | 0.02 | 0.04 | 0.08 | -0.20 | -0.16 | -0.18 | -0.05 | -0.08 |
| 6 | 0.53 | 0.40 | 0.54 | 0.61 | 0.56 | 1.00 | 0.71 | 0.57 | 0.27 | 0.20 | 0.24 | 0.24 | 0.14 | 0.08 | 0.14 | -0.01 | -0.09 | -0.12 | -0.12 | -0.38 | -0.42 | -0.35 | -0.26 | -0.18 |
| 7 | 0.41 | 0.25 | 0.59 | 0.77 | 0.40 | 0.71 | 1.00 | 0.78 | 0.28 | 0.14 | 0.21 | 0.21 | 0.08 | 0.27 | 0.37 | 0.15 | 0.01 | 0.07 | -0.04 | -0.39 | -0.41 | -0.22 | -0.23 | 0.00 |
| 8 | 0.36 | 0.26 | 0.61 | 0.71 | 0.40 | 0.57 | 0.78 | 1.00 | 0.68 | 0.47 | 0.20 | 0.08 | -0.06 | 0.10 | 0.25 | -0.02 | -0.04 | -0.00 | -0.19 | -0.48 | -0.45 | 0.03 | 0.06 | 0.06 |
| 9 | 0.03 | 0.31 | 0.40 | 0.28 | 0.30 | 0.27 | 0.28 | 0.68 | 1.00 | 0.69 | 0.18 | -0.08 | -0.21 | -0.28 | -0.05 | -0.12 | -0.15 | -0.14 | -0.18 | -0.17 | -0.36 | 0.21 | 0.22 | -0.05 |
| 10 | 0.16 | -0.02 | 0.11 | 0.23 | 0.28 | 0.20 | 0.14 | 0.47 | 0.69 | 1.00 | 0.48 | 0.03 | -0.21 | -0.22 | -0.01 | -0.01 | 0.19 | 0.22 | -0.04 | 0.07 | -0.09 | 0.37 | 0.49 | 0.13 |
| 11 | 0.22 | -0.14 | -0.19 | 0.12 | 0.24 | 0.24 | 0.21 | 0.20 | 0.18 | 0.48 | 1.00 | 0.66 | 0.37 | 0.38 | 0.29 | 0.28 | 0.35 | 0.33 | 0.13 | 0.17 | 0.06 | 0.17 | 0.33 | 0.32 |
| 12 | 0.25 | -0.03 | -0.23 | -0.03 | 0.19 | 0.24 | 0.21 | 0.08 | -0.08 | 0.03 | 0.66 | 1.00 | 0.74 | 0.59 | 0.49 | 0.39 | 0.33 | 0.18 | 0.08 | -0.02 | -0.10 | -0.03 | 0.16 | -0.04 |
| 13 | 0.06 | 0.00 | -0.24 | -0.21 | 0.07 | 0.14 | 0.08 | -0.06 | -0.21 | -0.21 | 0.37 | 0.74 | 1.00 | 0.71 | 0.51 | 0.46 | 0.29 | 0.15 | 0.21 | 0.05 | 0.09 | -0.12 | -0.19 | 0.12 |
| 14 | 0.13 | -0.16 | -0.15 | 0.00 | -0.05 | 0.08 | 0.27 | 0.10 | -0.28 | -0.22 | 0.38 | 0.59 | 0.71 | 1.00 | 0.79 | 0.63 | 0.48 | 0.39 | 0.33 | 0.04 | 0.09 | -0.04 | -0.10 | 0.24 |
| 15 | 0.19 | -0.03 | 0.03 | 0.19 | 0.10 | 0.14 | 0.15 | -0.02 | -0.04 | -0.01 | 0.29 | 0.49 | 0.51 | 0.79 | 1.00 | 0.80 | 0.58 | 0.51 | 0.37 | 0.05 | -0.07 | -0.01 | -0.11 | 0.04 |
| 16 | -0.02 | -0.18 | -0.17 | -0.05 | 0.08 | -0.01 | 0.15 | -0.02 | -0.12 | -0.01 | 0.28 | 0.39 | 0.46 | 0.63 | 0.80 | 1.00 | 0.70 | 0.60 | 0.58 | 0.37 | 0.12 | -0.03 | -0.15 | -0.06 |
| 17 | 0.20 | -0.32 | -0.20 | -0.01 | 0.02 | -0.09 | 0.01 | -0.04 | -0.15 | 0.19 | 0.35 | 0.33 | 0.29 | 0.48 | 0.58 | 0.70 | 1.00 | 0.82 | 0.48 | 0.44 | 0.20 | 0.21 | 0.16 | -0.04 |
| 18 | 0.17 | -0.23 | -0.17 | 0.06 | 0.04 | -0.12 | 0.07 | -0.00 | -0.14 | 0.22 | 0.33 | 0.18 | 0.15 | 0.39 | 0.51 | 0.60 | 0.82 | 1.00 | 0.57 | 0.48 | 0.20 | 0.32 | 0.27 | 0.11 |
| 19 | -0.30 | -0.32 | -0.25 | -0.27 | 0.08 | -0.12 | -0.05 | -0.19 | -0.19 | -0.04 | 0.13 | 0.08 | 0.21 | 0.33 | 0.37 | 0.58 | 0.48 | 0.57 | 1.00 | 0.65 | 0.51 | 0.10 | -0.03 | 0.05 |
| 20 | -0.37 | -0.35 | -0.42 | -0.51 | -0.20 | -0.38 | -0.39 | -0.48 | -0.17 | 0.07 | 0.17 | -0.02 | 0.05 | 0.04 | 0.05 | 0.37 | 0.44 | 0.48 | 0.65 | 1.00 | 0.63 | 0.36 | 0.18 | 0.01 |
| 21 | -0.34 | -0.45 | -0.45 | -0.45 | -0.16 | -0.42 | -0.41 | -0.45 | -0.36 | -0.09 | 0.06 | -0.01 | 0.09 | 0.09 | -0.07 | 0.12 | 0.20 | 0.20 | 0.51 | 0.63 | 1.00 | 0.30 | 0.32 | 0.25 |
| 22 | -0.12 | -0.24 | -0.14 | -0.08 | -0.18 | -0.35 | -0.22 | 0.03 | 0.21 | 0.37 | 0.17 | -0.10 | -0.12 | -0.04 | -0.01 | -0.03 | 0.21 | 0.32 | 0.10 | 0.36 | 0.30 | 1.00 | 0.68 | 0.31 |
| 23 | -0.02 | -0.25 | -0.21 | -0.05 | -0.05 | -0.26 | -0.23 | 0.06 | 0.22 | 0.49 | 0.33 | -0.03 | -0.19 | -0.10 | -0.11 | -0.15 | 0.16 | 0.27 | -0.03 | 0.18 | 0.32 | 0.68 | 1.00 | 0.61 |
| 24 | -0.18 | -0.33 | -0.27 | -0.14 | -0.08 | -0.18 | 0.00 | 0.06 | -0.05 | 0.14 | 0.32 | 0.16 | 0.12 | 0.24 | 0.04 | -0.06 | -0.04 | 0.11 | 0.05 | 0.01 | 0.25 | 0.31 | 0.61 | 1.00 |

**Table A.3:** Hourly mean and standard deviation for Stormy Summer.

| Time | Mean | Standard deviation |
|---|---|---|
| 1 | 1.03 | 15.77 |
| 2 | 1.21 | 21.98 |
| 3 | -0.83 | 14.34 |
| 4 | -0.22 | 12.15 |
| 5 | -0.89 | 13.98 |
| 6 | -0.62 | 13.40 |
| 7 | -0.87 | 11.80 |
| 8 | -1.70 | 13.38 |
| 9 | 5.71 | 37.42 |
| 10 | 6.94 | 23.94 |
| 11 | 4.82 | 16.97 |
| 12 | 3.84 | 14.09 |
| 13 | 2.59 | 15.26 |
| 14 | 0.56 | 11.42 |
| 15 | 1.82 | 11.55 |
| 16 | -0.88 | 10.83 |
| 17 | 0.68 | 14.08 |
| 18 | 2.60 | 26.99 |
| 19 | 4.82 | 28.62 |
| 20 | 10.55 | 54.45 |
| 21 | 7.40 | 31.57 |
| 22 | 7.01 | 29.34 |
| 23 | 3.61 | 18.66 |
| 24 | 1.93 | 16.89 |

**Table A.4:** Correlation matrix for Stormy Summer.

| | 1 | 2 | 3 | 4 | 5 | 6 | 7 | 8 | 9 | 10 | 11 | 12 | 13 | 14 | 15 | 16 | 17 | 18 | 19 | 20 | 21 | 22 | 23 | 24 |
|---|---|---|---|---|---|---|---|---|---|---|---|---|---|---|---|---|---|---|---|---|---|---|---|---|
| 1 | 1.00 | 0.52 | 0.50 | 0.69 | 0.44 | 0.40 | 0.48 | 0.31 | 0.07 | 0.45 | 0.11 | 0.01 | -0.13 | 0.19 | -0.18 | -0.20 | -0.03 | 0.09 | 0.33 | 0.15 | 0.30 | 0.20 | 0.12 | 0.28 |
| 2 | 0.52 | 1.00 | 0.54 | 0.44 | 0.48 | 0.48 | 0.48 | 0.26 | 0.61 | 0.18 | 0.12 | 0.03 | -0.29 | 0.03 | -0.28 | -0.24 | -0.04 | 0.64 | 0.51 | 0.70 | 0.23 | 0.08 | 0.03 | 0.28 |
| 3 | 0.50 | 0.54 | 1.00 | 0.73 | 0.75 | 0.65 | 0.57 | 0.36 | 0.18 | 0.27 | 0.18 | -0.00 | -0.03 | 0.11 | -0.12 | -0.09 | -0.08 | 0.16 | 0.30 | 0.22 | 0.25 | 0.06 | -0.10 | 0.11 |
| 4 | 0.69 | 0.44 | 0.73 | 1.00 | 0.67 | 0.57 | 0.62 | 0.29 | 0.02 | 0.47 | 0.28 | 0.11 | 0.01 | 0.18 | -0.14 | -0.06 | 0.00 | 0.04 | 0.31 | 0.07 | 0.19 | 0.06 | 0.16 | 0.09 |
| 5 | 0.44 | 0.48 | 0.67 | 0.67 | 1.00 | 0.85 | 0.66 | 0.54 | 0.23 | 0.38 | 0.34 | 0.07 | -0.05 | 0.09 | -0.16 | -0.07 | -0.19 | 0.12 | 0.26 | 0.19 | 0.42 | 0.33 | 0.05 | 0.25 |
| 6 | 0.40 | 0.48 | 0.65 | 0.57 | 0.85 | 1.00 | 0.74 | 0.56 | 0.35 | 0.44 | 0.38 | 0.20 | -0.02 | 0.15 | -0.11 | -0.05 | -0.23 | 0.27 | 0.29 | 0.40 | 0.41 | 0.17 | 0.40 | 0.28 |
| 7 | 0.48 | 0.48 | 0.57 | 0.62 | 0.66 | 0.74 | 1.00 | 0.56 | 0.43 | 0.59 | 0.50 | 0.31 | 0.09 | 0.19 | -0.01 | -0.22 | 0.33 | 0.48 | 0.40 | 0.41 | 0.33 | 0.29 | 0.37 | 0.28 |
| 8 | 0.31 | 0.26 | 0.36 | 0.29 | 0.54 | 0.56 | 0.56 | 1.00 | 0.29 | 0.48 | 0.29 | 0.20 | 0.09 | 0.08 | -0.32 | -0.11 | -0.06 | 0.14 | 0.28 | 0.48 | 0.48 | 0.16 | 0.45 | 0.16 |
| 9 | 0.07 | 0.61 | 0.18 | 0.02 | 0.23 | 0.35 | 0.43 | 0.29 | 1.00 | 0.25 | 0.36 | 0.36 | 0.06 | 0.07 | 0.03 | -0.08 | -0.31 | 0.20 | 0.53 | 0.27 | 0.24 | 0.24 | 0.31 | 0.45 |
| 10 | 0.45 | 0.18 | 0.27 | 0.47 | 0.38 | 0.44 | 0.59 | 0.48 | 0.25 | 1.00 | 0.68 | 0.61 | 0.33 | 0.29 | 0.19 | 0.10 | -0.31 | 0.20 | 0.53 | 0.27 | 0.24 | 0.24 | 0.31 | 0.47 |
| 11 | 0.11 | 0.12 | 0.18 | 0.28 | 0.34 | 0.38 | 0.50 | 0.29 | 0.36 | 0.68 | 1.00 | 0.71 | 0.49 | 0.38 | 0.24 | 0.34 | -0.05 | 0.32 | 0.49 | 0.49 | 0.53 | 0.39 | 0.48 | 0.41 |
| 12 | 0.01 | 0.03 | -0.00 | 0.11 | 0.07 | 0.20 | 0.31 | 0.20 | 0.36 | 0.61 | 0.71 | 1.00 | 0.67 | 0.53 | 0.47 | 0.13 | 0.45 | 0.51 | 0.40 | 0.43 | 0.41 | 0.49 | 0.39 | 0.51 |
| 13 | -0.13 | -0.29 | -0.03 | 0.01 | -0.05 | -0.02 | 0.09 | 0.09 | 0.06 | 0.33 | 0.49 | 0.67 | 1.00 | 0.68 | 0.65 | 0.51 | 0.33 | 0.19 | 0.36 | 0.08 | 0.38 | 0.27 | 0.32 | 0.24 |
| 14 | 0.19 | 0.03 | 0.11 | 0.18 | 0.09 | 0.15 | -0.11 | 0.08 | 0.07 | 0.29 | 0.38 | 0.53 | 0.68 | 1.00 | 0.63 | 0.63 | 0.51 | 0.33 | 0.46 | 0.14 | 0.30 | 0.25 | 0.43 | 0.41 |
| 15 | -0.18 | -0.28 | -0.12 | -0.14 | -0.16 | -0.11 | -0.01 | -0.32 | 0.03 | 0.19 | 0.24 | 0.47 | 0.65 | 0.63 | 1.00 | 0.69 | 0.45 | 0.26 | 0.30 | -0.03 | 0.09 | 0.07 | 0.15 | 0.14 |
| 16 | -0.20 | -0.24 | -0.09 | -0.06 | -0.07 | -0.05 | -0.22 | -0.11 | -0.08 | 0.10 | 0.34 | 0.13 | 0.51 | 0.63 | 0.69 | 1.00 | 0.55 | 0.25 | 0.23 | -0.04 | 0.10 | 0.05 | 0.25 | 0.11 |
| 17 | -0.03 | -0.04 | -0.08 | 0.00 | -0.19 | -0.23 | 0.33 | -0.06 | -0.08 | 0.04 | -0.05 | 0.45 | 0.33 | 0.51 | 0.45 | 0.55 | 1.00 | 0.22 | 0.23 | -0.06 | -0.23 | -0.23 | -0.19 | -0.11 |
| 18 | 0.09 | 0.64 | 0.16 | 0.04 | 0.12 | 0.27 | 0.48 | 0.14 | -0.31 | 0.20 | 0.32 | 0.51 | 0.19 | 0.33 | 0.26 | 0.25 | 0.22 | 1.00 | 0.77 | 0.87 | 0.27 | 0.20 | 0.28 | 0.45 |
| 19 | 0.33 | 0.51 | 0.30 | 0.31 | 0.26 | 0.36 | 0.40 | 0.28 | 0.53 | 0.53 | 0.49 | 0.40 | 0.36 | 0.46 | 0.30 | 0.23 | 0.23 | 0.77 | 1.00 | 0.71 | 0.50 | 0.49 | 0.62 | 0.11 |
| 20 | 0.15 | 0.70 | 0.22 | 0.07 | 0.19 | 0.29 | 0.41 | 0.48 | 0.27 | 0.27 | 0.49 | 0.43 | 0.08 | 0.14 | -0.03 | -0.04 | -0.06 | 0.87 | 0.71 | 1.00 | 0.45 | 0.26 | 0.64 | 0.45 |
| 21 | 0.30 | 0.23 | 0.25 | 0.19 | 0.42 | 0.41 | 0.33 | 0.48 | 0.24 | 0.24 | 0.53 | 0.41 | 0.38 | 0.30 | 0.09 | 0.10 | -0.23 | 0.27 | 0.50 | 0.45 | 1.00 | 0.45 | 0.72 | 0.29 |
| 22 | 0.20 | 0.08 | 0.06 | 0.06 | 0.33 | 0.39 | 0.33 | 0.48 | 0.24 | 0.52 | 0.39 | 0.41 | 0.34 | 0.28 | 0.13 | 0.07 | -0.23 | 0.20 | 0.45 | 0.30 | 0.82 | 1.00 | 0.45 | 0.72 |
| 23 | 0.12 | 0.03 | -0.10 | 0.16 | 0.05 | 0.17 | 0.29 | 0.16 | 0.24 | 0.62 | 0.53 | 0.49 | 0.27 | 0.25 | 0.31 | 0.15 | -0.19 | 0.20 | 0.45 | 0.26 | 0.32 | 0.45 | 1.00 | 0.51 |
| 24 | 0.28 | 0.28 | 0.11 | 0.09 | 0.25 | 0.40 | 0.38 | 0.45 | 0.31 | 0.48 | 0.41 | 0.39 | 0.26 | 0.41 | 0.14 | 0.14 | -0.11 | 0.43 | 0.62 | 0.45 | 0.64 | 0.72 | 0.51 | 1.00 |

**Table A.5:** Hourly mean and standard deviation for Cloudy Autumn.

| Time | Mean | Standard deviation |
|---|---|---|
| 1 | -1.32 | 25.55 |
| 2 | -0.30 | 23.25 |
| 3 | 0.22 | 24.46 |
| 4 | 1.42 | 24.25 |
| 5 | -2.53 | 24.48 |
| 6 | -4.09 | 30.23 |
| 7 | -5.22 | 43.74 |
| 8 | -7.04 | 40.55 |
| 9 | -7.07 | 36.43 |
| 10 | -6.99 | 32.39 |
| 11 | -6.77 | 31.24 |
| 12 | -5.66 | 30.78 |
| 13 | -4.24 | 37.29 |
| 14 | -3.99 | 37.19 |
| 15 | -4.22 | 38.32 |
| 16 | -3.30 | 42.72 |
| 17 | -3.55 | 45.25 |
| 18 | -7.80 | 49.25 |
| 19 | -9.08 | 40.16 |
| 20 | -9.83 | 45.79 |
| 21 | -5.98 | 40.30 |
| 22 | -5.09 | 38.32 |
| 23 | 2.91 | 38.99 |
| 24 | 9.69 | 39.59 |

**Table A.6:** Correlation matrix for Cloudy Autumn.

| | 1 | 2 | 3 | 4 | 5 | 6 | 7 | 8 | 9 | 10 | 11 | 12 | 13 | 14 | 15 | 16 | 17 | 18 | 19 | 20 | 21 | 22 | 23 | 24 |
|---|---|---|---|---|---|---|---|---|---|---|---|---|---|---|---|---|---|---|---|---|---|---|---|---|
| 1 | 1.00 | 0.70 | 0.64 | 0.61 | 0.62 | 0.51 | 0.42 | 0.32 | 0.28 | 0.25 | 0.28 | 0.26 | 0.23 | 0.23 | 0.13 | 0.01 | 0.01 | 0.01 | 0.04 | 0.10 | -0.05 | -0.01 | 0.11 | 0.12 |
| 2 | 0.70 | 1.00 | 0.69 | 0.65 | 0.60 | 0.54 | 0.43 | 0.36 | 0.38 | 0.28 | 0.28 | 0.29 | 0.25 | 0.23 | 0.22 | 0.12 | 0.08 | 0.05 | 0.09 | 0.13 | 0.00 | 0.08 | 0.11 | 0.12 |
| 3 | 0.64 | 0.69 | 1.00 | 0.77 | 0.69 | 0.56 | 0.40 | 0.37 | 0.33 | 0.31 | 0.29 | 0.30 | 0.28 | 0.32 | 0.29 | 0.14 | 0.14 | 0.02 | 0.12 | 0.20 | 0.01 | 0.06 | 0.13 | 0.12 |
| 4 | 0.61 | 0.65 | 0.77 | 1.00 | 0.79 | 0.58 | 0.48 | 0.40 | 0.36 | 0.33 | 0.31 | 0.31 | 0.27 | 0.23 | 0.14 | 0.11 | 0.03 | 0.03 | 0.07 | -0.10 | -0.02 | 0.08 | 0.10 | 0.09 |
| 5 | 0.62 | 0.60 | 0.69 | 0.79 | 1.00 | 0.66 | 0.54 | 0.45 | 0.40 | 0.37 | 0.30 | 0.27 | 0.23 | 0.16 | 0.09 | 0.07 | 0.01 | 0.04 | 0.09 | -0.11 | -0.03 | 0.13 | 0.16 | 0.16 |
| 6 | 0.51 | 0.54 | 0.56 | 0.58 | 0.66 | 1.00 | 0.73 | 0.60 | 0.54 | 0.46 | 0.34 | 0.31 | 0.24 | 0.19 | 0.12 | -0.01 | -0.03 | -0.01 | 0.09 | 0.16 | -0.04 | 0.04 | 0.18 | 0.16 |
| 7 | 0.42 | 0.43 | 0.40 | 0.48 | 0.54 | 0.73 | 1.00 | 0.74 | 0.67 | 0.59 | 0.44 | 0.38 | 0.29 | 0.21 | 0.10 | -0.01 | -0.02 | -0.01 | 0.06 | 0.05 | -0.04 | -0.03 | 0.12 | 0.11 |
| 8 | 0.32 | 0.36 | 0.37 | 0.40 | 0.40 | 0.60 | 0.74 | 1.00 | 0.80 | 0.68 | 0.56 | 0.41 | 0.32 | 0.27 | 0.18 | 0.10 | 0.10 | 0.14 | 0.16 | 0.17 | 0.09 | 0.08 | 0.19 | 0.21 |
| 9 | 0.28 | 0.38 | 0.33 | 0.36 | 0.36 | 0.54 | 0.67 | 0.80 | 1.00 | 0.78 | 0.60 | 0.45 | 0.36 | 0.32 | 0.16 | 0.16 | 0.21 | 0.21 | 0.23 | 0.13 | 0.11 | 0.18 | 0.18 | 0.18 |
| 10 | 0.25 | 0.28 | 0.31 | 0.33 | 0.33 | 0.46 | 0.59 | 0.68 | 0.78 | 1.00 | 0.75 | 0.59 | 0.51 | 0.44 | 0.35 | 0.33 | 0.30 | 0.32 | 0.29 | 0.27 | 0.22 | 0.25 | 0.26 | 0.26 |
| 11 | 0.28 | 0.28 | 0.29 | 0.31 | 0.30 | 0.34 | 0.44 | 0.56 | 0.60 | 0.75 | 1.00 | 0.75 | 0.64 | 0.44 | 0.35 | 0.33 | 0.30 | 0.31 | 0.29 | 0.27 | 0.26 | 0.26 | 0.27 | 0.27 |
| 12 | 0.26 | 0.29 | 0.30 | 0.31 | 0.27 | 0.31 | 0.38 | 0.41 | 0.45 | 0.59 | 0.75 | 1.00 | 0.81 | 0.69 | 0.59 | 0.52 | 0.44 | 0.38 | 0.41 | 0.29 | 0.30 | 0.33 | 0.30 | 0.32 |
| 13 | 0.23 | 0.25 | 0.28 | 0.27 | 0.23 | 0.24 | 0.29 | 0.32 | 0.36 | 0.51 | 0.64 | 0.81 | 1.00 | 0.80 | 0.66 | 0.59 | 0.55 | 0.50 | 0.54 | 0.35 | 0.38 | 0.36 | 0.28 | 0.32 |
| 14 | 0.23 | 0.23 | 0.32 | 0.23 | 0.16 | 0.19 | 0.21 | 0.27 | 0.32 | 0.44 | 0.44 | 0.69 | 0.80 | 1.00 | 0.64 | 0.64 | 0.53 | 0.53 | 0.51 | 0.39 | 0.40 | 0.39 | 0.31 | 0.23 |
| 15 | 0.13 | 0.12 | 0.29 | 0.14 | 0.09 | 0.12 | 0.10 | 0.18 | 0.16 | 0.35 | 0.35 | 0.59 | 0.66 | 0.64 | 1.00 | 0.75 | 0.69 | 0.65 | 0.64 | 0.58 | 0.48 | 0.42 | 0.36 | 0.35 |
| 16 | 0.01 | 0.08 | 0.14 | 0.11 | 0.07 | -0.01 | -0.01 | 0.10 | 0.16 | 0.33 | 0.33 | 0.52 | 0.59 | 0.64 | 0.75 | 1.00 | 0.85 | 0.84 | 0.84 | 0.80 | 0.69 | 0.65 | 0.69 | 0.71 |
| 17 | 0.01 | 0.05 | 0.14 | 0.03 | 0.01 | -0.03 | -0.02 | 0.10 | 0.16 | 0.30 | 0.30 | 0.44 | 0.55 | 0.53 | 0.69 | 0.85 | 1.00 | 0.94 | 0.91 | 0.80 | 0.80 | 0.85 | 0.91 | 0.92 |
| 18 | 0.01 | 0.09 | 0.02 | 0.03 | 0.04 | -0.01 | -0.01 | 0.14 | 0.21 | 0.32 | 0.31 | 0.38 | 0.50 | 0.53 | 0.65 | 0.84 | 0.94 | 1.00 | 0.96 | 0.84 | 0.79 | 0.88 | 0.89 | 0.86 |
| 19 | 0.04 | 0.13 | 0.12 | 0.07 | 0.09 | 0.09 | 0.06 | 0.16 | 0.21 | 0.29 | 0.29 | 0.41 | 0.54 | 0.51 | 0.64 | 0.84 | 0.91 | 0.96 | 1.00 | 0.92 | 0.84 | 0.88 | 0.93 | 0.88 |
| 20 | 0.10 | 0.00 | 0.20 | -0.10 | -0.11 | 0.16 | 0.05 | 0.17 | 0.23 | 0.27 | 0.27 | 0.29 | 0.35 | 0.39 | 0.58 | 0.80 | 0.80 | 0.84 | 0.92 | 1.00 | 0.85 | 0.87 | 0.94 | 0.85 |
| 21 | -0.05 | 0.08 | 0.01 | -0.02 | -0.03 | -0.04 | -0.04 | 0.09 | 0.13 | 0.22 | 0.26 | 0.30 | 0.38 | 0.40 | 0.48 | 0.69 | 0.80 | 0.79 | 0.84 | 0.85 | 1.00 | 0.95 | 0.94 | 0.81 |
| 22 | -0.01 | 0.11 | 0.06 | 0.08 | 0.13 | 0.04 | -0.03 | 0.08 | 0.11 | 0.25 | 0.26 | 0.33 | 0.36 | 0.39 | 0.42 | 0.65 | 0.85 | 0.88 | 0.88 | 0.87 | 0.95 | 1.00 | 0.96 | 0.78 |
| 23 | 0.11 | 0.12 | 0.13 | 0.10 | 0.16 | 0.18 | 0.12 | 0.19 | 0.18 | 0.26 | 0.27 | 0.30 | 0.28 | 0.31 | 0.36 | 0.69 | 0.91 | 0.89 | 0.93 | 0.94 | 0.94 | 0.96 | 1.00 | 0.87 |
| 24 | 0.12 | 0.12 | 0.12 | 0.09 | 0.16 | 0.16 | 0.11 | 0.21 | 0.18 | 0.26 | 0.27 | 0.32 | 0.32 | 0.23 | 0.35 | 0.71 | 0.92 | 0.86 | 0.88 | 0.85 | 0.81 | 0.78 | 0.87 | 1.00 |

**Table A.7:** Hourly mean and standard deviation for Windy Winter.

| Time | Mean | Standard deviation |
|---|---|---|
| 1 | 2.03 | 7.75 |
| 2 | 1.47 | 7.92 |
| 3 | -0.10 | 9.65 |
| 4 | -1.49 | 12.09 |
| 5 | -3.73 | 13.05 |
| 6 | -3.27 | 12.57 |
| 7 | -1.41 | 12.72 |
| 8 | 2.43 | 13.21 |
| 9 | 3.18 | 12.34 |
| 10 | 3.88 | 12.21 |
| 11 | 5.10 | 13.16 |
| 12 | 4.06 | 9.94 |
| 13 | 2.89 | 11.16 |
| 14 | 1.46 | 9.08 |
| 15 | 1.01 | 8.78 |
| 16 | 0.59 | 8.60 |
| 17 | 0.91 | 9.11 |
| 18 | 1.71 | 8.40 |
| 19 | 2.00 | 14.86 |
| 20 | 0.19 | 9.39 |
| 21 | -0.10 | 8.72 |
| 22 | 0.25 | 8.46 |
| 23 | 1.30 | 7.69 |
| 24 | 0.83 | 6.99 |

**Table A.8:** Correlation matrix for Windy Winter.

| | 1 | 2 | 3 | 4 | 5 | 6 | 7 | 8 | 9 | 10 | 11 | 12 | 13 | 14 | 15 | 16 | 17 | 18 | 19 | 20 | 21 | 22 | 23 | 24 |
|---|---|---|---|---|---|---|---|---|---|---|---|---|---|---|---|---|---|---|---|---|---|---|---|---|
| 1 | 1.00 | 0.37 | 0.39 | 0.24 | 0.10 | 0.03 | 0.12 | 0.23 | 0.23 | 0.35 | 0.41 | 0.25 | 0.19 | 0.01 | -0.07 | -0.12 | -0.02 | -0.20 | 0.03 | 0.15 | 0.07 | 0.04 | -0.16 | -0.17 |
| 2 | 0.37 | 1.00 | 0.60 | 0.61 | 0.53 | 0.55 | 0.24 | 0.04 | 0.14 | 0.04 | 0.15 | 0.30 | 0.04 | -0.03 | -0.03 | -0.14 | -0.17 | 0.01 | -0.04 | 0.11 | 0.13 | 0.06 | -0.01 | -0.07 |
| 3 | 0.39 | 0.60 | 1.00 | 0.72 | 0.54 | 0.45 | 0.42 | 0.10 | 0.19 | 0.12 | 0.18 | 0.31 | 0.19 | 0.05 | -0.00 | -0.11 | 0.02 | -0.01 | 0.08 | 0.14 | 0.13 | -0.02 | -0.07 | -0.04 |
| 4 | 0.24 | 0.61 | 0.72 | 1.00 | 0.70 | 0.67 | 0.29 | 0.01 | -0.00 | 0.07 | 0.09 | 0.17 | 0.06 | 0.07 | 0.03 | -0.09 | 0.01 | -0.02 | 0.08 | 0.17 | 0.12 | 0.04 | -0.03 | -0.14 |
| 5 | 0.10 | 0.53 | 0.54 | 0.70 | 1.00 | 0.75 | 0.44 | -0.02 | -0.24 | -0.12 | -0.15 | 0.04 | -0.07 | -0.17 | -0.17 | -0.32 | -0.23 | -0.13 | -0.10 | -0.02 | 0.02 | -0.06 | -0.13 | -0.15 |
| 6 | 0.03 | 0.55 | 0.45 | 0.67 | 0.75 | 1.00 | 0.48 | 0.10 | 0.08 | -0.06 | -0.10 | 0.06 | -0.17 | -0.14 | -0.07 | -0.19 | -0.20 | -0.06 | -0.06 | -0.07 | 0.03 | -0.01 | -0.07 | -0.12 |
| 7 | 0.12 | 0.24 | 0.42 | 0.29 | 0.44 | 0.48 | 1.00 | 0.34 | 0.31 | 0.13 | 0.09 | 0.21 | 0.10 | -0.01 | -0.05 | -0.21 | -0.17 | -0.18 | -0.02 | -0.07 | -0.08 | -0.13 | 0.01 | -0.13 |
| 8 | 0.23 | 0.04 | 0.10 | 0.01 | -0.02 | 0.10 | 0.34 | 1.00 | 0.49 | 0.42 | 0.52 | 0.40 | 0.39 | 0.30 | 0.21 | 0.09 | 0.09 | -0.14 | -0.00 | 0.08 | -0.05 | -0.00 | -0.04 | 0.08 |
| 9 | 0.23 | 0.14 | 0.19 | -0.00 | -0.24 | 0.08 | 0.31 | 0.49 | 1.00 | 0.46 | 0.51 | 0.44 | 0.30 | 0.33 | 0.28 | 0.19 | 0.05 | 0.13 | 0.03 | 0.16 | 0.11 | -0.02 | 0.12 | 0.15 |
| 10 | 0.35 | 0.04 | 0.12 | 0.07 | -0.12 | -0.06 | 0.13 | 0.42 | 0.46 | 1.00 | 0.77 | 0.59 | 0.53 | 0.42 | 0.23 | 0.18 | 0.28 | 0.02 | 0.12 | 0.14 | 0.28 | 0.16 | 0.10 | 0.07 |
| 11 | 0.41 | 0.15 | 0.18 | 0.09 | -0.15 | -0.10 | 0.09 | 0.52 | 0.51 | 0.77 | 1.00 | 0.68 | 0.69 | 0.55 | 0.40 | 0.30 | 0.32 | 0.28 | 0.20 | 0.15 | 0.11 | 0.07 | 0.05 | 0.01 |
| 12 | 0.25 | 0.30 | 0.31 | 0.17 | 0.04 | 0.06 | 0.21 | 0.40 | 0.44 | 0.59 | 0.68 | 1.00 | 0.67 | 0.64 | 0.54 | 0.29 | 0.32 | 0.02 | 0.24 | 0.19 | 0.21 | 0.18 | 0.20 | 0.10 |
| 13 | 0.19 | 0.04 | 0.19 | 0.06 | -0.07 | -0.17 | 0.10 | 0.39 | 0.30 | 0.53 | 0.69 | 0.67 | 1.00 | 0.51 | 0.24 | 0.32 | 0.17 | 0.18 | 0.25 | 0.12 | 0.20 | 0.01 | 0.08 | -0.05 |
| 14 | 0.01 | -0.03 | 0.05 | 0.07 | -0.17 | -0.14 | -0.01 | 0.30 | 0.33 | 0.42 | 0.55 | 0.64 | 0.51 | 1.00 | 0.52 | 0.48 | 0.36 | 0.20 | 0.24 | 0.17 | 0.20 | -0.09 | 0.16 | 0.09 |
| 15 | -0.07 | -0.03 | -0.00 | 0.03 | -0.17 | -0.07 | -0.05 | 0.21 | 0.28 | 0.23 | 0.40 | 0.54 | 0.24 | 0.52 | 1.00 | 0.60 | 0.57 | 0.45 | 0.24 | 0.30 | 0.09 | -0.05 | 0.09 | 0.02 |
| 16 | -0.12 | -0.14 | -0.11 | -0.09 | -0.32 | -0.19 | -0.21 | 0.09 | 0.19 | 0.18 | 0.30 | 0.29 | 0.32 | 0.48 | 0.60 | 1.00 | 0.68 | 0.67 | 0.63 | 0.32 | 0.37 | -0.03 | 0.08 | -0.09 |
| 17 | -0.02 | -0.17 | 0.02 | 0.01 | -0.23 | -0.20 | -0.17 | 0.09 | 0.05 | 0.28 | 0.32 | 0.32 | 0.17 | 0.36 | 0.57 | 0.68 | 1.00 | 0.67 | 0.34 | 0.30 | 0.30 | 0.07 | 0.14 | -0.05 |
| 18 | -0.20 | 0.01 | -0.01 | -0.02 | -0.13 | -0.06 | -0.18 | -0.14 | 0.13 | 0.02 | 0.28 | 0.02 | 0.18 | 0.20 | 0.45 | 0.67 | 0.67 | 1.00 | 0.39 | 0.26 | 0.32 | -0.12 | 0.06 | -0.03 |
| 19 | 0.03 | -0.04 | -0.01 | 0.08 | -0.10 | -0.06 | -0.02 | -0.00 | 0.03 | 0.12 | 0.20 | 0.24 | 0.25 | 0.24 | 0.24 | 0.63 | 0.34 | 0.39 | 1.00 | 0.41 | 0.46 | -0.01 | 0.11 | -0.01 |
| 20 | 0.15 | 0.11 | -0.02 | 0.17 | -0.02 | -0.07 | -0.07 | 0.08 | 0.16 | 0.14 | 0.15 | 0.19 | 0.12 | 0.17 | 0.30 | 0.32 | 0.30 | 0.26 | 0.41 | 1.00 | 0.54 | -0.11 | 0.03 | -0.01 |
| 21 | 0.07 | 0.13 | -0.07 | 0.12 | 0.02 | 0.03 | -0.08 | -0.05 | 0.11 | 0.28 | 0.11 | 0.21 | 0.20 | 0.20 | 0.09 | 0.37 | 0.30 | 0.32 | 0.46 | 0.54 | 1.00 | -0.00 | -0.00 | 0.01 |
| 22 | 0.04 | 0.06 | -0.02 | 0.04 | -0.06 | -0.01 | -0.13 | -0.00 | -0.02 | 0.16 | 0.07 | 0.18 | 0.01 | -0.09 | -0.05 | -0.03 | 0.07 | -0.12 | -0.01 | -0.11 | -0.00 | 1.00 | -0.06 | -0.01 |
| 23 | -0.16 | -0.01 | -0.07 | -0.03 | -0.13 | -0.07 | 0.01 | -0.04 | 0.12 | 0.10 | 0.05 | 0.20 | 0.08 | 0.16 | 0.09 | 0.08 | 0.14 | 0.06 | 0.11 | 0.03 | -0.00 | -0.06 | 1.00 | -0.02 |
| 24 | -0.17 | -0.07 | -0.04 | -0.14 | -0.15 | -0.12 | -0.13 | 0.08 | 0.15 | 0.07 | 0.01 | 0.10 | -0.05 | 0.09 | 0.02 | -0.09 | -0.05 | -0.03 | -0.01 | -0.01 | 0.01 | -0.01 | -0.02 | 1.00 |

## A.2. Additional runtime examples

The following examples are supporting the choice made in Section 7.2 for 250 scenarios.

**Table A.9:** Results DORH and SORH for a PHS for Spring Weekend.

| Number of scenarios | DORH profit | SORH profit | Stochastic value | Maximum runtime |
|---|---|---|---|---|
| 50 | 124.95 | 339.47 | 171.7% | 8s |
| 100 | 124.95 | 336.07 | 169.0% | 17s |
| 250 | 124.95 | 335.17 | 168.2% | 62s |
| 500 | 124.95 | 340.28 | 172.3% | 178s |
| 750 | 124.95 | 338.26 | 170.7% | 372s |
| 1000 | 124.95 | 334.06 | 167.4% | 616s |

**Table A.10:** Results DORH and SORH for a PHS for Stormy Summer.

| Number of scenarios | DORH profit | SORH profit | Stochastic value | Maximum runtime |
|---|---|---|---|---|
| 50 | 212.80 | 459.40 | 119.5% | 10s |
| 100 | 212.80 | 440.51 | 107.0% | 16s |
| 250 | 212.80 | 449.74 | 111.3% | 50s |
| 500 | 212.80 | 444.84 | 109.0% | 194s |
| 750 | 212.80 | 445.00 | 109.1% | 315s |
| 1000 | 212.80 | 439.79 | 106.7% | 498s |

**Table A.11:** Results DORH and SORH for a BESS for Cloudy Autumn.

| Number of scenarios | DORH profit | SORH profit | Stochastic value | Maximum runtime |
|---|---|---|---|---|
| 50 | 1004.55 | 2424.09 | 141.3% | 10s |
| 100 | 1004.55 | 2421.42 | 141.0% | 17s |
| 250 | 1004.55 | 2379.05 | 136.8% | 59s |
| 500 | 1004.55 | 2389.13 | 137.8% | 120s |
| 750 | 1004.55 | 2402.12 | 137.8% | 214s |
| 1000 | 1004.55 | 2357.15 | 134.6% | 358s |

**Table A.12:** Results DORH and SORH for a BESS for Windy Winter.

| Number of scenarios | DORH profit | SORH profit | Stochastic value | Maximum runtime |
|---|---|---|---|---|
| 50 | 653.30 | 873.98 | 33.8% | 10s |
| 100 | 653.30 | 923.23 | 41.3% | 20s |
| 250 | 653.30 | 918.66 | 40.6% | 50s |
| 500 | 653.30 | 897.31 | 37.4% | 165s |
| 750 | 653.30 | 903.36 | 38.3% | 283s |
| 1000 | 653.30 | 897.13 | 37.3% | 344s |